Analysis of BJT Colpitts Oscillators - Empirical and Mathematical Methods for Predicting Behavior

Nicholas Jon Stave
Marquette University

ANALYSIS OF BJT COLPITTS OSCILLATORS – EMPIRICAL AND MATHEMATICAL METHODS FOR PREDICTING BEHAVIOR

by

Nicholas J. Stave, B.Sc.

A Thesis submitted to the Faculty of the Graduate School,
Marquette University,
in Partial Fulfillment of the Requirements for
the Degree of Master of Science

Milwaukee, Wisconsin

August 2019

ABSTRACT
ANALYSIS OF BJT COLPITTS OSCILLATORS –
EMPIRICAL AND MATHEMATICAL
METHODS FOR PREDICTING
BEHAVIOR

Nicholas J. Stave, B.Sc.

Marquette University, 2019

Oscillator circuits perform two fundamental roles in wireless communication – the local oscillator for frequency shifting and the voltage-controlled oscillator for modulation and detection. The Colpitts oscillator is a common topology used for these applications. Because the oscillator must function as a component of a larger system, the ability to predict and control its output characteristics is necessary. Textbooks treating the circuit often omit analysis of output voltage amplitude and output resistance and the literature on the topic often focuses on gigahertz-frequency chip-based applications. Without extensive component and parasitics information, it is often difficult to make simulation software predictions agree with experimental oscillator results.

The oscillator studied in this thesis is the bipolar junction Colpitts oscillator in the common-base configuration and the analysis is primarily experimental. The characteristics considered are output voltage amplitude, output resistance, and sinusoidal purity of the waveform. The contributions of each of the components of the oscillator to the output voltage waveform are investigated and methods to predict and control amplitude are discussed. The relationships of the output resistance and waveform shape to the inductor are also studied. Two example Colpitts oscillators with different design criteria are constructed for the benefit of the reader and to test the methods identified in the work.

TABLE OF CONTENTS

LIST OF TABLES v

LIST OF FIGURES vi

1 INTRODUCTION 1

1.1 Electronic Oscillators 1

1.1.1 Colpitts Oscillator Family 1

1.1.2 Colpitts Oscillator 4

1.2 Previous Work 5

1.2.1 Exact Calculation of Oscillation Amplitude and Predicting Power Consumption for CMOS Colpitts Oscillators [7] 5

1.2.2 Frequency and Power Scaling in mm-Wave Colpitts Oscillators [8] 6

1.2.3 Everything You Always Wanted to Know About Colpitts Oscillators [17] 7

1.3 Thesis Objective 7

1.4 Thesis Outline 8

2 THEORY 10

2.1 BJT Colpitts Oscillator 10

2.1.1 Common-Base Amplifier 11

2.1.2 Criteria for Oscillation 16

2.1.3 Common-Base Oscillator 18

2.2 Output Characteristics 25

2.2.1 Output Voltage Amplitude 26

2.2.2 Output Impedance 49

2.2.3 Phase Noise and Distortion 59

3 EXPERIMENTAL DATA AND RESULTS 62

3.1 Output Voltage Amplitude Experiments 63

3.1.1 V_o Experiment 1: Dependence on Inductance (Constant C_1) . . 64

3.1.2 V_o Experiment 2: Dependence on Inductance (Constant f_0) . . 65

3.1.3 V_o Experiment 3: Saturation Dependence on Inductance (Constant C) 68

3.1.4 V_o Experiment 4: Dependence on C 76

3.1.5 V_o Experiment 5: Dependence on n 77

3.1.6 V_o Experiment 6: Dependence on Biasing 78

3.1.7 V_o Experiment 7: Large Inductance Oscillator 82

3.1.8 V_o Experiment 8: Added Resistance in Series with Inductor . . 83

3.2 Output Resistance Experiments 85

3.2.1 R_o Experiment 1: Constant C_1 86

3.2.2 R_o Experiment 2: Constant f_0 87

3.2.3 R_o Experiment 3: Large L, Small C 88

3.2.4 R_o Experiment 4: Added Resistance in Series with Inductor . . 89

3.3 Frequency Domain Experiments 90

3.3.1 Frequency Domain Experiment 1: Baseline Oscillator 91

3.3.2 Frequency Domain Experiment 2: Large L, Small C 93

3.3.3 Frequency Domain Experiment 3: Added Resistance in Series with Inductor 97

4 DISCUSSION 101

4.1 Output Voltage Amplitude 101

4.1.1 Feedback Gain vs Output Voltage Amplitude 102

4.1.2 Output Voltage as a Function of Inductance 102

4.1.3 V_o-Inductance Slope 103

4.2 Output Impedance 103

4.3 Waveform Distortion 103

4.4 Guidelines for Oscillator Construction 104

4.4.1 Oscillator 1 105

4.4.2 Oscillator 2 109

5 CONCLUSIONS AND SUGGESTIONS FOR FURTHER RESEARCH 114

5.1 Contributions 114

5.1.1 Output Voltage Amplitude Guidelines 115

5.1.2 Output Resistance Guideline 116

5.2 Suggestions for Further Research 116

BIBLIOGRAPHY 117

A OUTPUT IMPEDANCE OF COMMON-BASE AMPLIFIER 119

B RESONANT FREQUENCY, MAXIMUM EQUIVALENT SERIES RESISTANCE, AND NEGATIVE RESISTANCE 122

B.1 Resonant Frequency 124

B.2 Condition for Oscillation 125

B.3 Negative Resistance 125

C CONTRIBUTION OF EQUIVALENT SERIES RESISTANCE OF INDUCTOR TO OUTPUT IMPEDANCE 127

D DERIVATION OF LARGE-SIGNAL EMITTER CURRENT AND TRANSCONDUCTANCE FOR SINUSOIDAL INPUT 129

E PLOTS OF RELEVANT BESSEL FUNCTIONS 133

E.1 Bessel Functions of the First Kind 133

E.2 Modified Bessel Functions of the First Kind 134

E.3 Small-Angle Approximations 134

LIST OF TABLES

2.1 Output Resistance - Clarke-Hess Circuit, Smith Method 58

3.1 R_L and V_o for Large L Oscillator 88

3.2 Theoretical Output Resistances of Oscillator with Added Resistance r 90

3.3 Baseline Oscillator Component and Bias Values 91

3.4 Baseline Oscillator - Relative Power at Harmonics 93

3.5 Large-Inductor Oscillator (Saturated) - Relative Power at Harmonics 96

3.6 Oscillator with No Added Resistance - Relative Power at Harmonics 98

3.7 Oscillator with Added Resistance - Relative Power at Harmonics 100

LIST OF FIGURES

1.1 Simplified BJT Colpitts Oscillator 2

1.2 Feedback Gains in LC Oscillators 3

1.3 BJT Oscillators in the Colpitts Family 4

2.1 Common-Base Amplifier with Voltage-Divider Biasing 12

2.2 Common-Base Amplifier with Dual-Supply Biasing 13

2.3 Simplified Hybrid-π Model in Common-Base Configuration 14

2.4 Simplified Common-Base Amplifier Small-Signal Equivalent Circuit 14

2.5 More Robust Representation of the Common-Base Amplifier 16

2.6 Generic Feedback Amplifier Block Diagram 17

2.7 Dual-Supply Common-Base Colpitts Oscillator 19

2.8 Small-Signal Equivalent Common-Base Colpitts Oscillator 20

2.9 Rearranged Small-Signal Equivalent Common-Base Colpitts Oscillator 20

2.10 Small-Signal Equivalent Oscillator with Feedback Loop Opened 22

2.11 Admittance to be Transformed 22

2.12 Approximate Transformed Admittance, Valid if $R^2\omega^2(C_1 + C_2)^2 \gg 1$ 23

2.13 Oscillator with Transformed Admittance 24

2.14 Hagen Colpitts Oscillator Example 27

2.15 Hagen Oscillator Circuit in LTSpice 28

2.16 Hagen Simulation: No Initial Conditions, $0 < t < 5\ \mu s$ 29

2.17 Hagen Simulation: No Initial Conditions, $495\ \mu s < t < 500\ \mu s$ 29

2.18 Hagen Simulation: No Initial Conditions, $1495\ \mu s < t < 1500\ \mu s$ 30

2.19 Hagen Simulation: *startup* Applied, $432\ \mu s < t < 480\ \mu s$ 31

2.20 Hagen Simulation: *uic* Applied, 322 $\mu s < t < 392\ \mu s$ 31

2.21 Hagen Simulation: $V_{CC} = 7\ V$, *uic* Applied, 1.400 $ms < t < 1.404\ ms$ 32

2.22 Protoboard Hagen Colpitts Oscillator Circuit Diagram 33

2.23 Protoboard Hagen Colpitts Oscillator 33

2.24 Protoboard Hagen Oscillator Simulation: *startup* Applied, 428 $\mu s < t < 472\ \mu s$. 34

2.25 Protoboard Hagen Oscillator Output Voltage Waveform 34

2.26 Modified Protoboard Hagen Colpitts Oscillator Circuit Diagram 35

2.27 Modified Protoboard Hagen Colpitts Oscillator 36

2.28 Modified Protoboard Hagen Oscillator Simulation: *startup* Applied, 452 $\mu s < t < 476\ \mu s$ 37

2.29 Modified Protoboard Hagen Oscillator Output Voltage Waveform 37

2.30 Breadboard Hagen Colpitts Oscillator Circuit Diagram 38

2.31 Breadboard Hagen Colpitts Oscillator 39

2.32 Breadboard Hagen Oscillator Simulation: *startup* Applied, 380 $\mu s < t < 390\ \mu s$ 40

2.33 Breadboard Hagen Oscillator Output Voltage Waveform 40

2.34 Clarke-Hess Common-Base Oscillator, Alternate Topology 42

2.35 Clarke-Hess Oscillator with Incorporated Input Resistors 43

2.36 Final Clarke-Hess Oscillator 43

2.37 Clarke-Hess Colpitts Oscillator Example 45

2.38 Clarke-Hess Simulation: *startup* Applied, 900 $\mu s < t < 905\ \mu s$ 46

2.39 Constructed Clarke-Hess Oscillator 47

2.40 Modified Clarke-Hess Oscillator Simulation: *startup* Applied, 270 $\mu s < t < 275\ \mu s$ 47

2.41 Breadboard Modified Clarke-Hess Oscillator Output Voltage Waveform 48

2.42 $G_m(x)/g_{mQ}$ with x Extracted 49

2.43 Smith Colpitts Oscillator Example 50

2.44 Smith Simulation: *startup* Applied, $0 < t < 1\ ms$ 51

2.45 Smith Simulation: $0 < t < 1\ ms$ 52

2.46 Smith Simulation: $0 < t < 1\ ms$ 52

2.47 Constructed Smith Oscillator 53

2.48 Smith Simulation: $0 < t < 1\ ms$ 54

2.49 Breadboard Modified Smith Oscillator Output Voltage Waveform 54

2.50 Smith Oscillator Small-Signal Equivalent 55

2.51 Loaded and Unloaded Output Voltages 59

2.52 163 kHz Oscillator on Spectrum Analyzer 60

3.1 Small Inductance Measurement Method 62

3.2 Colpitts Oscillator for Extracting Output Voltage Data 63

3.3 First Data Set - V_o vs L, Constant C_1, Slope ($n = 0.31$): $0.68\ V/\mu H$ 65

3.4 Second Data Set - f_0 vs L, Constant f_0 66

3.5 Second Data Set - V_o vs L, Constant f_0, Slope ($n = 0.3$): $1.64\ V/\mu H$ 67

3.6 Experiment 3 Circuit 68

3.7 Experiment 3, Data Set 1 69

3.8 Unsaturated Region of Experiment 3, Data Set 1 70

3.9 Experiment 3, Data Set 2 71

3.10 Experiment 3, Data Set 3 71

3.11 Experiment 3, Data Set 4 72

3.12 Experiment 3, Data Set 1 73

3.13 Experiment 3, Data Set 2 73

3.14 Experiment 3, Data Set 3 74

3.15 Experiment 3, Data Set 4 74

3.16 Experiment 3, Data Set 1 75

3.17 Experiment 4 - V_o vs C 77

3.18 Experiment 5 - V_o vs n 78

3.19 V_o Experiment 6 - $V_o(pp) = f(V_{CC}, V_{EE})$ 79

3.20 Oscillator without Positive DC Voltage Supply 80

3.21 Single-Supply Oscillator: Saturated and Unsaturated Output Voltages 81

3.22 Corrected Output Voltage 81

3.23 Oscillator with Large Inductor, Small Capacitors 82

3.24 Output Waveform for Large Inductance Oscillator 83

3.25 Oscillator with Added Resistance r' 84

3.26 Output Voltages of Original and Augmented Circuits 85

3.27 R_o vs L, Constant C_1, Slope ($n = 0.31$): 0.25 $k\Omega/\mu H$ 86

3.28 R_o vs L, Constant f_0, Slope ($n = 0.3$): 0.43 $k\Omega/\mu H$ 87

3.29 Oscillator with Added Resistance r' 89

3.30 Baseline Oscillator Waveform 92

3.31 Baseline Oscillator Harmonics 93

3.32 Large-Inductor Oscillator - Unsaturated Waveform 94

3.33 Large-Inductor Oscillator Harmonics - Unsaturated 94

3.34 Large-Inductor Oscillator - Saturated Waveform 95

3.35 Large-Inductor Oscillator Harmonics - Saturated 96

3.36 Oscillator with No Added Resistance - Waveform 97

3.37 Oscillator with No Added Resistance - Harmonics 98

3.38 Oscillator with Added Resistance - Waveform 99

3.39 Oscillator with Added Resistance - Harmonics 99

4.1 Resonant Frequency vs Inductance Curve, $C = 4.7\ nF$ 106

4.2 First Example Oscillator Circuit 107

4.3 First Example Oscillator Waveforms 108

4.4 First Example Oscillator Simulation: No Initial Conditions 108

4.5 Second Example Oscillator Waveform - Dual Supply 110

4.6 Second Example Oscillator Circuit 111

4.7 Second Example Oscillator Waveform - Single Supply 111

4.8 Second Example Oscillator Simulation: *uic* Applied 112

4.9 Second Example Oscillator Simulation: No Initial Conditions 112

A.1 Common-Base Amplifier Small-Signal Equivalent Circuit Including r_o and R_S . 119

A.2 CB Amplifier Equivalent Circuit for Calculating Z_o 120

B.1 Generalized Positive Feedback Transistor Oscillator 122

B.2 Complete Generalized KCL Matrix 123

B.3 Reduced KCL Matrix 123

B.4 Common-Base Colpitts Oscillator - Alternative View 126

C.1 Inductor Admittance Transformation 127

D.1 Common-Base Amplifier with Simplified Biasing 129

E.1 $J_n(x)$ 133

E.2 $I_n(x)$ 134

E.3 $J_0(x)$ 135

E.4 $J_n(x)$, $n > 0$, even 136

E.5 $J_n(x)$, $n > 1$, odd 136

CHAPTER 1

INTRODUCTION

Oscillators are ubiquitous in electronics. While exotic components are necessary for very high frequency oscillation, discrete transistor oscillators can produce signals over a significant portion of the RF spectrum. Many oscillators output a sinusoidal, or harmonic, signal which finds several applications in wireless communication. Harmonic oscillators may be used in conjunction with a mixer to shift the frequency of a signal in a wireless receiver or transmitter. With a slight alteration to the circuit described in this work, the voltage-controlled oscillator may be used as a component of a phase-locked loop for detection and modulation. Other electronic oscillator circuits provide periodic signals of different waveforms, such as a sawtooth or square wave.

1.1 Electronic Oscillators

"An electronic oscillator is a circuit with a periodic output signal but with no periodic input signal [18, p. 241]." Because the primary function of the oscillator is to output a signal with a predictable rate of repetition, oscillators require a frequency selection mechanism. Frequency selection is provided by an LC-tank circuit in all the oscillators in this thesis, but electronic oscillators can use a variety of methods such as phase shifting or a resonant cavity to perform this function.

All frequency selectors or resonators suffer loss due to resistance and must be resupplied with energy to maintain oscillation. This is accomplished through a positive-feedback amplifier for the oscillators investigated in the following chapters. Oscillation could also be maintained directly using negative resistance, for example, with a Gunn diode [10].

1.1.1 Colpitts Oscillator Family

The Colpitts oscillator consists of an amplifier and a feedback network. The feedback network consists of an inductor and two capacitors with a portion of the output

signal being directed back to the input through one of the reactive elements. This network provides the two functions of frequency selection and signal reinforcement (positive feedback). As will be seen in the following chapter, there must be no net phase shift (or an integer multiple of 2π radians of phase shift) for a signal going around the feedback loop to achieve oscillation. Figure 1.1 is a simplified diagram of the Colpitts oscillator.

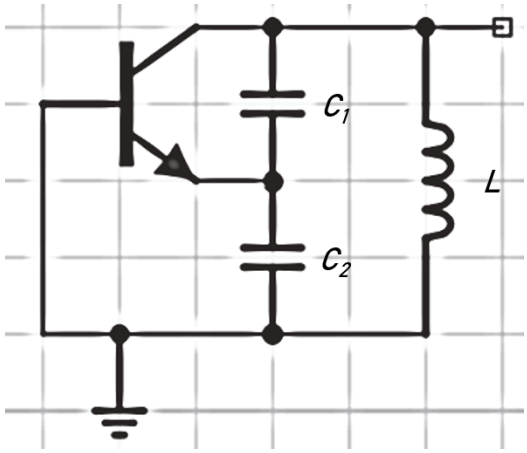

Figure 1.1: Simplified BJT Colpitts Oscillator

The satisfaction of the requirements for oscillation are demonstrated in the following chapter for the bipolar junction transistor Colpitts oscillator in the common-base configuration. They can similarly be met by a number of oscillators which have slight modifications from the circuit under investigation. The active component could be a field-effect transistor or an op-amp. For a BJT oscillator, the base need not be the common node. If the amplifier inverts its output signal relative to its input signal as in the case of the common-emitter or common-source amplifiers, the feedback network must also be inverting to provide no net phase shift around the loop. This can be accomplished with a rearrangement of the elements of the LC feedback network as shown in figure 1.2.

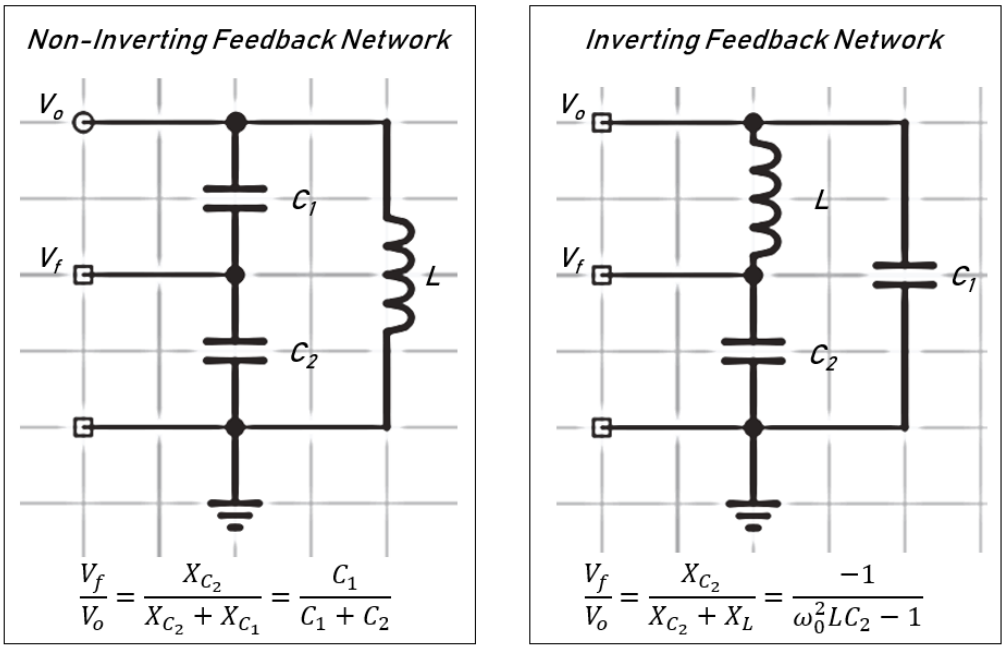

Figure 1.2: Feedback Gains in LC Oscillators

A Colpitts-type oscillator with an inverted feedback signal is often called a Pierce oscillator. An oscillator using a resonator with two inductors and one capacitor is termed a Hartley oscillator, and a Colpitts oscillator with an extra capacitor in series with the inductor is called a Clapp oscillator. Finally, a crystal component can be used in place of the inductor in a Colpitts oscillator to improve frequency stability [14]. Simplified diagrams of some of the oscillators in the Colpitts family are displayed in figure 1.3.

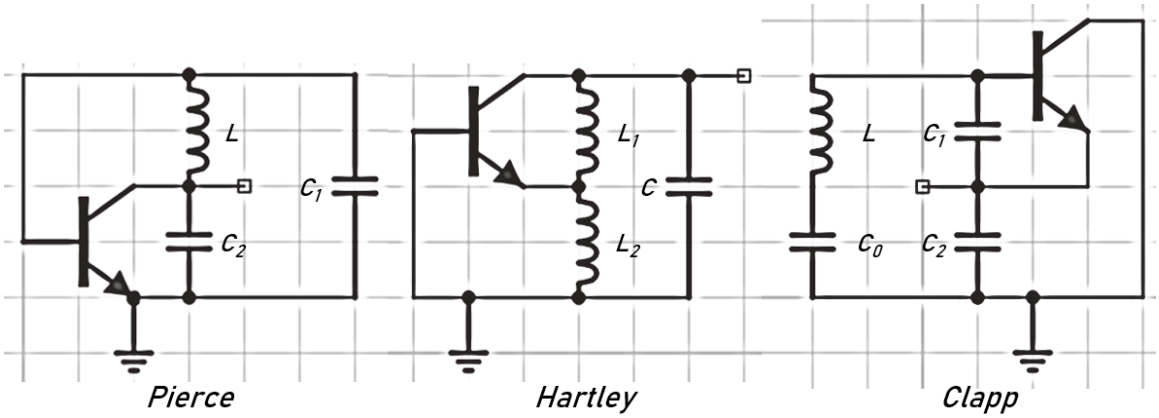

Figure 1.3: BJT Oscillators in the Colpitts Family

1.1.2 Colpitts Oscillator

The circuit treated in this thesis is the BJT Colpitts oscillator. Because most of the investigation was experimental and not simulated, practicality took priority in component selection and circuit design. The Colpitts oscillator, unlike the Hartley, requires more capacitors than inductors and the former are generally much more abundant. Because the focus of this thesis is on the relationships of the components of the circuit to the output characteristics, the BJT was chosen as the active component instead of a field-effect transistor. Virtually any desired oscillator that can be built with one component can also be built with the other, but calculating biasing and gains for large numbers of oscillators is simpler when dealing with linear and not quadratic relationships. Various test oscillators were constructed using op-amps as well, but their slew rates confine them to the hundreds of kilohertz – below the general range of interest of this thesis.

The frequencies for most of the oscillators investigated are in the low megahertz range, and this was again selected for practicality. At lower frequencies, coupling and bypass capacitors become large and tuning becomes cumbersome. Above approximately 10 megahertz, junction capacitances and parasitics become very relevant and disruptive to resonant frequency prediction.

The AC ground point for all circuits in this work is the base but as seen in the previous section, common-emitter or common-collector configurations are also possible. In the textbooks referenced, the term "Colpitts oscillator" often implies the common-base configuration and the analysis focuses on it. Further, the analysis for the common-base configuration is often simpler than for other configurations as evidenced by the feedback gain calculations displayed in figure 1.2.

1.2 Previous Work

A search of the term "Colpitts" on the IEEE digital library returns hundreds of articles on the subject. Many of the articles discuss novel application methods for Colpitts oscillators in the gigahertz frequency range and many others investigate chaotic oscillators whose output voltage amplitudes never repeat. Some of the articles do discuss fundamental Colpitts oscillator construction – specifically biasing and component selection (see [12] and [15]). Three articles were found that relate specifically to this work. Their results as they pertain to this thesis are summarized here.

1.2.1 Exact Calculation of Oscillation Amplitude and Predicting Power Consumption for CMOS Colpitts Oscillators [7]

The circuit considered by the author Qiuting Huang was the common-drain CMOS Colpitts oscillator. This oscillator differs from the one in this thesis by a substitution of the active device and by a rearrangement of the feedback network. The small-signal equivalent circuit is virtually the same. Huang begins the analysis by introducing negative resistance – a concept that was mentioned above for the Gunn diode oscillator. While covered only briefly in appendix B, the Colpitts oscillator is in fact a negative-resistance oscillator. Oscillation is only possible if the resistance in the circuit is overcome by the negative resistance of the combination of the active device and the reactive components.

From this expression for negative resistance, Huang terms "critical transconductance" the minimum transconductance g_m required to balance the resistance

of the circuit with negative resistance and achieve oscillation. He then derives an expression for the current through the transistor at the resonant frequency and solves the output voltage amplitude as a function of the same. Through more manipulation, Huang finally arrives at an expression for the output voltage amplitude as a function of the component and bias values of the circuit:

$$V_m \approx \frac{I_o(5+x)}{12R_s}\frac{L}{C}, \qquad C = \frac{C_1}{2} = \frac{C_2}{2}, \qquad x = \frac{V_T - V_B}{V_m} \tag{1.1}$$

where I_o is the average current through the transistor, R_S is the combination of all of the resistance causing loss in the resonator, V_m is the output voltage amplitude, V_T is the thermal voltage, and V_B is the gate-source bias voltage.

While this analysis pertains to the CMOS transistor, the relationships of the quiescent current, inductance and capacitance to the output voltage of equation 1.1 will all be shown to be consistent with the experiments conducted in chapter 3.

1.2.2 Frequency and Power Scaling in mm-Wave Colpitts Oscillators [8]

The circuit discussed in this article is very extreme compared to those covered in the following chapters. The active device used by the author Alireza Imani is the 130-nm silicon-germanium heterojunction bipolar transistor in a CMOS environment. This transistor is intended for millimeter and sub-millimeter signals and the frequencies cited for analysis in this article are 106 and 148 GHz. Finally, the circuit diagram includes only L and C_2 as the other capacitance is provided by the C_π and C_μ effective capacitances seen in the complete hybrid-π small-signal equivalent circuit model. [1]

While the circuit and its applications are beyond the scope of this thesis, Imani does provide a derivation and expression for the amplitude of oscillation:

$$a_{pp,S} \approx \frac{4I_{BIAS}L_S}{K_S(R_{B,S}+R_{L,S})C_{2,S}(1+\beta_S)} \tag{1.2}$$

where a_{pp} is the amplitude of oscillation; I_{bias} is the average emitter current; L is the inductance; C_2 is the discrete capacitor; K is a function of intrinsic and external

[1] The simplified hybrid-π model is discussed in section 2.1.1.

capacitances; R_B and R_L are the base and inductance resistances; and β is a ratio of capacitances. The subscript S indicates that all values are scaled by a set of constants. The current, inductance and capacitance are in the same positions as those in equation 1.1 from the Huang article [7]. While the derivation and many of the other variables of equation 1.2 are not directly applicable to work at much lower frequencies, at least two sources agree on some of the factors contributing to the output voltage amplitude.

1.2.3 Everything You Always Wanted to Know About Colpitts Oscillators [17]

Many of the mathematical methods investigated in this thesis are seen in this comprehensive article by Ulrich L. Rohde and Anisha M. Apte. The concept of negative resistance is explained using the common-collector oscillator variant. Large-signal current and voltage analysis similar to the Clarke-Hess [3] method seen in section 2.2.1 is elucidated. The article does not provide an equation for output voltage amplitude as a function of circuit parameters but instead provides the value as a function of power and load resistance.

Output voltage amplitude is a byproduct of power for the authors of this article. A desired resonant frequency and output power are first selected and the component values are determined one at a time to arrive at an oscillator that meets the specifications with the lowest possible phase noise. The example circuit that they developed features a resonant frequency of 350 MHz. The capacitors required to achieve this frequency were in the single-digit picofarads and the inductor value was 21 nanohenries - all well below the component values available in the laboratory while working on this thesis. While the specific oscillator tested was not directly applicable to this work, their methods are the same as those of the textbook authors.

1.3 Thesis Objective

The purpose of this thesis is to develop a method to control the output voltage amplitude, output resistance, and waveform purity of the Colpitts oscillator in its discrete form. Given enough resistors, inductors, and capacitors, it does not take long to produce

an oscillating signal. Given more time, one can achieve oscillation at the desired frequency. From the perspective of an oscillator as a single stage or component in a complicated system, producing a signal at the required frequency is not sufficient.

Depending on the components used, the output impedance of the oscillation could be on the order of megohms. Again, circuit dependent, the output voltage amplitude could be twice or more the supply voltage – a problem for the follow-on buffer that will certainly be required if the output impedance is very high. A further issue is the distortion of the waveform and its accompanying increase in the power of frequency harmonics, depending on the selection of the reactive components.

There are an infinite number of combinations that will produce a specified resonant frequency using two capacitors and one inductor. Many of those combinations will not produce a functional Colpitts oscillator. Using the methods in this thesis, suitable components can be determined.

A search of the literature provides indications of the solution to this problem though applied to circuits with very different components and operating conditions. While a comprehensive equation predicting each of the output characteristics is beyond the scope of this work, methods to correct undesirable attributes or to achieve oscillation in a nonfunctioning circuit are developed. These methods are tested in the example circuits of Chapter 4.

1.4 Thesis Outline

The purpose of chapter 2 (Theory) is to develop the analysis methods and establish the terminology for the common-base Colpitts oscillator. In the first part of the chapter, the common-base amplifier is introduced and analyzed. The concept of positive feedback is discussed and finally the oscillator is examined. The second part of the chapter investigates the methods used by difference sources to determine the output characteristics of voltage amplitude, impedance, and phase noise.

In chapter 3 (Experimental Data and Results), experiments are conducted to ascertain the relationships of the components of the Colpitts oscillator to its output

characteristics. Chapter 4 (Discussion) summarizes the observations and emphasizes remarkable discoveries. Chapter 5 (Conclusions) discusses the comprehensive experience of this work and ideas for future work.

CHAPTER 2

THEORY

The first purpose of this chapter is to introduce the concept of the oscillator – its basis as an amplifier and the requirements to achieve oscillation. The second purpose is to investigate the current methods available for oscillator analysis and behavior prediction. Finally, this chapter seeks to demonstrate that more analysis is required to account for the output characteristics of physically-constructed oscillators.

2.1 BJT Colpitts Oscillator

There are many methods for constructing an oscillator and not all oscillators produce sinusoidal, or harmonic, output signals. Those that do find very important applications as carrier frequency producers in every radio transmitter and receiver. The harmonic oscillator circuit presented in this thesis is the BJT common-base Colpitts oscillator.

The Colpitts oscillator requires an amplifier. The amplifier in this circuit is provided by a bipolar junction transistor. BJTs are easily obtained and their characteristics are well known. Counterpart oscillators can certainly be constructed using field-effect transistors but their variety makes the BJT a simpler choice to form a basis for analysis. The selected active component could also be an operational amplifier, but common op-amps cannot produce harmonic output into the megahertz frequency range.

Colpitts oscillators can be grounded at any node, but the relatively simple gain calculations and the preponderance of literature favor the common-base version. Selecting the Colpitts over the Hartley oscillator is a matter of practicality – the Colpitts uses two capacitors and one inductor versus only one capacitor and two inductors for the Hartley, and capacitors are more readily available than inductors. Finally, higher-frequency harmonic oscillators can be constructed using special diodes and resonator cavities, but their construction and analysis are more complicated. All of these factors contribute to the selection of the oscillator circuit design used in this study.

2.1.1 Common-Base Amplifier

The common-base amplifier is one of three basic configurations for a single-transistor amplifier. It is a voltage amplifier and current buffer. From the perspective of passing along a voltage signal from one stage to the next, it is not the obvious choice. Compared to the common-collector and common-emitter amplifiers, the input impedance of the common-base amplifier is low but its output impedance is high. A follow-on voltage buffer will generally be necessary to provide enough current to drive a low-impedance load.

This little-used amplifier is the opposite of the common-collector amplifier in many of its impedance and gain characteristics but it has important applications. While its input impedance, on the order of tens of ohms in many cases, is too low to pass along a voltage signal, it can easily be transformed a bit higher to match an impedance for maximum power transfer (e.g. a 50 Ω antenna [6, p. 73]). This amplifier configuration also exhibits the capacity for tremendous voltage gain (easily 22 dB), with the added benefit that the amplified output signal is in phase with the input signal.

Common-Base Amplifier Circuit

The common-emitter amplifier is perhaps the most readily useable configuration because of its single-stage power gain. The common-base amplifier, because of its niche uses and because it is the basis for the common-base oscillator, bears some investigation.

Figure 2.1 is a common-base amplifier using voltage-divider biasing, coupled to an AC source and a resistive load. A more complete diagram would include the source impedance, but this complicates the analysis and is not a factor in the oscillator circuit modification. Compared to the common-emitter amplifier, this configuration takes input at the emitter and outputs through the collector. The base is grounded in the AC circuit with the bypass capacitor but uses R_1, R_2, and R_E to maintain the base at a higher DC voltage than the emitter.

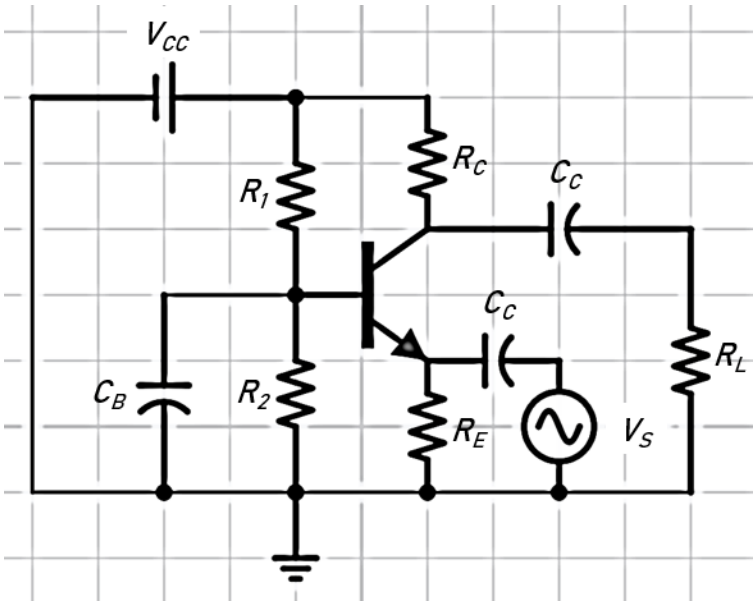

Figure 2.1: Common-Base Amplifier with Voltage-Divider Biasing

Figure 2.2 is the same amplifier but uses two DC supplies to bias the transistor. This method is less practical from a device standpoint but makes biasing much simpler in the lab. Whichever biasing method is used, the AC-equivalent circuit is the same.

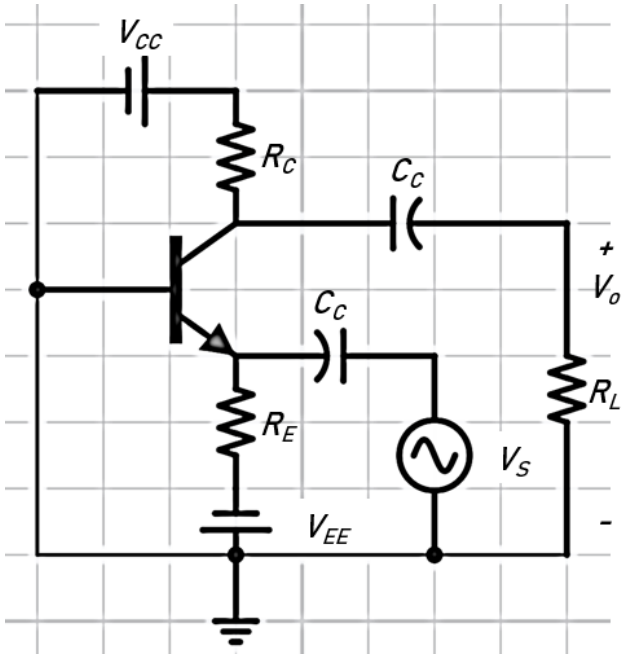

Figure 2.2: Common-Base Amplifier with Dual-Supply Biasing

To determine the parameters of input and output impedance and current and voltage gain, the transistor symbol in a circuit diagram must be replaced by an equivalent circuit model before analyzing. There are three linear circuit models commonly taught in transistor textbooks [2, ch. 7], [13, ch. 6]: the hybrid model, the hybrid-π model, and the r_e model. The hybrid model, with its ubiquitous h_{fe} factor, appears on most transistor datasheets. The r_e model is very simple, which is an advantage and a disadvantage. The hybrid-π model in its fullness is very robust but can be simplified to two components if rigor is not necessary. Because of this versatility, the same model can be used to describe the simple mid-frequency amplifier and the more parasitic-susceptible microwave amplifier. The hybrid-π model will be used throughout this thesis. Figure 2.3 is the simplified hybrid-π circuit with the base, emitter and collector terminals labeled.

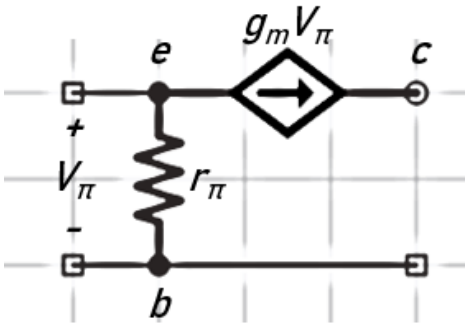

Figure 2.3: Simplified Hybrid-π Model in Common-Base Configuration

The reciprocal of the resistor $r_\pi = V_T / I_{BQ}$ is the slope of the i_b vs v_{be} curve at the quiescent point. Similarly, the small-signal transconductance g_m is the slope of the i_c vs v_{be} curve at the quiescent point, or $g_m = I_{CQ}/V_T$ [13, p. 379]. The common-emitter current gain is $\beta = i_c/i_b = g_m r_\pi$.

Common-Base Amplifier Analysis

To analyze the AC-equivalent circuit, the DC voltage sources, bypass capacitors, and coupling capacitors are shorted and the transistor is replaced by its equivalent small-signal model. The components are then rearranged for simplification. Figure 2.4 is the small-signal equivalent circuit for the common-base amplifier of figure 2.2.

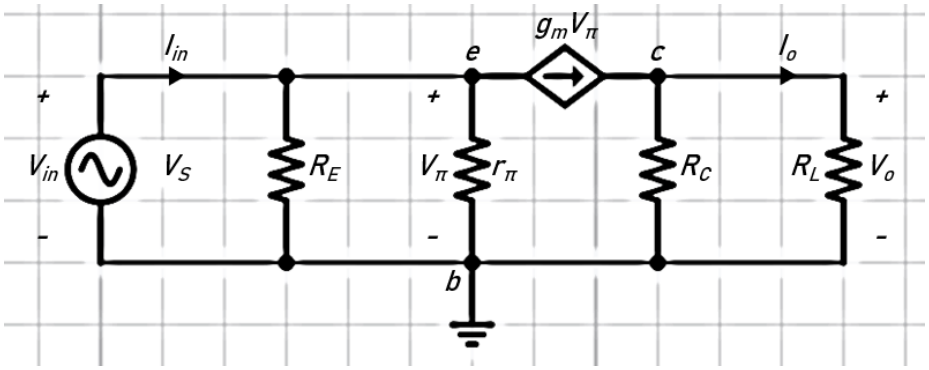

Figure 2.4: Simplified Common-Base Amplifier Small-Signal Equivalent Circuit

To calculate voltage and current gain, the input and output voltages and currents are first determined:

- The input voltage is the source voltage, V_S, which is also the base-emitter voltage V_π.
- The output current is the portion of the dependent source current through the load resistance: $I_o = g_m V_\pi \frac{R_C}{R_C + R_L}$
- The output voltage is the dependent source current multiplied by the output resistance: $V_o = g_m V_\pi R_o$, where $R_o = R_C || R_L$.
- The input current is the dependent source current plus the current through the input-side resistors: $I_{in} = g_m V_\pi + \frac{V_\pi}{R_{in}}$, where $R_{in} = R_E || r_\pi$.

The voltage and current gains are calculated as follows:

$$A_V = \frac{V_o}{V_{in}} = g_m R_o \tag{2.1}$$

$$A_I = \frac{I_o}{I_{in}} = g_m \Big(\frac{R_C}{R_C + R_L} \Big) \Big(\frac{r_\pi}{\beta + 1} || R_E \Big) \tag{2.2}$$

The input impedance is calculated as follows:

$$Z_{in} = \frac{V_{in}}{I_{in}} = \frac{1}{\frac{1}{r_\pi} + g_m} = \frac{r_\pi}{\beta + 1} \tag{2.3}$$

The intrinsic output resistance r_o of the npn transistor in the common-base configuration could be on the order of megohms. Connected in parallel with the effective input resistance $r_\pi / (\beta + 1)$, its effect is negligible. This resistance dominates the output resistance of the amplifier however and is included in its calculation. The circuit with the resistance r_o included is shown in figure 2.5.

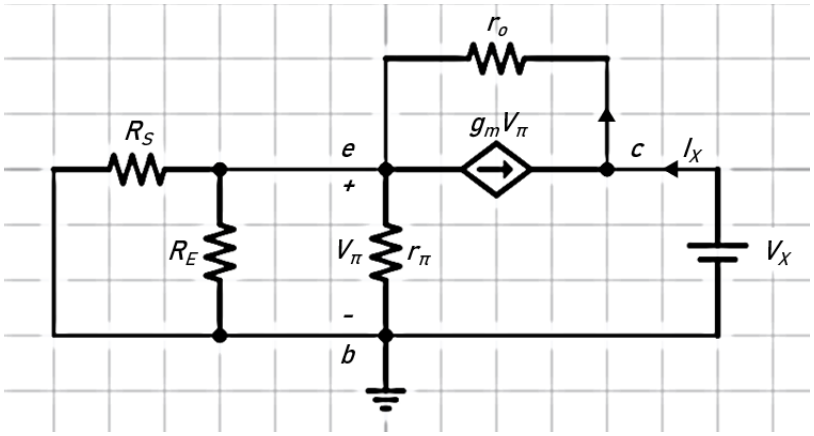

Figure 2.5: More Robust Representation of the Common-Base Amplifier

For the algebraic procedure, see appendix A. The result is as follows:

$$Z_o = \frac{V_X}{I_X} = r_o(1 + g_m R_{eq}) + R_{eq}, \qquad R_{eq} = R_S||R_E||r_\pi. \tag{2.4}$$

2.1.2 Criteria for Oscillation

The fundamental concept of operation for the Colpitts oscillator is positive feedback. While positive feedback in amplifiers is usually an undesireable side effect of frequency response, it is required in this type of oscillator. Because there is no input signal, the oscillator must be self-starting and self-sustaining. This is possible only by achieving a zero in the denominator of the oscillator's transfer function to offset the factor of 0 contributed by the input voltage.

Feedback

Figure 2.6 is a simple block diagram of a generic feedback amplifier.

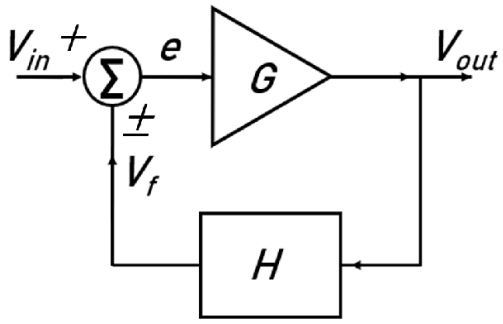

Figure 2.6: Generic Feedback Amplifier Block Diagram

Conceptually, feedback provides the system information about the output and allows the system to correct to the desired output. In the ubiquitous case of negative feedback, the output signal is sent through a feedback network and then subtracted from (added out of phase to) the input signal.

Negative feedback provides several advantages: increased bandwidth; increased signal-to-noise ratio; higher input impedance; and lower output impedance, etc [2, p. 751]. The primary cost is a decrease in gain. Referring to figure 2.6 and assuming that the error signal $e = V_{in} - V_f$ where V_f is the feedback signal,

$$V_{out} = G \times e \qquad V_f = HV_{out},$$

so

$$\frac{V_{out}}{V_{in}} = \frac{G}{1 + HG} \tag{2.5}$$

where V_{out}/V_{in} is the closed-loop gain, G is the gain of the amplifier, H is the gain of the feedback network, and HG is termed the loop gain. The gain of the system including negative feedback is reduced by the factor $1 + HG$.

Nyquist and Barkhausen Criteria

If the amplifier and feedback gains are functions of frequency, the loop gain could conceivably exhibit a phase shift such that the feedback signal adds to the input signal constructively. This resulting positive feedback causes instability and oscillation. The

Nyquist criterion for stability instructs that a negative-feedback amplifier is stable at all frequencies provided that at no frequency is the loop gain less than or equal to –1 [2, p. 766].

If instead the feedback signal is intentionally added in phase to the input signal, the system becomes a positive-feedback amplifier and its gain, or transfer function, is

$$\frac{V_{out}}{V_{in}} = \frac{G}{1 - HG}. \tag{2.6}$$

Equation 2.6 exhibits a simple pole at $HG = 1$. The Barkhausen criteria for oscillation states that oscillation is possible provided that the loop gain attains a value of unity with no net phase shift around the closed loop. Equation 2.6 rearranged yields

$$V_{out} = \frac{GV_{in}}{1 - HG} \tag{2.7}$$

and with equation 2.7, the oscillator form becomes clear. As the oscillator generates its own signal, V_{in} equals zero. Because thermal noise exists in any electrical system, a properly-designed high-Q reactive feedback circuit selects the resonant frequency signal from this thermal noise and amplifies it repeatedly until it self-limits (as in the case of the Colpitts oscillator).

2.1.3 Common-Base Oscillator

Figure 2.7 is an example of a complete dual-supply common-base Colpitts oscillator.

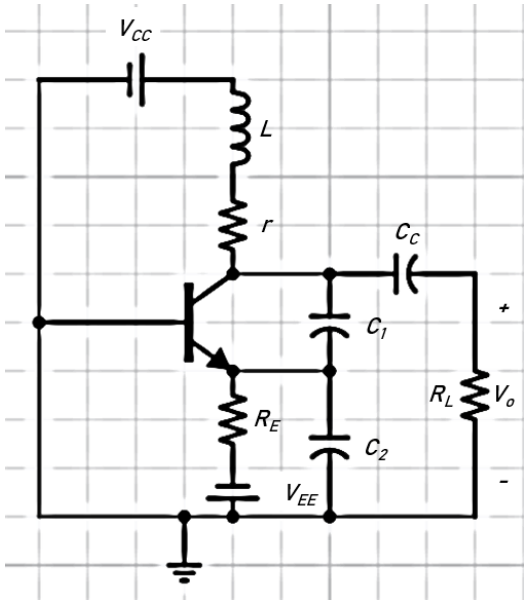

Figure 2.7: Dual-Supply Common-Base Colpitts Oscillator

This circuit resembles the amplifier from figure 2.2 with only a few important differences. First, in place of the collector resistor there is an inductor. In series with the inductor is its equivalent series resistance *r* which can have a large effect on oscillator performance. Second, there is no source, as the tank circuit formed from the components C_1, C_2, and *L* effectively acts as the source. Finally, there is a feedback path from collector to emitter through C_1.

The ideal LC tank circuit with its perpetual sinusoidal current does not appear distinctly in figure 2.7 or in its small-signal equivalent in figure 2.8. Note that the reactive components remain in the small-signal circuit while the coupling capacitor is replaced with a short circuit because its impedance at the resonant frequency is insignificant.

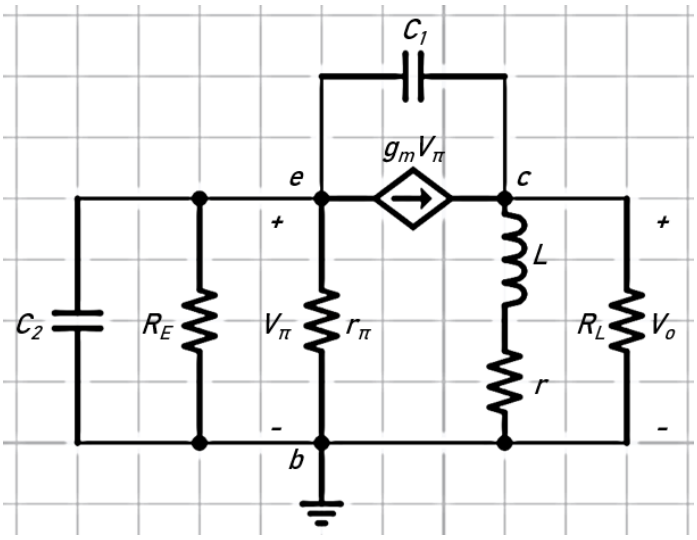

Figure 2.8: Small-Signal Equivalent Common-Base Colpitts Oscillator

Rearranging the terminals of figure 2.8 vertically results in the circuit of figure 2.9 in which the tank circuit appears, albeit with the small equivalent series resistance *r*.

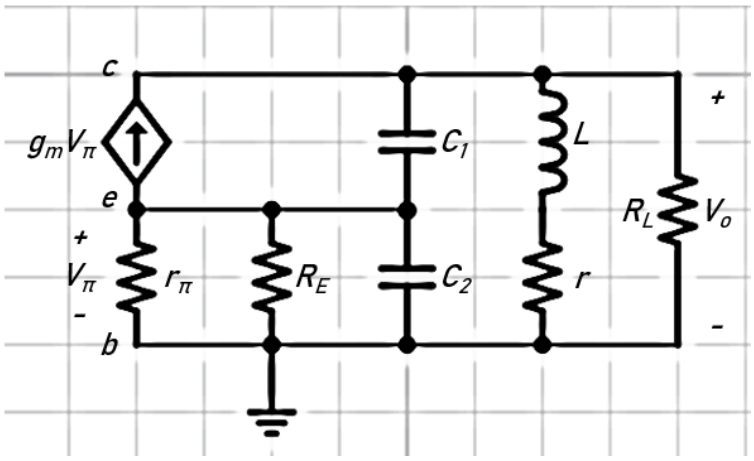

Figure 2.9: Rearranged Small-Signal Equivalent Common-Base Colpitts Oscillator

The appearance of the LC resonator indicates that oscillation may be possible, but several requirements must first be met.

Satisfaction of Oscillation Criteria

As shown in section 2.1.2, the oscillator's transfer function must have a zero in the denominator. The magnitude of the loop gain must be at least unity and there must be no phase shift at the resonant frequency. The phase shift of the transfer function is readily calculated using either figure 2.7 or 2.9.

The common-base amplifier takes input at the emitter, outputs to the collector, and the signal is not inverted. This means that the feedback network must output a non-inverted signal. The capacitor C_1 is the feedback path. Its input voltage is V_o and its output voltage is V_π. C_1 and C_2 form a voltage divider between the collector and emitter such that

$$A_{V_f} = \frac{V_\pi}{V_o} = \frac{X_{C_2}}{X_{C_1} + X_{C_2}} = \frac{C_1}{C_1 + C_2} = n, \tag{2.8}$$

where n is termed the capacitive ratio. Neither the feedback network nor the amplifier gain exhibit a shift in phase, so the first criterion is met.

Equation 2.8 also provides a piece of the second requirement for oscillation – that the loop gain have a magnitude of one. As in section 2.1.2, the loop gain is the product of the amplifier and feedback network gains. Equation 2.8 is the feedback network gain. From equation 2.1, the amplifier gain is $g_m R_o$, where R_o is the combined resistance between the collector and the base. Often, loop gain is initially greater than one but settles to unity as oscillation builds.

Figure 2.9 does not present an immediately clear output impedance, so rearrangement and combination is necessary. The obstacle to a clear output impedance is the feedback path through C_1. An equivalent output signal could be generated by breaking the feedback path and applying a sinusoidal signal at that point [18, p. 245], given that the applied signal encounters the same impedance as the original circuit [19, p. 460]. The applied signal is V_π and the impedance it must see is the input impedance of the common-base amplifier. From equation 2.3, the input resistance is $\frac{r_\pi}{\beta+1}$, relabeled as r_i. With the feedback loop broken, the resulting circuit is shown in figure 2.10.

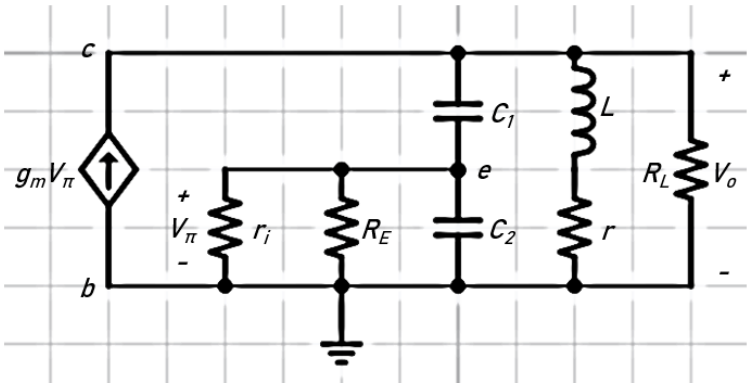

Figure 2.10: Small-Signal Equivalent Oscillator with Feedback Loop Opened

Figure 2.10 could be analyzed in terms of an output current and a load but a simplification can make the messy analysis clearer. A parallel LC circuit has infinite impedance at the resonant frequency but the two resistors shunting C_2 in figure 2.10 must first be repositioned. By solving for the combined admittance of C_1, C_2, r_i, and R_E in terms of a conductance and a susceptance, the two resistors are moved to the output and the capacitors are, within an approximation, left alone [18, p. 127].

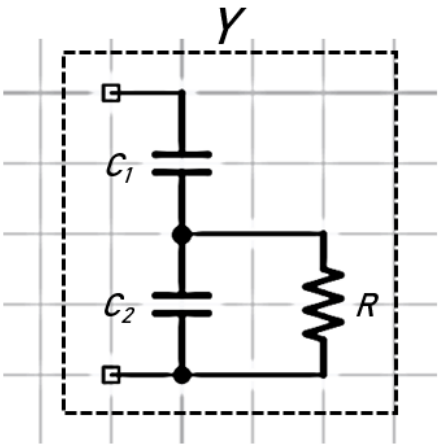

Figure 2.11: Admittance to be Transformed

Figure 2.11 is the admittance to be transformed. The resistor R is the parallel combination of r_i and R_E. The impedance of the combination is

$$Z = \frac{1}{j\omega C_1} + \frac{R}{1 + jR\omega C_2}$$

and the admittance is

$$Y = \frac{R\omega^2 C_1^2}{1 + R^2\omega^2(C_1 + C_2)^2} + \frac{j\omega C_1(1 + R^2\omega^2 C_2(C_1 + C_2))}{1 + R^2\omega^2(C_1 + C_2)^2}.$$

The admittance leads to a parallel resistance

$$R_{eq} = \frac{1 + R^2\omega^2(C_1 + C_2)^2}{\omega^2 R C_1^2} \tag{2.9}$$

which can be approximated as

$$R_{eq} \approx R\left(\frac{C_1 + C_2}{C_1}\right)^2 = \frac{R}{n^2}$$

if the second term in the numerator of equation 2.9 is much larger than one. The admittance also contains a parallel capacitance

$$C_{eq} = \frac{C_1 + R^2\omega^2 C_1 C_2(C_1 + C_2)}{1 + R^2\omega^2(C_1 + C_2)^2} \tag{2.10}$$

which can be approximated as

$$C_{eq} \approx \frac{R^2\omega^2 C_1 C_2(C_1 + C_2)}{R^2\omega^2(C_1 + C_2)^2} = \frac{C_1 C_2}{C_1 + C_2} = C_1 || C_2$$

using the same criterion as for the equivalent resistance. The final approximate transformation is shown in figure 2.12.

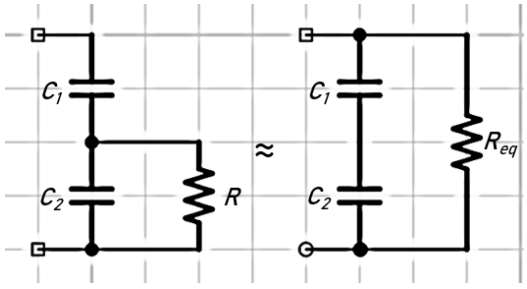

Figure 2.12: Approximate Transformed Admittance, Valid if $R^2\omega^2(C_1 + C_2)^2 \gg 1$

The resulting oscillator is shown in figure 2.13.

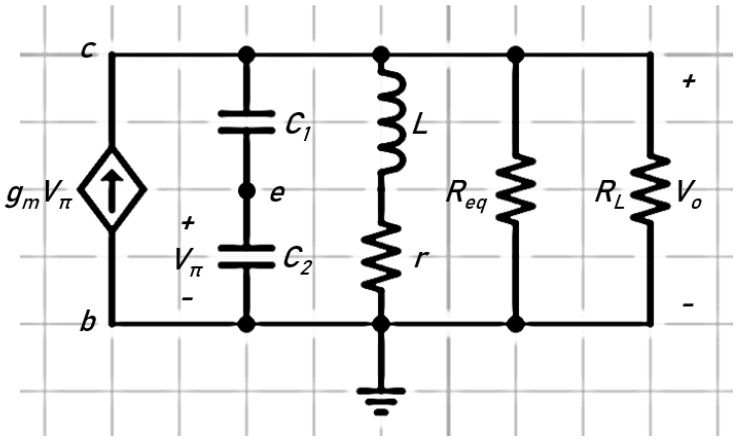

Figure 2.13: Oscillator with Transformed Admittance

The same admittance transformation should be performed for the small resistance r in the inductor when calculating the output impedance for follow-on stages. Ignoring r until section 2.2.2 and appendix C, figure 2.13 exhibits a tank circuit of infinite impedance at resonance and a combined resistance of $R_{eq}||R_L$. As in equation 2.1, the voltage gain of the amplifier at resonance is simply:

$$A_{V_{amp}} = g_m(R_{eq}||R_L) = g_m R_o \tag{2.11}$$

where R_o is the combined output impedance of the oscillator and the load. The oscillation requirement that the loop gain must have unity magnitude requires that the oscillator satisfy:

$$A_{V_{loop}} = g_m(R_{eq}||R_L)\frac{C_1}{C_1 + C_2} = n g_m R_o = 1. \tag{2.12}$$

Other Results

Methods for predicting the frequency of oscillation and the maximum allowable equivalent series resistance in the inductor can be found in appendix B. The results are:

$$\omega^2 = \frac{1}{L}\left(\frac{1}{C_1} + \frac{1}{C_2} + \frac{r}{r_\pi C_2}\right) \tag{2.13}$$

and

$$rr_\pi = \frac{\beta+1}{\omega^2 C_1 C_2} - \frac{L}{C_2} \quad \Rightarrow \quad r_{max} = \frac{\beta+1}{\omega^2 C_1 C_2 r_\pi} - \frac{L}{C_2 r_\pi}. \tag{2.14}$$

All inductors contain equivalent series resistance. Equation 2.14 quantifies the maximum equivalent series resistance allowable such that oscillation can still occur. The equation predicts the possibility of adding resistance to the inductor which would have the effect of lowering the output resistance. An experiment testing this phenomenon is conducted in section 3.2.4.

2.2 Output Characteristics

Because the oscillator must function as a component of a system, its output characteristics must be known. Of course the most important characteristic for an oscillator is the resonant frequency. Absent any resistance, the resonant frequency of a tank circuit is $f_0 = \frac{1}{2\pi\sqrt{LC}}$. This is generally a close approximation for Colpitts oscillators with resonant frequencies in the single-digit megahertz, and it is improved by the inclusion of resistance as in equation 2.13 and equation B.6.

Transistors under operation develop small capacitances at their junctions. This effect is significant when these capacitances are of the same order of magnitude as the reactive components used for oscillation. With a small C_1, it is even possible to produce a clean sinusoidal output waveform with no C_2 capacitor. Predicting resonant frequency accurately and precisely is a matter of including all circuit factors and characterizing the active component to account for parasitics.

The other output characteristics are also important. While the only input to the oscillator is the DC supply voltage, the output voltage amplitude can range from a fraction of a volt to more than twice the value of the positive supply. For a multi-stage device with a single DC supply, a very high oscillator output voltage may not work well with a follow-on amplifier stage. While automatic gain control circuits can resize the oscillator output voltage amplitude, they cannot correct saturated waveforms. The extra

active devices also add unnecessary noise to the system, especially if the oscillator's output voltage can be controlled.

The output impedance has been shown to be resistive in the previous section. While that simplifies the problem, the magnitude of the output resistance is still an important factor. Most of the oscillators in the Results chapter have output resistances in the range of hundreds of ohms to tens of kilohms. These values can be more easily matched to a system with an emitter follower circuit than can a large-inductor oscillator whose output resistance is on the order of megohms.

Finally, improperly designed oscillators yield distorted waveforms. From clipping and sawtooth waveforms to near-sinusoids with abrupt linear segments, these distortions increase the power of harmonics visible in the frequency-domain representation of the output voltage signal.

The references treat these characteristics to varying extents. The following sections are an investigation of some of the reference analysis methods along with investigations of their example circuits.

2.2.1 Output Voltage Amplitude

Only two of the textbook references (Hagen [5] and Clarke-Hess [3]) make a prediction of the output voltage amplitude for the BJT Colpitts oscillator.[1] In the first case, Hagen provides a circuit and states that its peak output amplitude will equal the supply voltage. While the experimental circuit required alteration to achieve oscillation, the predicted waveform could be obtained through simulation given certain conditions. The coincidence of the equality of the two voltages is shown through simulation to be specific to the values of the components of the circuit and not generally true.

The method of Clarke and Hess is much more complicated. The premise of these authors is that small-signal analysis is not appropriate for oscillators or indeed most transistor amplifiers. Through analysis of the Shockley diode equation, they develop a

[1] The Huang [7] and Imani [8] articles make predictions for the output voltage amplitude but for significantly different circuits.

characteristic curve of the emitter current given a sinusoidal input signal. From this solution for the emitter current, they develop an expression for the large-signal transconductance.

Set equal to this expression is the analysis of the specific oscillator configuration, reconfigured in terms of transconductance. The method consists of determining the value of transconductance that places the poles of the oscillator exactly on the imaginary axis, yielding unity loop gain and steady oscillation. The example circuit is constructed as specified but requires alteration to achieve experimentally measurable oscillation.

Hagen Output Voltage Method

Analysis The Hagen example [5, p. 130] is a common-base Colpitts oscillator using voltage-divider biasing with a single DC source. The inductor is assumed to have no equivalent series resistance. The load is coupled with a capacitor and both the base and the supply are tied to AC ground with bypass capacitors. Figure 2.14 is the circuit diagram including component values. The transistor specified is the 2N3904.

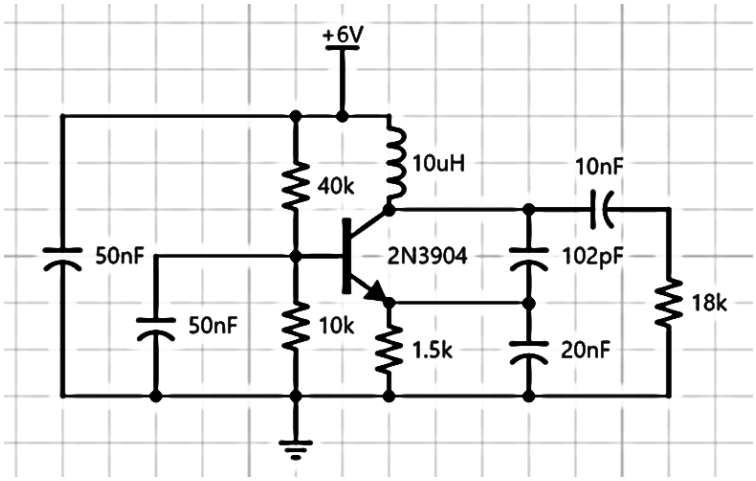

Figure 2.14: Hagen Colpitts Oscillator Example

Assuming a standard base-emitter voltage drop of 0.7 V, the biasing scheme provides an emitter current of 0.33 mA. Treating the coupling and bypass capacitors as

AC short circuits, the frequency of oscillation from equation B.5 with $r = 0$ is approximately 5 MHz. The textbook predicts a peak output voltage amplitude of 6 V – the value of the DC supply.

Simulation The circuit from figure 2.14 was simulated in LTspice [4].The schematic is shown in figure 2.15. With no startup conditions specified, the simulated output waveform from $t = 0$ to $t = 5\ \mu s$ is shown in figure 2.16.

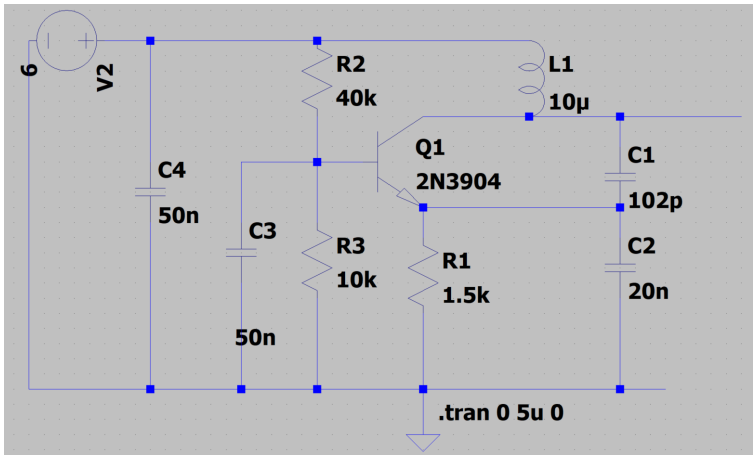

Figure 2.15: Hagen Oscillator Circuit in LTSpice

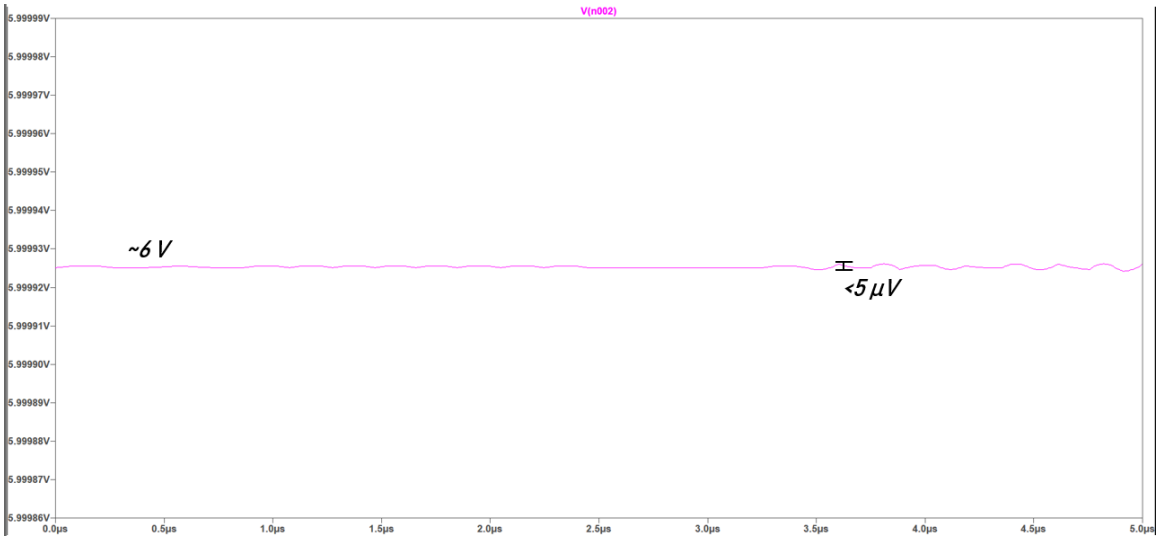

Figure 2.16: Hagen Simulation: No Initial Conditions, $0 < t < 5\ \mu s$

The simulated waveform of figure 2.16 shows some oscillatory behavior at the end of the time sample. Allowing approximately 2,500 cycles, figure 2.17 displays a 5 μs sample of the output voltage waveform after a warmup period of 495 μs.

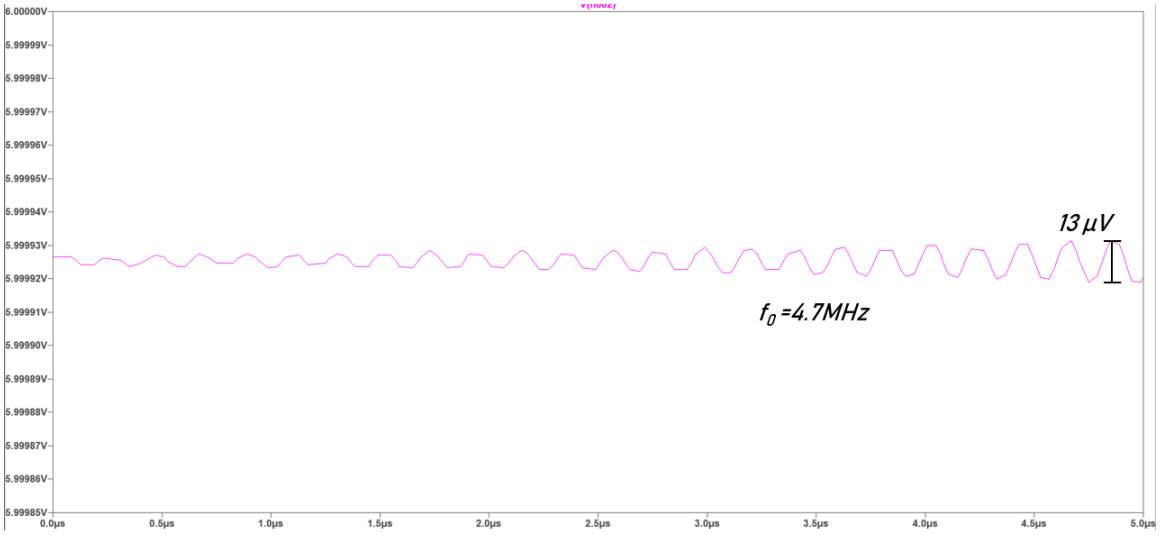

Figure 2.17: Hagen Simulation: No Initial Conditions, $495\ \mu s < t < 500\ \mu s$

Figure 2.17 displays oscillation at the correct frequency but of amplitude on the order of microvolts. Increasing the warmup time still further results in no discernable oscillation, as seen in figure 2.18.

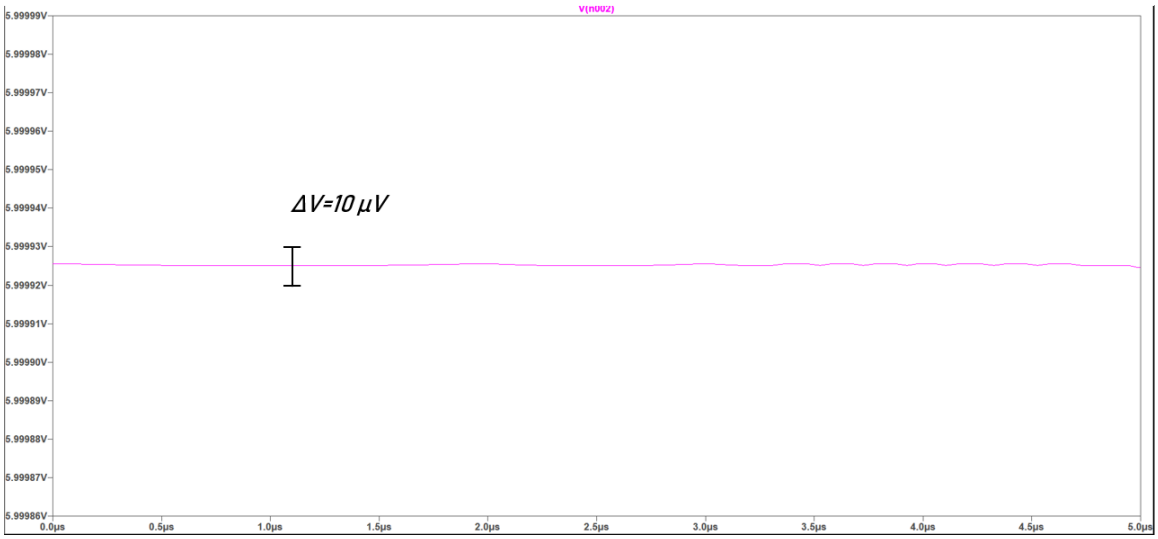

Figure 2.18: Hagen Simulation: No Initial Conditions, 1495 $\mu s < t < 1500\ \mu s$

LTspice includes the initial condition modifiers *uic* and *startup*. The former stands for *use initial conditions* and it involves skipping the DC operating point analysis and applying nonphysical conditions to the circuit. The latter modifier ramps the independent sources during the first 20 μs of the simulation [4]. Because real transistor oscillators rely on noise present in the circuit to begin oscillation and this noise is not present in simulation, these modifiers assist with oscillation stimulation.

Applying the *startup* modifier results in the waveform of figure 2.19.

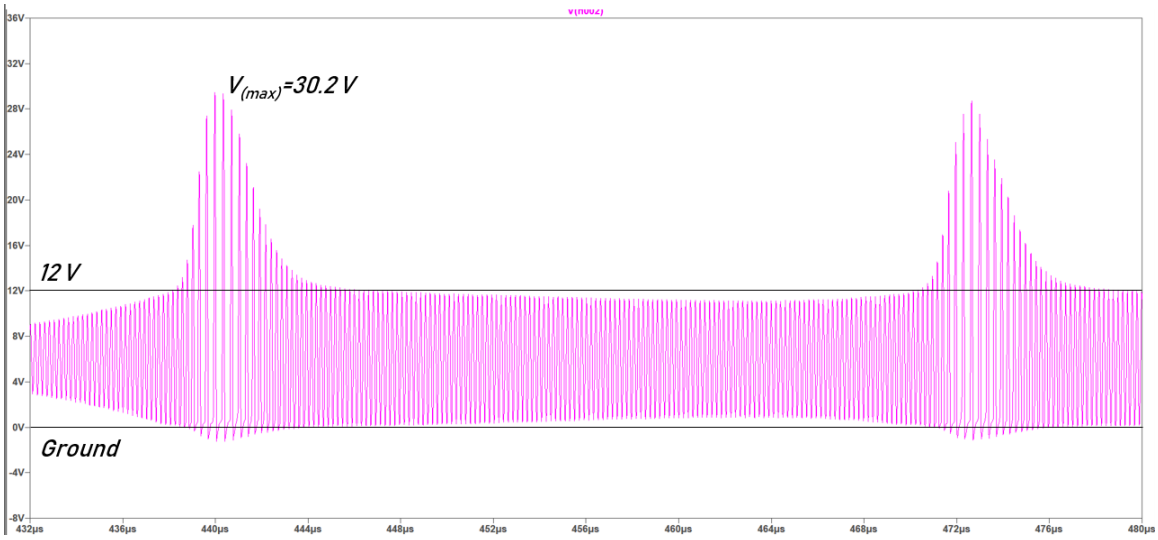

Figure 2.19: Hagen Simulation: *startup* Applied, 432 $\mu s < t <$ 480 μs

The simulated waveform of figure 2.19 alternates every 35 μs between periods of generally stable 12-Vpp oscillation and 30-V saturated output voltage. The frequency is 4.8 MHz.

If the modifier *uic* is applied, the waveform in figure 2.20 is generated.

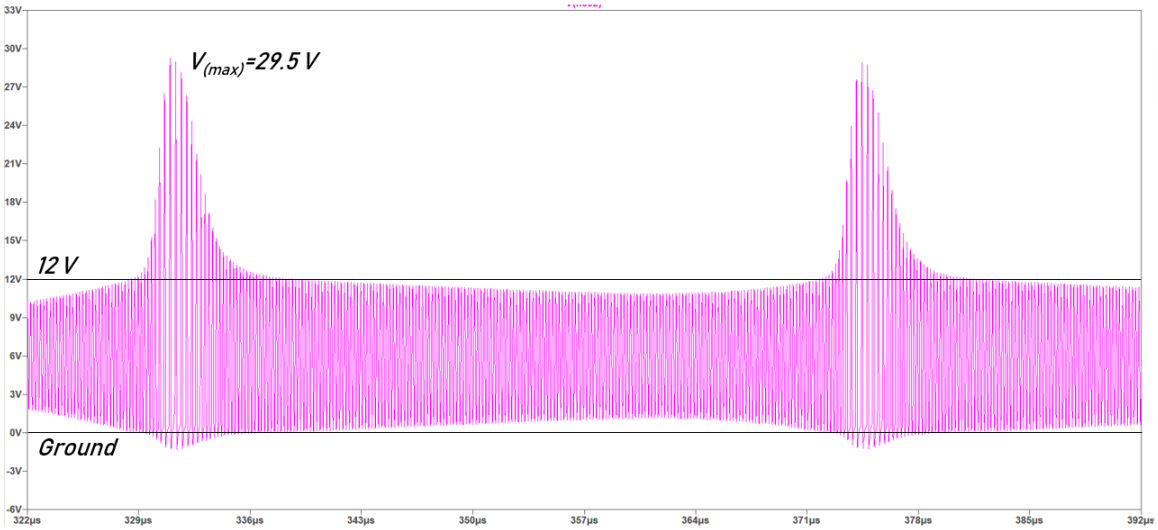

Figure 2.20: Hagen Simulation: *uic* Applied, 322 $\mu s < t <$ 392 μs

The waveform of figure 2.20 is very similar to that of figure 2.19 – alternating between 12-V sinusoidal behavior and almost 30-V saturated output voltage.

The supply voltage and the peak output voltage (when not saturated) are both 6 V. To show that the coincidence of these values is not true generally, the supply is increased to 7 V with all other components kept constant. Figure 2.21 is the output voltage waveform under these conditions.

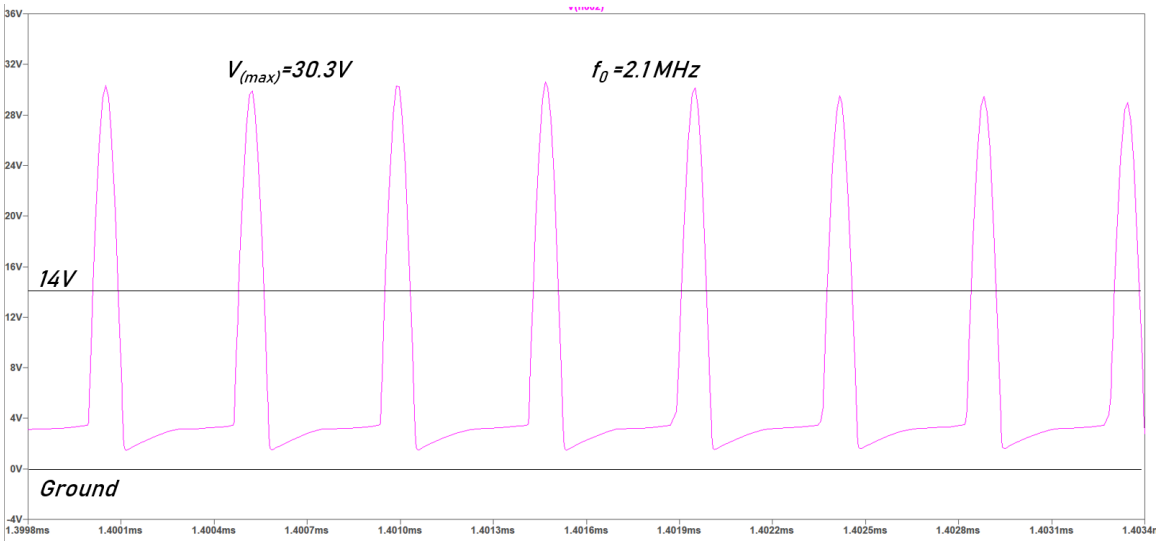

Figure 2.21: Hagen Simulation: $V_{CC} = 7\ V$, *uic* Applied, 1.400 $ms < t <$ 1.404 ms

While the waveform in figure 2.21 does not drop precisely to ground, the maximum output is significantly higher than twice V_{CC}. The waveform is very distorted and the frequency is less than half the desired value.

Protoboard Hagen Circuit Figure 2.22 is the circuit diagram of the Hagen oscillator using the closest practically-achievable component values and figure 2.23 is the oscillator constructed on protoboard. All component values are measured.

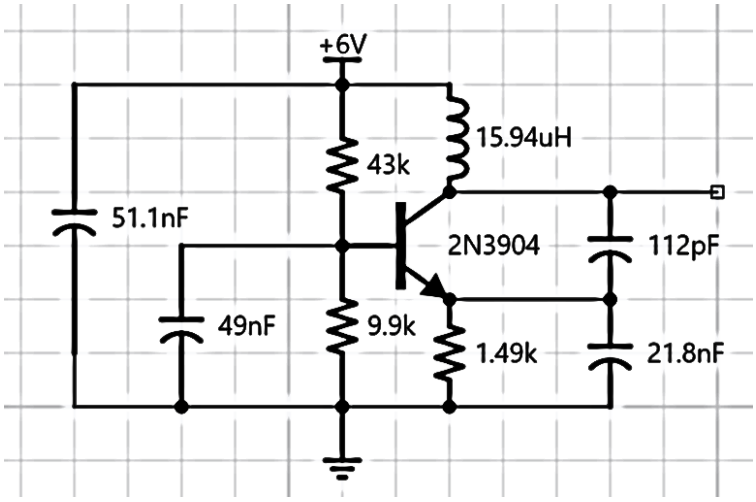

Figure 2.22: Protoboard Hagen Colpitts Oscillator Circuit Diagram

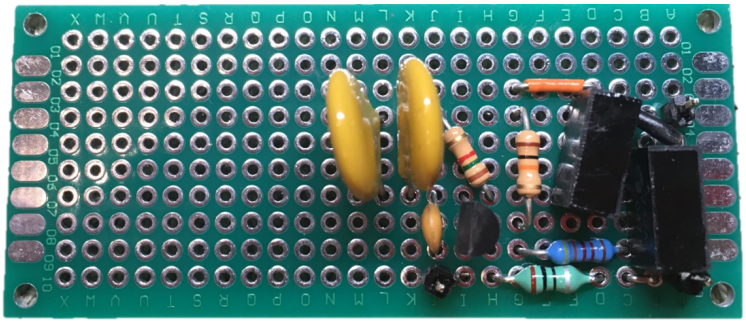

Figure 2.23: Protoboard Hagen Colpitts Oscillator

The simulated output waveform using the compoenent values of figure 2.22 and applying the *startup* modifier is displayed in figure 2.24. The waveform is very similar to the previous simulated waveforms. Figure 2.25 is the output waveform for the constructed circuit.

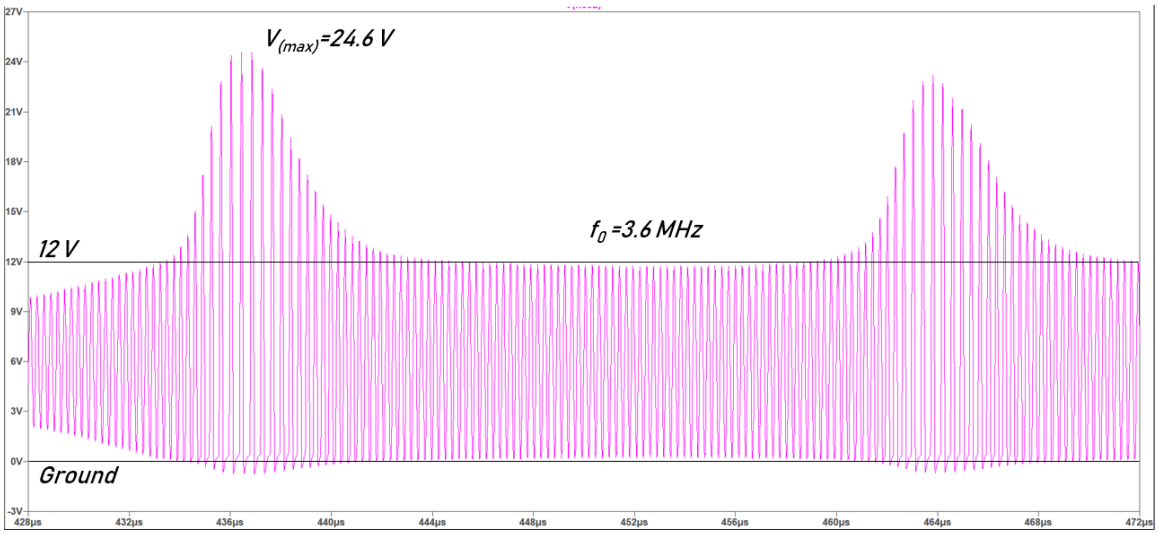

Figure 2.24: Protoboard Hagen Oscillator Simulation: *startup* Applied, 428 $\mu s < t <$ 472 μs

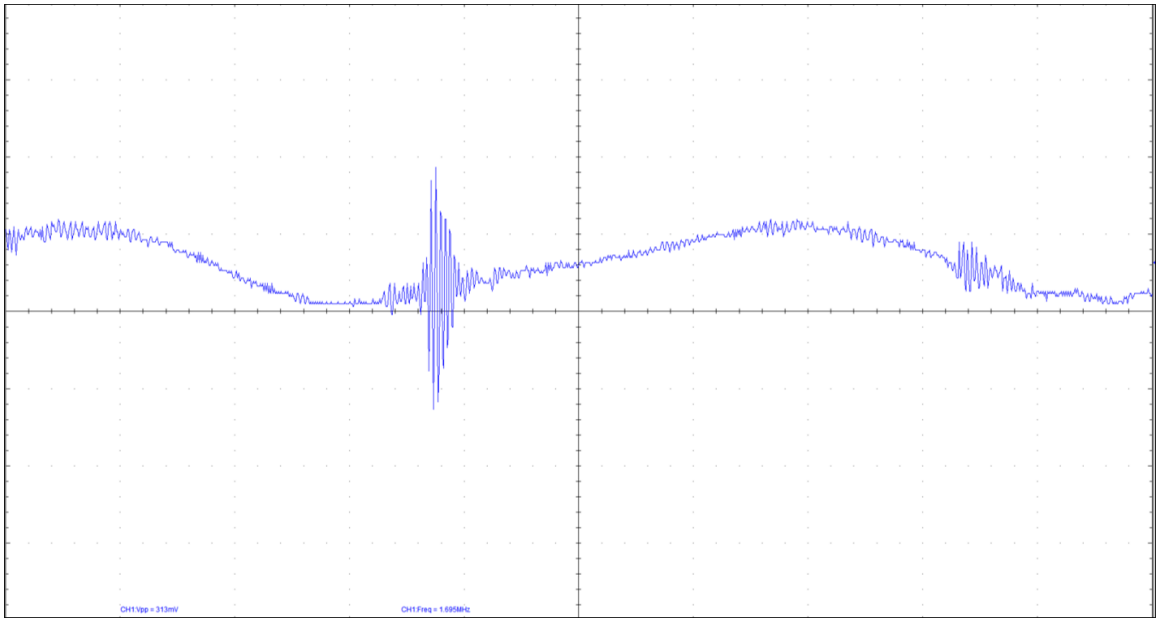

Figure 2.25: Protoboard Hagen Oscillator Output Voltage Waveform

Simulations predict very similar behavior to the specified circuit but in practice, no oscillation was achieved.

Modified Protoboard Hagen Circuit To enable the circuit to function in practice, it is modified in two ways. The capacitor shunting the input voltage in figures 2.14 and 2.22 removes AC components from the power supply but has the effect of decreasing the output voltage amplitude. It is removed. Next, the C_2 capacitor is approximately 200 times the C_1 capacitor. Because these two capacitors act as a voltage divider of ratio n, this very small ratio results in very little feedback voltage returning to the input. The C_2 capacitor is replaced with a smaller value. The circuit diagram for the modified Hagen oscillator with measured component values identified is displayed in figure 2.26 and the protoboard circuit is shown in figure 2.27.

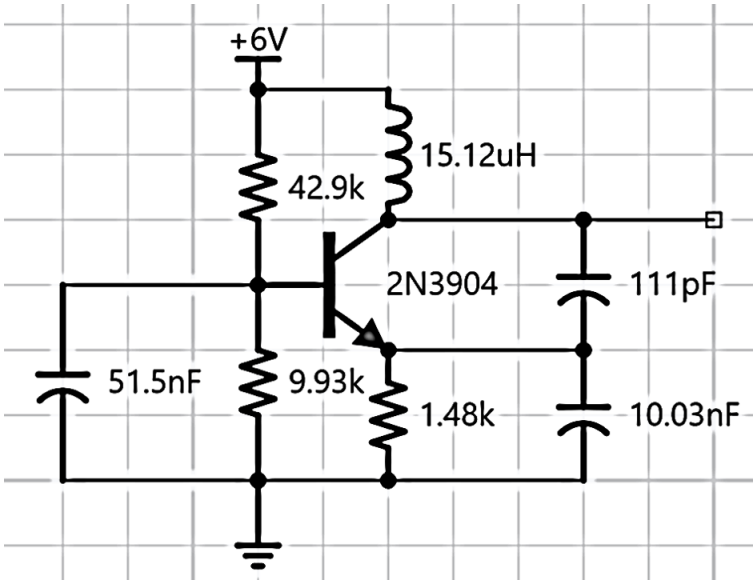

Figure 2.26: Modified Protoboard Hagen Colpitts Oscillator Circuit Diagram

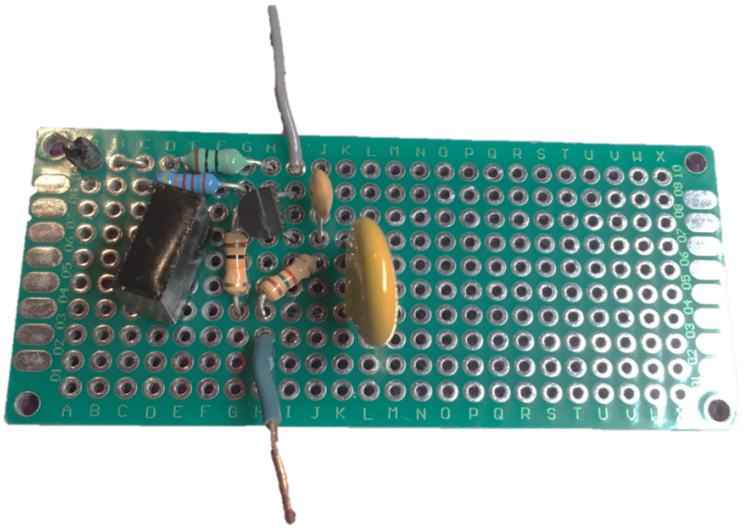

Figure 2.27: Modified Protoboard Hagen Colpitts Oscillator

The simulated output waveform using the component values of the circuit in figure 2.26 and applying the *startup* modifier is displayed in figure 2.28. The waveform does not exhibit the intermittent periods of saturation as did the previous simulations for the Hagen circuit. Instead the waveform is constantly saturated and the maximum voltage fluctuates between 15 V and 16 V. The frequency of this circuit is 3.4 MHz. This is lower than the specified 5-MHz frequency but is explained by the larger inductor. Figure 2.29 is the output waveform for the constructed circuit.

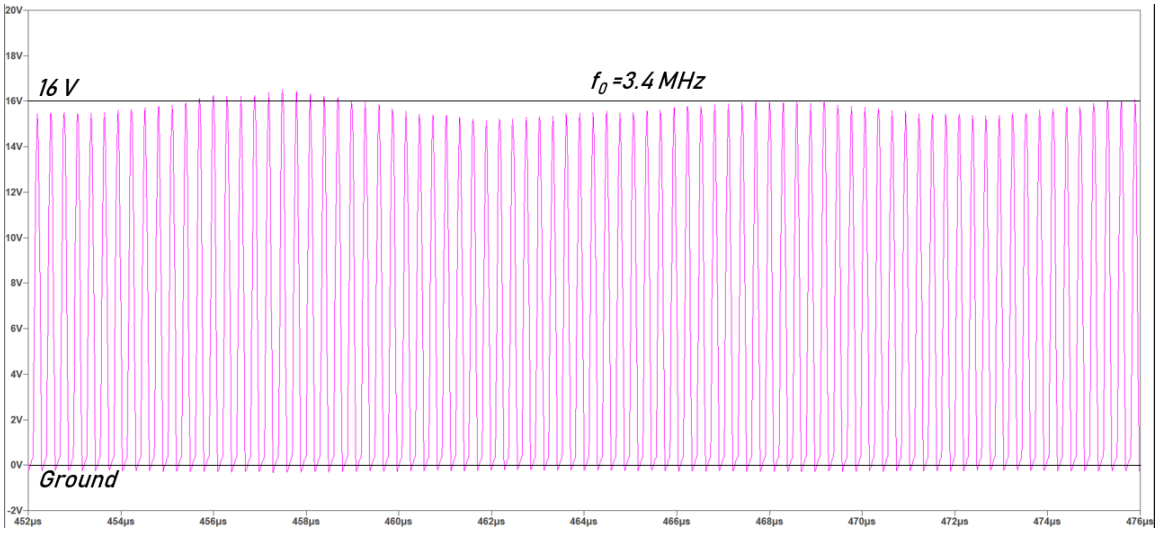

Figure 2.28: Modified Protoboard Hagen Oscillator Simulation: *startup* Applied, 452 μs < t < 476 μs

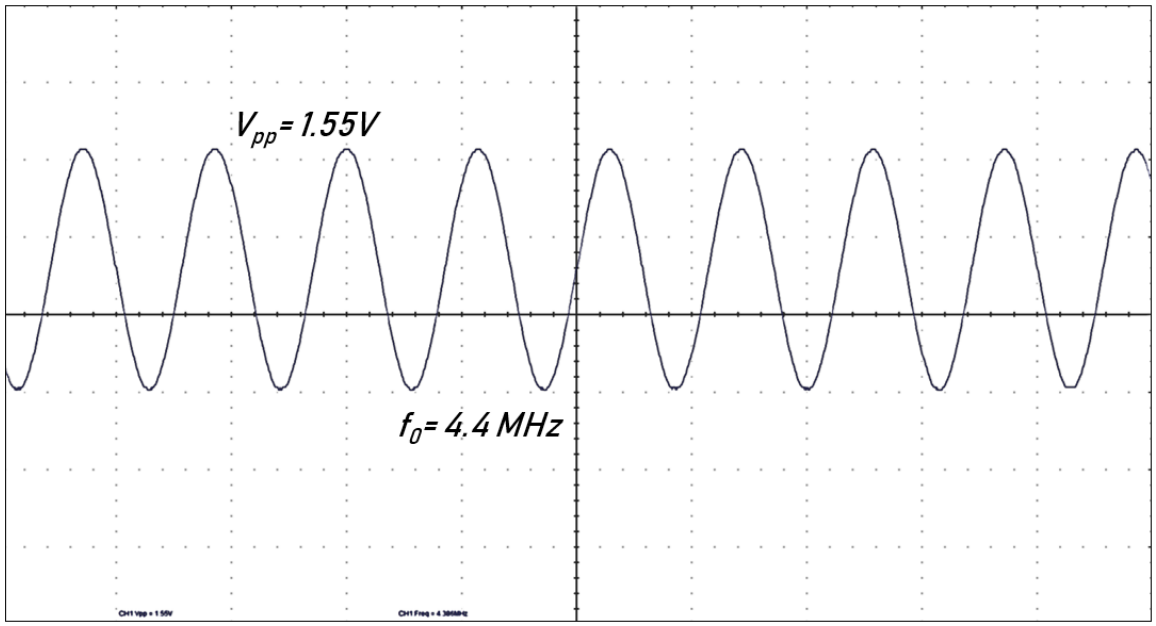

Figure 2.29: Modified Protoboard Hagen Oscillator Output Voltage Waveform

The protoboard circuit produces oscillation in practice but with an output voltage amplitude much smaller than the simulated value and at a significantly higher resonant

frequency.

Breadboard Hagen Circuit Soldering circuits onto protoboard is time consuming. To accelerate the process of testing oscillators, the modified Hagen oscillator is constructed on a breadboard. While breadboards contain parasitics due to the large amount of interconnection material, the detrimental effects can be mitigated by maintaining a low resonant frequency. The leads of the components are also kept short to prevent adding their parasitic effects.

Figure 2.30 is the circuit diagram for the breadboard Hagen oscillator with measured component values identified and figure 2.31 is the circuit as constucted. When constructed with a 10-nF C_2 capacitor as in the modified protoboard circuit, the circuit did not produce oscillation. The C_2 capacitor was replaced by a smaller value and oscillation was achieved.

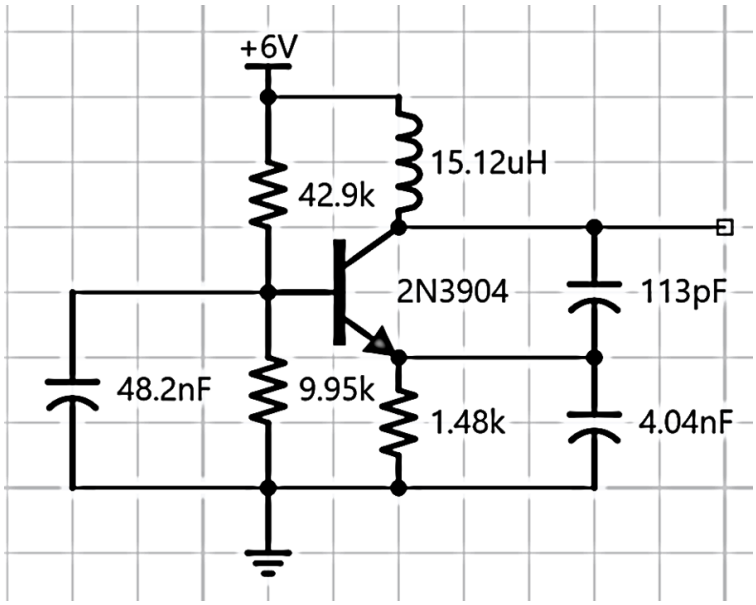

Figure 2.30: Breadboard Hagen Colpitts Oscillator Circuit Diagram

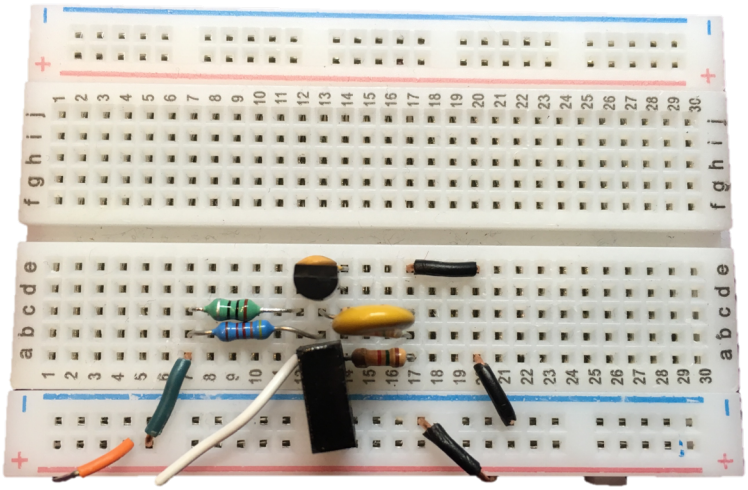

Figure 2.31: Breadboard Hagen Colpitts Oscillator

The simulated output waveform for this circuit using the *startup* modifier is displayed in figure 2.32. The change in the C_2 capacitor did not alter the waveform significantly from figure 2.28 – the waveform is still saturated and the maximum value is approximately 16 V, though there is less fluctuation in the circuit with the smaller C_2 capacitor.

Figure 2.33 is the output voltage for the breadboard-constructed circuit. The output voltage amplitude is much larger than that of figure 2.29, though the C_2 capacitor is significantly smaller.

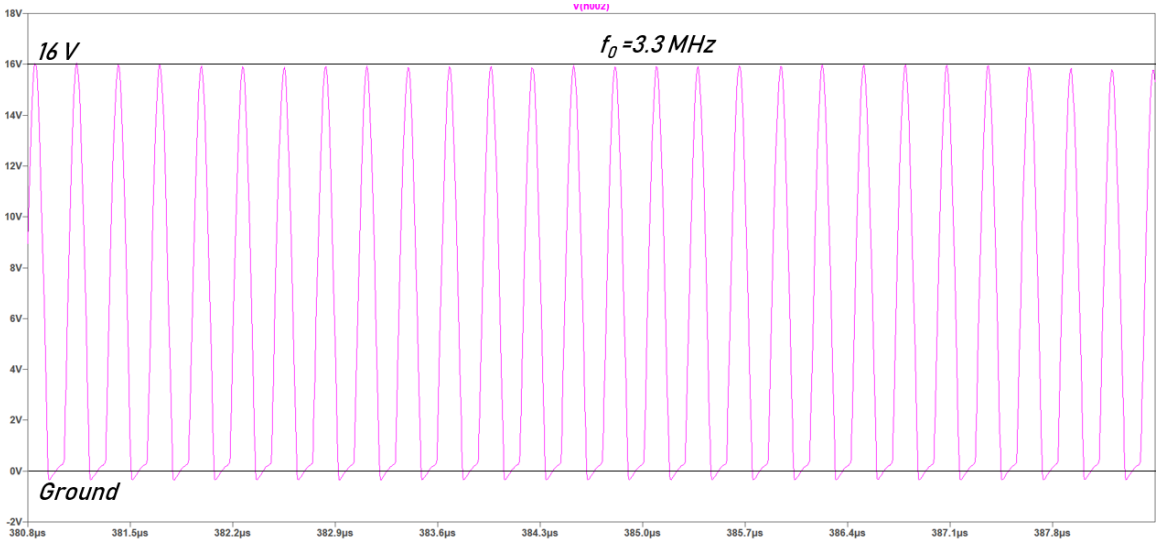

Figure 2.32: Breadboard Hagen Oscillator Simulation: *startup* Applied, 380 $\mu s < t < 390\ \mu s$

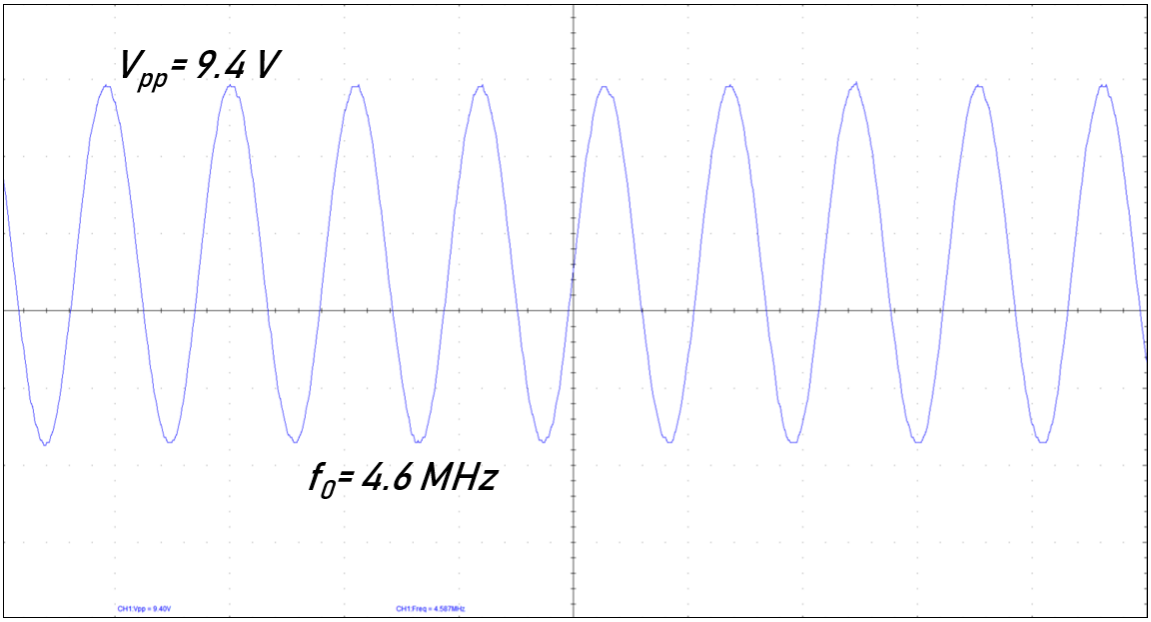

Figure 2.33: Breadboard Hagen Oscillator Output Voltage Waveform

Hagen Circuit Conclusion Experiment and simulation agree that the Hagen circuit topology produces oscillation. Simulation indicates that the output voltage should

usually oscillate between ground and 12 V, though there are regular periods of saturation as well. The coincidence of the supply and output voltages is specific to the circuit components and is not a general trend. The modified circuits exhibited larger inductors and their simulated output voltage amplitudes were also larger than that of the Hagen-specified circuit. This agrees with the equations of Imani [8] and Huang [7].

The data seem to show that experimental circuits require more feedback voltage (i.e. larger capacitive ratio n) to oscillate and that the output voltage for the experimental circuit will be smaller than that of the simulated circuit. The breadboard circuit required a larger n than the protoboard circuit. Whether breadboard parasitics are the cause or differences in transistor characteristics is undetermined.

Clarke-Hess Output Voltage Method

Analysis The Clarke-Hess [3] method of oscillator analysis makes use of three concepts unique among the oscillator references: large-signal vs. small-signal analysis; capacitive transformers; and the expression of oscillator currents and voltages as expansions of Bessel functions. Small-signal analysis assumes small perturbation around a DC operating point, but oscillators can output a voltage more than twice the value of the DC supply.

While approximated in small-signal analysis, the Shockley diode equation (D.1) indicates that the current through a diode is a function of the voltage across it. If that voltage is sinusoidal and sufficiently large, the current is proportional to $e^{x\cos(\omega t)}$, which can be expanded using Bessel functions. The introduction of the transformer to the analysis is an extension of the admittance transformation from section 2.1.3, though the ideal transformer circuit component was not used explicitly there.

The circuit used for demonstration by Clarke-Hess is that of figure 2.7, though that specific topology is not required for this analysis. The circuit may be redrawn as in figure 2.34.

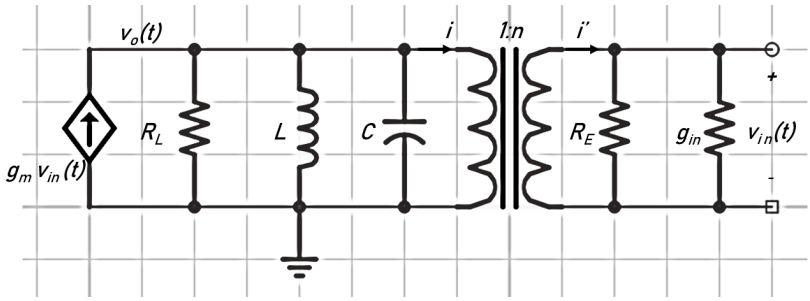

Figure 2.34: Clarke-Hess Common-Base Oscillator, Alternate Topology

Figure 2.34 makes use of the capacitive transformer, where the two oscillator capacitors form a voltage divider $n = \frac{C_1}{C_1+C_2}$ as in equation 2.8. The capacitor C from figure 2.34 is the series-combined capacitor $C = \frac{C_1 C_2}{C_1+C_2}$. As the input is at the emitter, the input conductance g_{in} is simply the Shockley diode equation applied to the emitter, so that $g_{in} = g_{mQ}/\alpha$. The output voltage to be determined is $v_o(t)$.

To satisfy the Barkhausen criterion for amplitude, the loop gain must be unity at the resonant frequency. From the circuit of figure 2.34, the following relationships are known:

$$v_{in} = nv_o \qquad i = ni'$$
$$G_L = 1/R_L \qquad G_E = 1/R_E.$$

With these, the total output conductance can be calculated:

$$i' = v_{in}(g_{in} + G_E) = \frac{i}{n}$$
$$i = nv_{in}(g_{in} + G_E) = n^2 v_o(g_{in} + G_E)$$
$$\frac{i}{v_o} = G = n^2(g_{in} + G_E), \tag{2.15}$$

where G is the conductance from the input-side resistors taking into account the transformer. The circuit can now be redrawn as in figure 2.35.

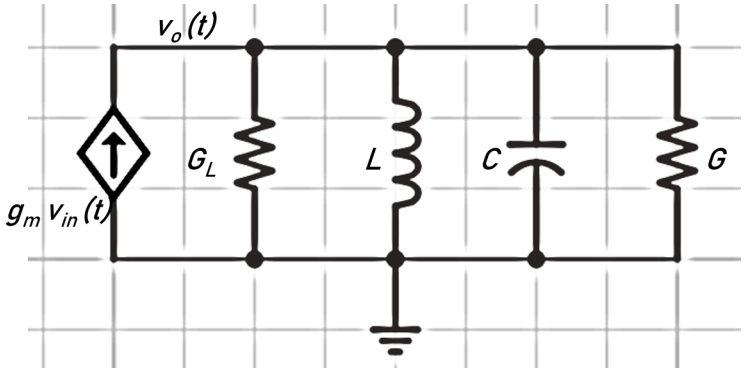

Figure 2.35: Clarke-Hess Oscillator with Incorporated Input Resistors

Finally, the two conductors can be combined to form a total conductance, G_T:

$$G_T = G_L + G, \tag{2.16}$$

and the circuit redrawn one final time, as in figure 2.36.

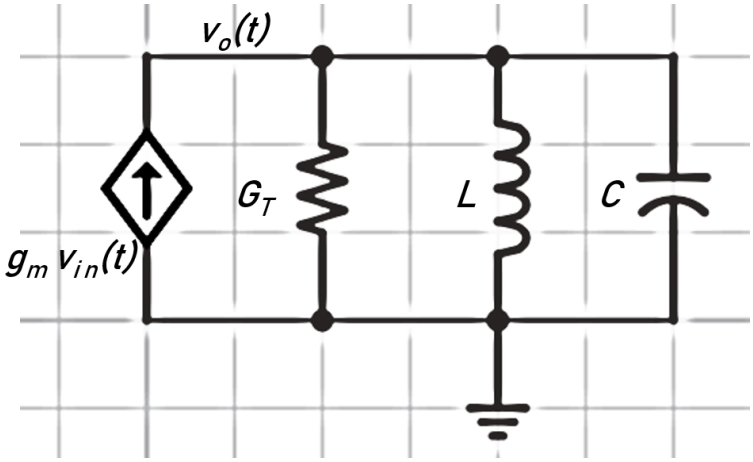

Figure 2.36: Final Clarke-Hess Oscillator

The loop gain, $A_L(s)$, of this simple RLC circuit is calculated using the following relationships:

$$|A_{L_{min}}(s)| = 1 \qquad \frac{v_o}{g_m v_{in}} = \frac{1}{Y}$$

$$Y = G_T + \frac{1}{sL} + sC \qquad v_{in} = nv_o.$$

Rewriting the current source as a function of the output voltage,

$$\frac{v_o}{g_m v_{in}} = \frac{v_o}{g_m n v_o} = Z = \frac{1}{Y} = \left(G_T + \frac{1}{sL} + sC\right)^{-1},$$

then

$$A_{L_{min}}(s) = \frac{v_o}{v_o} = 1 = \frac{ng_m}{Y} = \frac{ng_m}{G_T + \frac{1}{sL} + sC}.$$

Rewriting the quotient with a single zero in the numerator and two simple poles in the denominator yields

$$A_{L_{min}}(s) = 1 = \frac{ng_m\left(\frac{1}{C}\right)s}{s^2 + s\frac{G_T}{C} + \frac{1}{LC}}.$$

Solving for the poles yields

$$s = -\frac{G_T}{2C} \pm \sqrt{\left(\frac{G_T}{2C}\right)^2 - \frac{1}{LC}}. \tag{2.17}$$

Using the substitution $\gamma = \frac{G_T}{2C}$ and $\omega_0^2 = \frac{1}{LC}$,

$$A_{L_{min}}(s) = 1 = \frac{(2\gamma s)ng_m/G_T}{s^2 + 2\gamma s + \omega_0^2}. \tag{2.18}$$

From equation 2.18, the minimum transconductance that will provide a unity loop gain at resonance and place the poles directly on the imaginary axis is

$$g_{mQ_{min}} = \frac{G_T}{n}. \tag{2.19}$$

Combining both the transconductance terms on the left-hand side of the equation results in

$$g_{mQ_{min}} = \frac{G_L + n^2 G_E}{n(1 - n/\alpha)}. \tag{2.20}$$

Converting equation 2.20 to its large-signal equivalent involves simply relabeling the transconductance as $G_m(x)$ [3, p. 225].

$$G_m(x) = \frac{G_L + n^2 G_E}{n(1 - n/\alpha)}. \tag{2.21}$$

Dividing equation 2.21 by g_{mQ} and setting it equal to equation D.15[2] results in the method for determining the voltage at which the oscillator stabilizes:

$$\frac{G_m(x)}{g_{mQ}} = \frac{G_L + n^2 G_E}{g_{mQ} n(1 - n/\alpha)} = \frac{2I_1(x)}{xI_0(x)}\left(1 + \frac{\ln(I_0(x))}{V_\lambda / V_T}\right). \tag{2.22}$$

[2]See appendix D for the derivation of equation D.15.

The right-hand side of equation 2.22 is a function of x and V_λ, where $x = V_1/V_T$ and V_λ is the voltage drop across the emitter resistor. The left-hand side is a function of the readily-determined variables from the oscillator circuit. The right-hand side is plotted and the ordinate is identified whose value is that of the left-hand side. The corresponding abscissa is extracted as x, and $V_1 = xV_T$, where V_1 is the amplitude of the input voltage. Finally, V_1 is related to the output voltage by the equation $V_o = V_1/n$.

Example The Clarke-Hess example oscillator is exhibited in figure 2.37. The authors predict an output voltage of 7.9 V peak and a frequency of 1.6 MHz [3, p. 227]. The simulated output voltage waveform is exhibited in figure 2.38. The authors did not specify a transistor so the 2N2222 was used for simulation.

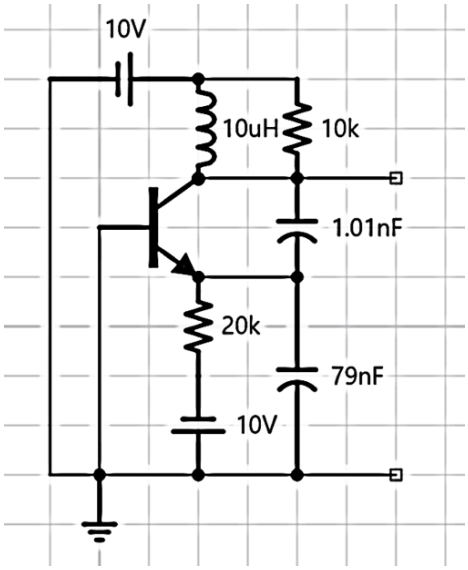

Figure 2.37: Clarke-Hess Colpitts Oscillator Example

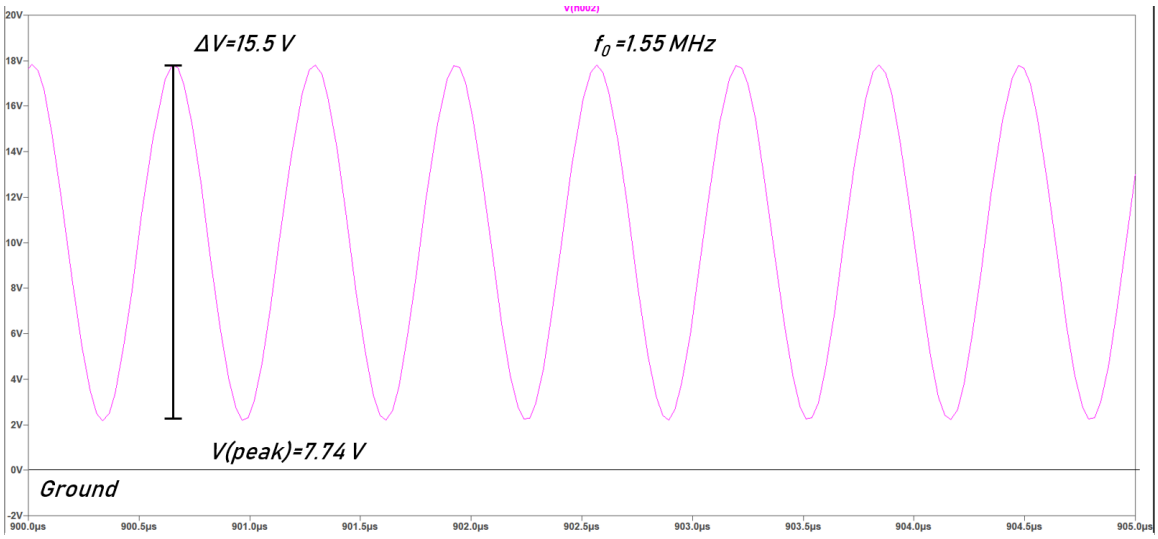

Figure 2.38: Clarke-Hess Simulation: *startup* Applied, 900 $\mu s < t < 905\ \mu s$

The simulated values are very close to the theoretical. When constructed on a breadboard however, the circuit yields no oscillation. As seen in the Hagen circuit, increasing the capacitance ratio can stimulate oscillation, so the C_2 capacitor is replaced with a 22.4 nF capacitor. The experimental circuit is shown in figure 2.39, noting that the resistor in series with the inductor is the resistance of the inductor. Figure 2.40 is the simulated output waveform for the modified circuit of figure 2.39 and figure 2.41 its experimental output voltage.

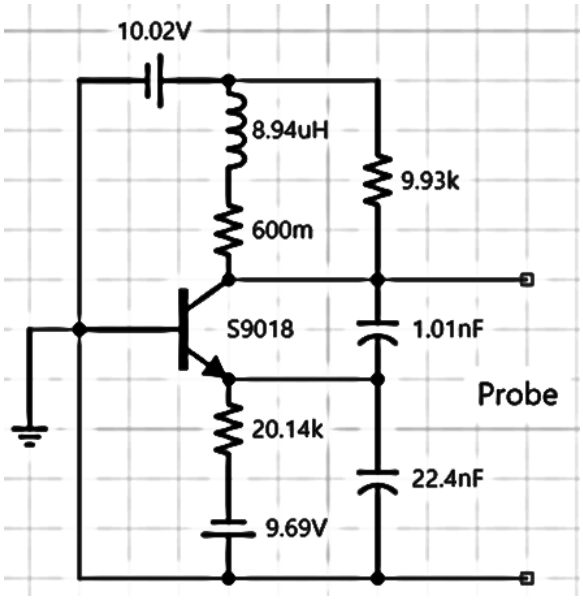

Figure 2.39: Constructed Clarke-Hess Oscillator

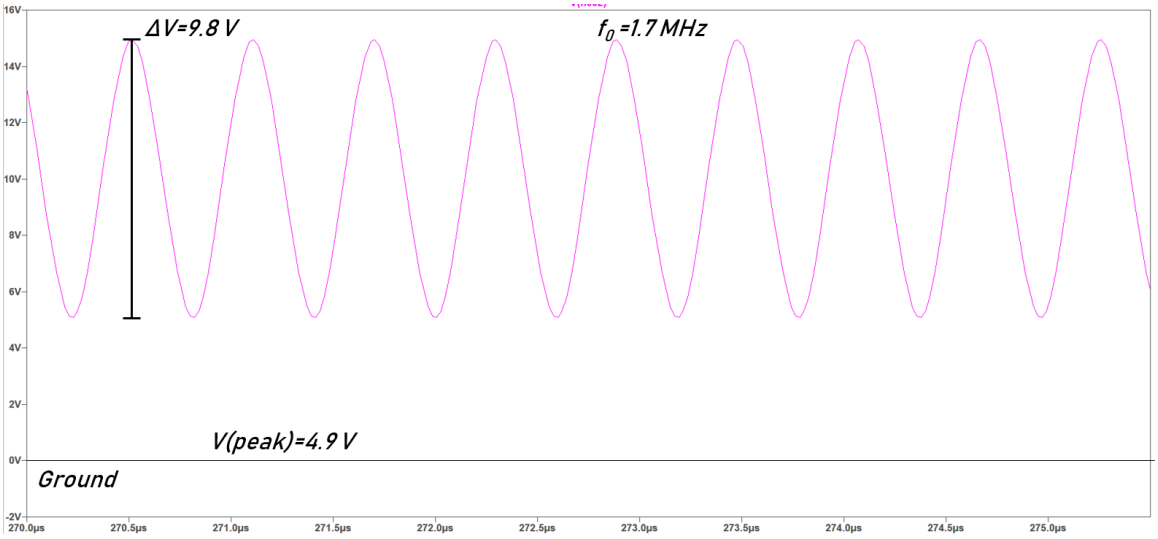

Figure 2.40: Modified Clarke-Hess Oscillator Simulation: *startup* Applied, 270 $\mu s < t <$ 275 μs

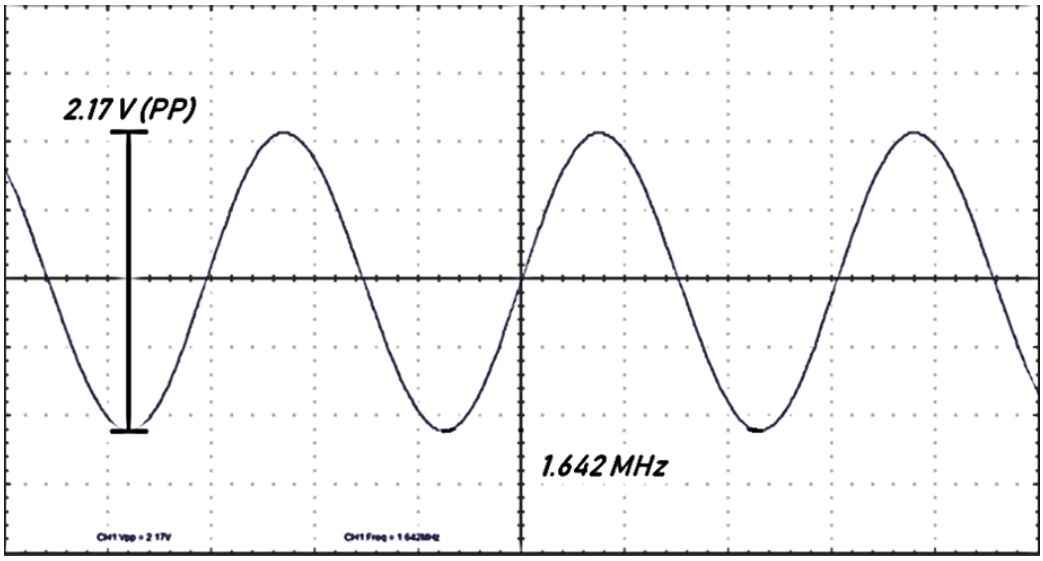

Figure 2.41: Breadboard Modified Clarke-Hess Oscillator Output Voltage Waveform

After averaging to account for phase and amplitude jitter, the experimental peak amplitude is 1.085 V, much smaller than the simulated peak amplitude of 4.86 V. A smaller experimental output voltage compared to its simulated counterpart was also seen in the Hagen circuit.

The theoretical expected output voltage amplitude is calculated as follows. The capacitor transformer ratio is $n = \frac{C_1}{C_1+C_2} = 0.043$. With the reactive components removed to prevent oscillation, $V_{BEQ} = 0.71$ V and $\alpha = 0.998$. $V_\lambda = V_{EE} - V_{BEQ} = 8.98$ V and the quiescent emitter current is $I_{EQ} = V_\lambda / R_E = 445.9\ \mu A$. The quiescent collector current is $I_{CQ} = \alpha I_{EQ} = 445.0\ \mu A$ and the transconductance is $g_{mQ} = I_{CQ}/V_T = 17.11\ mS$. The input conductance is $g_{in} = \frac{g_{mQ}}{\alpha} = 17.15\ mS$. The left-hand side of equation 2.22 is completed by applying equation 2.21 and dividing by the quiescent transconductance.

$$\frac{G_m(x)}{g_{mQ}} = \frac{G_L + n^2 G_E}{g_{mQ} n(1 - n/\alpha)} = 0.143. \tag{2.23}$$

This value is equated to the right-hand side of equation 2.22,

$$\frac{G_m(x)}{g_{mQ}} = \frac{2I_1(x)}{xI_0(x)}\left(1 + \frac{\ln I_0(x)}{8.98V/.026V}\right)$$

which is a plot of the variable x as seen in figure 2.42.

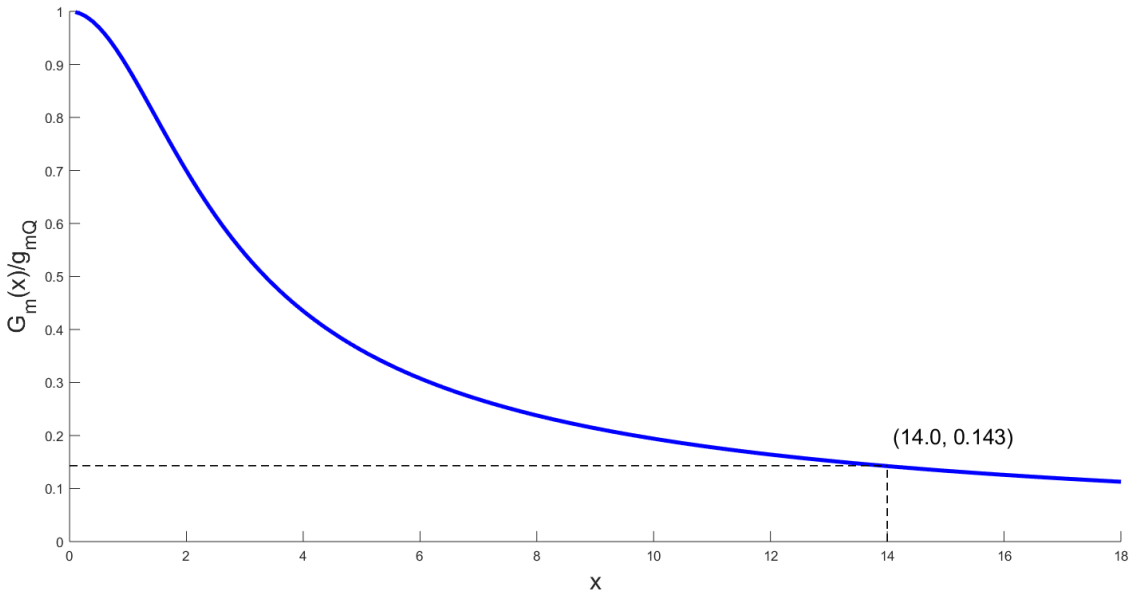

Figure 2.42: $G_m(x)/g_{mQ}$ with x Extracted

As indicated by the plot in figure 2.42, the x value corresponding to the $G_m(x)/g_{mQ}$ value from equation 2.23 is 14.0. As $x = V_1/V_T$, $V_1 = 0.364$ V. The output voltage is related to the input voltage by the equation $V_1 = nV_o$, so $V_o = 8.44$ V is the calculated amplitude of the output voltage $v_o(t) = V_o \cos(2\pi(1.72 \times 10^6)t)$. Without taking into account the inductor's equivalent series resistance or the emitter resistor in the calculation of the predicted frequency (see equation B.6), the frequency is close to the experimental value. The calculated amplitude however is much larger than both the experimental and simulated values of 1.1 V and 4.9 V respectively.

2.2.2 Output Impedance

The two output impedance methods discussed in this section are the methods of Smith [18] and Clarke-Hess [3]. The methods differ, but the results are identical. As seen in section 2.1.3, the common-base oscillator sees an output impedance even when it is unloaded. The feedback signal sees a combination of the input and emitter resistances. When this resistance is transformed across the load, it becomes a frequency-dependent function of the two oscillator capacitors.

The analysis of section 2.1.3 is the Smith method [18]. It is a brute-force method of transforming an impedance into an equivalent conductance and susceptance. By using an approximation (equation 2.9), the result is reasonably concise.

The Clarke-Hess method makes the same approximation to calculate R_o and notes that the result resembles a similar circuit using a transformer with a turns ratio equal to n, the capacitive ratio. Because the Clarke-Hess method produces the conductance G_T and not R_o directly, the final equation is clearer because it is not obfuscated by parallel resistors. The example circuits from both methods are presented, as well as the results using the alternate method to show equivalency.

Smith Output Impedance Method

Smith Circuit Figure 2.43 is the example 20 MHz common-base Colpitts oscillator from the Smith textbook [18, p. 246]. Smith makes no prediction for the output voltage amplitude.

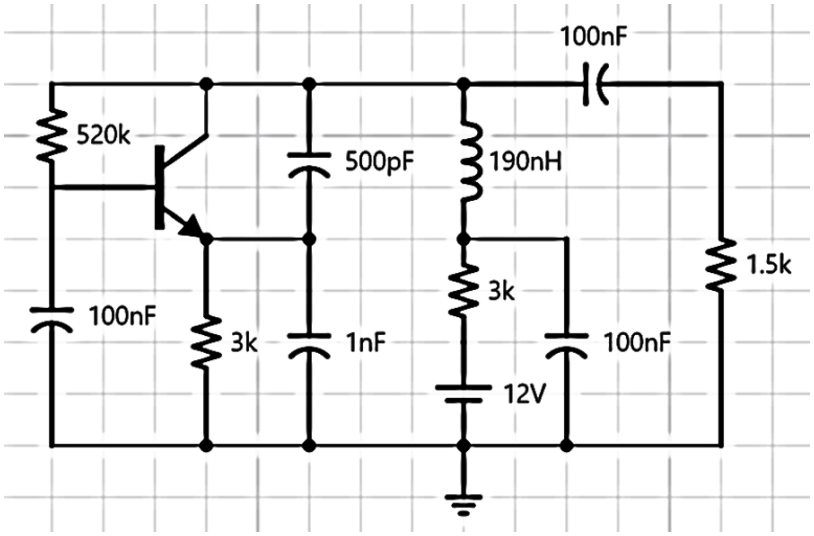

Figure 2.43: Smith Colpitts Oscillator Example

To determine the expected output voltage amplitude, the ciruit is simulated with no load. The 2N2222 is selected in the absence of a specified transistor and because the

experimental S9018 transistor was not available. Applying the same *startup* modifier to the simulation software and letting the circuit run for 1 ms produces the waveform of figure 2.44.

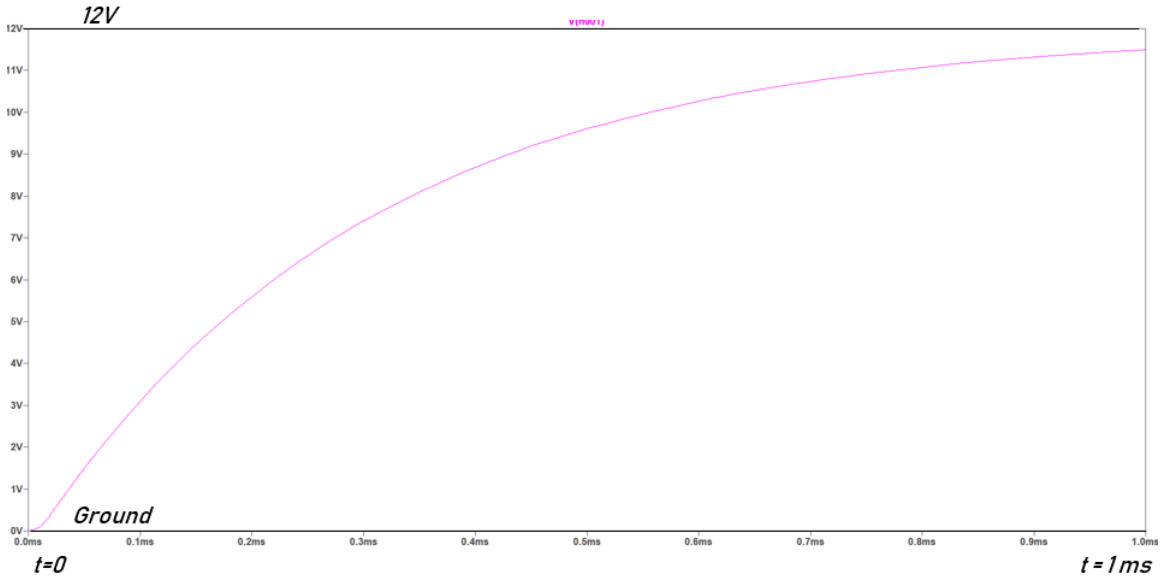

Figure 2.44: Smith Simulation: *startup* Applied, $0 < t < 1$ *ms*

Applying the modifier *uic* resulted in a virtually identical output waveform to figure 2.44. Increasing the warmup time did not yield oscillation. Removing all modifiers resulted in the waveform of figure 2.45.

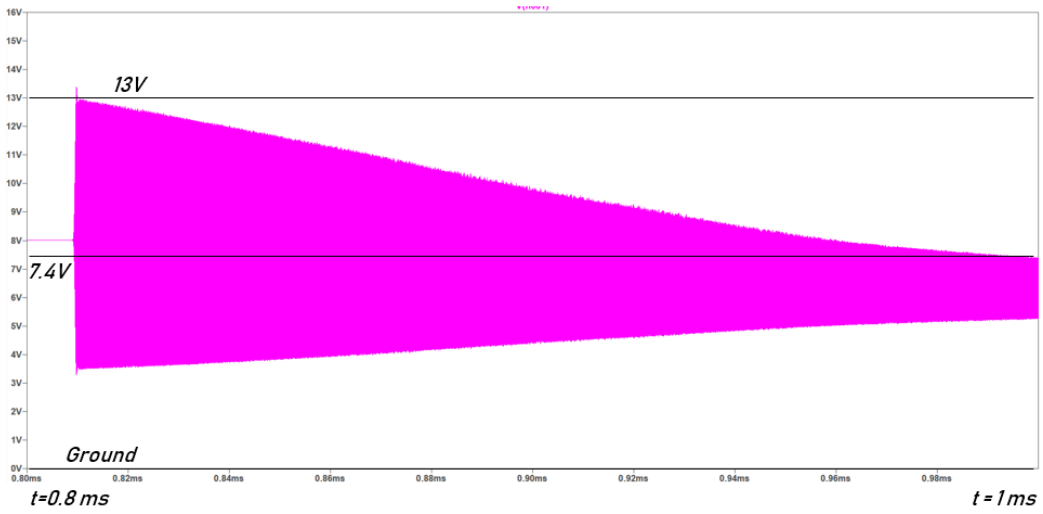

Figure 2.45: Smith Simulation: $0 < t < 1\ ms$

The simulation produces oscillation but with decreasing amplitude. Increasing the time did not result in a stabilized waveform and setting the final time to 2 ms resulted in no oscillation whatsoever. The best available simulation is that of figure 2.45. Figure 2.46 is a closer inspection of the oscillating waveform near $t = 1\ ms$ where the simulation appears to be stabilizing.

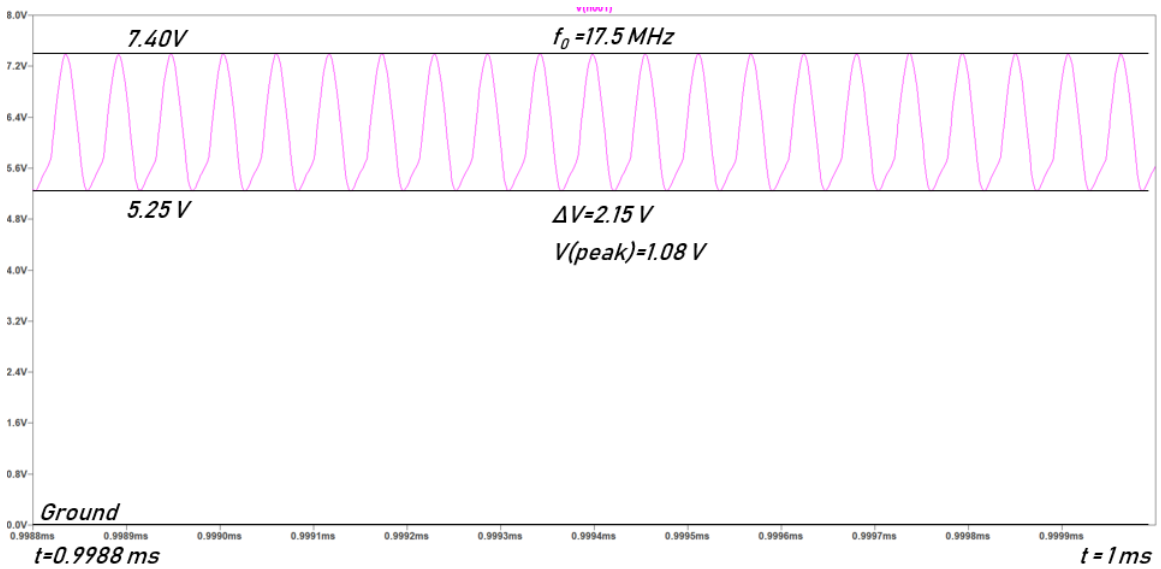

Figure 2.46: Smith Simulation: $0 < t < 1\ ms$

While the simulation predicts an oscillating (albeit distorted) output of 2.2 volts peak-to-peak, the circuit did not yield an oscillating signal experimentally when constructed on a breadboard. Oscillation was achieved by boosting the DC supply voltage. The modified circuit with measured component values identified is exhibited in figure 2.47. The simulated waveform for the modified circuit with no special initial conditions applied and using the 2N2222 transistor is shown in figure 2.48 and the unloaded experimental output waveform is seen in figure 2.49.

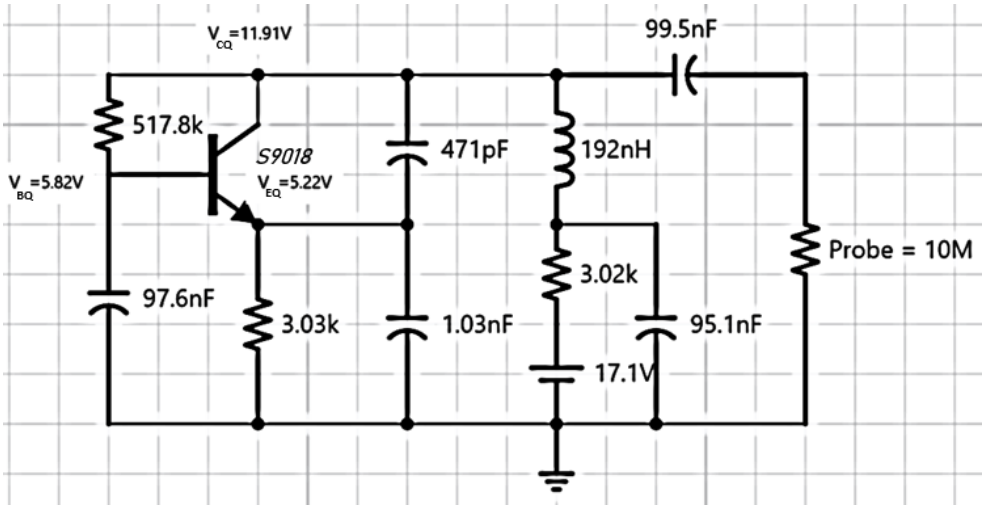

Figure 2.47: Constructed Smith Oscillator

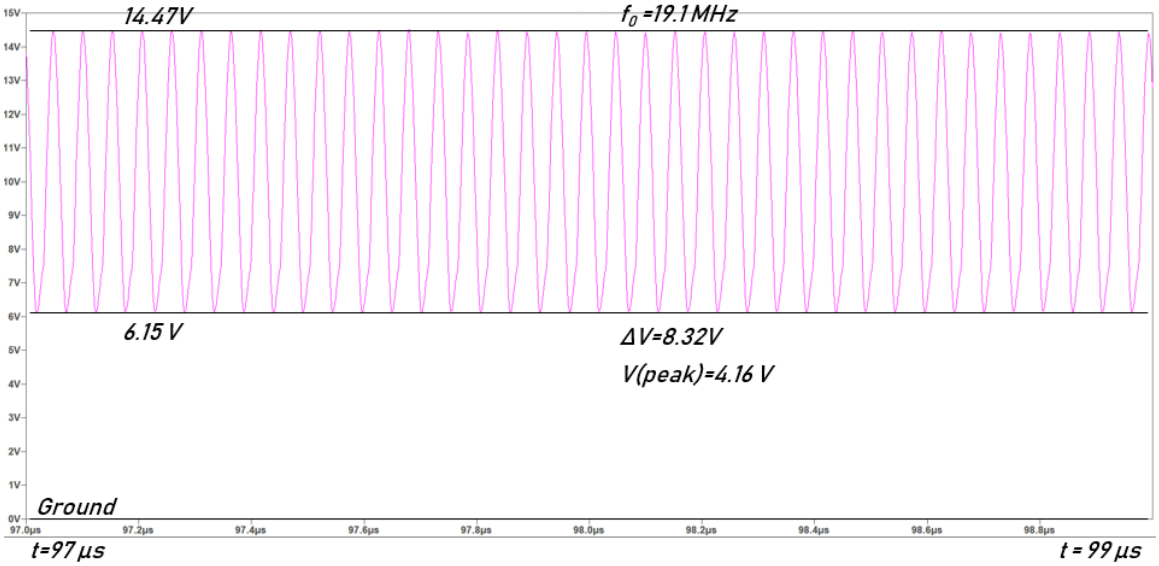

Figure 2.48: Smith Simulation: $0 < t < 1\ ms$

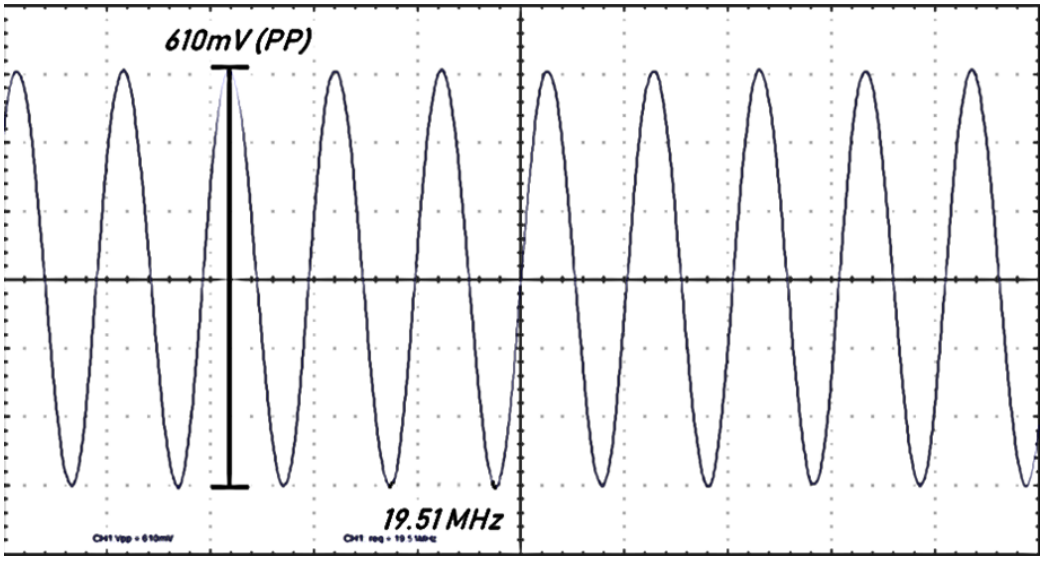

Figure 2.49: Breadboard Modified Smith Oscillator Output Voltage Waveform

To the extent that the simulation is predictive in this instance, the breadboard circuit's output voltage amplitude is significantly smaller than the simulated value. The two frequencies match much more closely.

Output Resistance To calculate the theoretical output resistance, the circuit is presented as its small-signal equivalent as seen in figure 2.50.

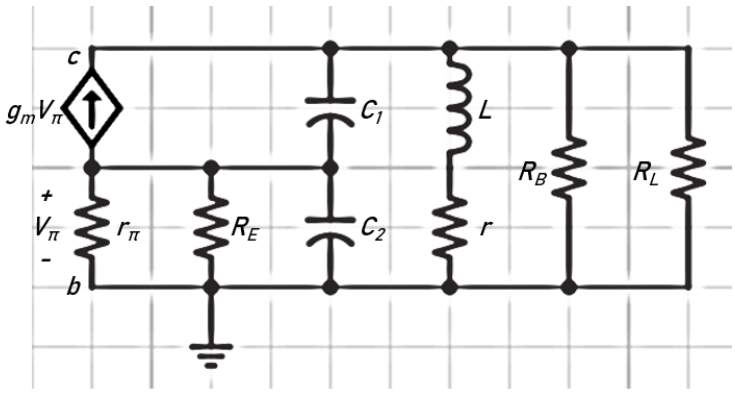

Figure 2.50: Smith Oscillator Small-Signal Equivalent

As in section 2.1.3, the first step in determining output impedance is to break the feedback loop and apply the same signal to the input that would be provided by the feedback signal. To do so requires that the input signal sees the same resistance from the unbroken loop. The base-emitter resistor is therefore replaced by the input resistor $r_i = r_\pi/(\beta+1)$. This resistance, in parallel with the emitter resistor is termed R, and it must be transformed across the output. The required values are calculated.

$$I_{EQ} = \frac{V_{EQ}}{R_E} = 1.72\ \ mA \qquad r_i = \frac{V_T}{I_{EQ}} = 15.1\ \ \Omega$$

$$R = r_i||R_E = 15.0\ \ \Omega \qquad r \approx 100\ \ m\Omega$$

$$n = \frac{C_1}{C_1 + C_2} = 0.31 \qquad \omega_0 = 122.6\ \ Mrad/s$$

There are four possible options for settling on a final unloaded output resistance value depending on whether to include the effects of frequency and the resistance of the inductor. To clarify, these output resistances will be termed $R_{o,approx}$ for the R/n^2 approximation value; $R_{o,\omega}$ for the value taking into account only the frequency effect of the admittance transformation; $R_{o,r}$ for the value taking into account only the resistance of the inductor; and $R_{o,\omega,r}$ for the value taking into account both effects. While the base

resistor in this circuit acts as a load, its value is so large that it is virtually an open circuit from the standpoint of output resistance. It will be ignored in the subsequent calculations.

The first output resistance value, from the approximation of equation 2.9, assumes that $R\omega^2(C_1 + C_2)^2 \gg 1$. That value in this case is 0.51, so the assumption does not hold. Going ahead with the approximation anyway yields an equivalent resistance of $R_{o,approx} = 152.5\ \Omega$.

Using the full expression of equation 2.9 to account for the frequency effect of the admittance transformation results in $R_{o,\omega} = 172.5\ \Omega$

Including only the equivalent series resistance of the inductor (see equation C.1) yields an output resistance of $R_{o,r} = 148.4\ \Omega$.

Finally, taking into account both the frequency effect of the transformation and the resistance of the inductor provides an output resistance of $R_{o,\omega,r} = 167.3\ \Omega$.

As will be discussed in the following section, the Clarke-Hess method calculates $G_T = G_L + n^2(G_E + g_{in})$, where $G_T = 1/R_o$. Using this method without a load conductance, the necessary additional variables are calculated.

$$G_E = \frac{1}{R_E} = 330\ \mu S \qquad g_{in} = \frac{I_{EQ}}{V_T} = 66.3\ mS$$

The unloaded output conductance is then 6.6 mS and the output resistance is $R_o = 152.5\ \Omega$, identical to the value using the Smith method without the two extra considerations.

The textbook's original load of 1.5 kΩ is approximately ten times larger than any of the calculated output resistances and should not load the circuit much. To determine the experimental output resistance, a capacitively-coupled potentiometer is applied across the output and varied until the output voltage amplitude is half of its unloaded value, at which point the output impedance of the oscillator equals the resistance of the potentiometer. The value of the capacitor was 25 μF – large enough to provide a negligible impedance to the circuit at the resonant frequency. In fact, the potentiometer read 609 Ω as the output resistance. A second potentiometer showed 587 Ω, which is within the expected measurement variance. The specified load resistor is only 2.5 times

the experimental output resistance and will certainly cause a significant drop in the output voltage amplitude.

In the case of this oscillator, the effects of frequency and inductor resistance did not much alter the calculated value of the output resistance. There was a substantial percentage difference with the experimental value, however. Using the Clarke-Hess expression because it is the most concise, the only value in that expression that could account for the discrepancy is the transconductance. Perhaps if the actual average emitter current is larger than the measured quiescent emitter current, this method could be reconciled with experiment.

Clarke-Hess Output Impedance Method

As described in section 2.2.1 and equation 2.16, the output conductance using the Clarke-Hess [3] method is

$$G_T = G_L + n^2(g_{in} + G_E),$$

or for the unloaded oscillator,

$$G_{unloaded} = n^2(g_{in} + G_E).$$

The output resistance is then $R_{o,unloaded} = 1/G_{unloaded}$. Using a circuit similar to the one shown in figure 2.39 using the S9018 transistor and with the load removed, the variables are calculated.

$$R_E = 20.12\ k\Omega \qquad G_E = \frac{1}{R_E} = 49.7\ \mu S$$

$$V_{EE} = 9.68\ V \qquad V_{EQ} = -0.71\ V$$

$$I_{EQ} = \frac{V_{EQ} + V_{EE}}{R_E} = 445.8\ \mu A \qquad g_{in} = \frac{I_{EQ}}{V_T} = 17.15\ mS$$

$$C_1 = 1043\ pF \qquad C_2 = 23.1\ nF$$

$$n = \frac{C_1}{C_1 + C_2} = 0.043 \qquad L = 8.94\ \mu H$$

$$r \approx 600\ m\Omega \qquad \omega_0 = 10.47\ Mrad/s$$

Using these values, the theoretical total unloaded conductance and unloaded output resistance are calculated as $G_o = 32.1\ \ \mu S$ and $R_o = 31.16\ \ k\Omega$.

Using a potentiometer to vary the amplitude until it reaches $V_{o,unloaded}/2$ yields an experimental output resistance of 10.79 kΩ. The Clarke-Hess output resistance prediction varies from experimental by almost 200%.

Turning to the Smith [18] method, the additional required values are calculated.

$$r_i = \frac{V_T}{I_{EQ}} = 58.3\ \ \Omega \qquad R = r_i||R_E = 58.2\ \ \Omega$$

Table 2.1 records the possible output resistances in the style of section 2.2.2.

Resistance Type	Value (kΩ)
$R_{o,approx}$	31.16
$R_{o,\omega}$	31.30
$R_{o,r}$	9.95
$R_{o,\omega,r}$	9.96

Table 2.1: Output Resistance - Clarke-Hess Circuit, Smith Method

Again, the Clarke-Hess and Smith results are identical for the simplest case. The approximation requiring that $R\omega^2(C_1 + C_2)^2 \gg 1$ is somewhat more valid for this oscillator as that value is 3.7. As seen in table 2.1, factoring in the frequency effect does not result in a value much different from the approximate value, but including the resistance of the inductor places the theoretical value quite close to its experimental value.

As a final point on this circuit, the load resistor is specified to be directly coupled – that is, there is no capacitor between the oscillator and the load. For the preceding experiment, this load was removed and the output resistance was measured by coupling a potentiometer with a large capacitor. Because the inductor is effectively a short circuit for the purpose of biasing, the load resistor shunting it should have little loading effect. Figure 2.51 is a superposition of the waveforms from the unloaded circuit, the circuit constructed as specified, and the circuit with the same load resistor coupled with a large capacitor ($10\mu F$).

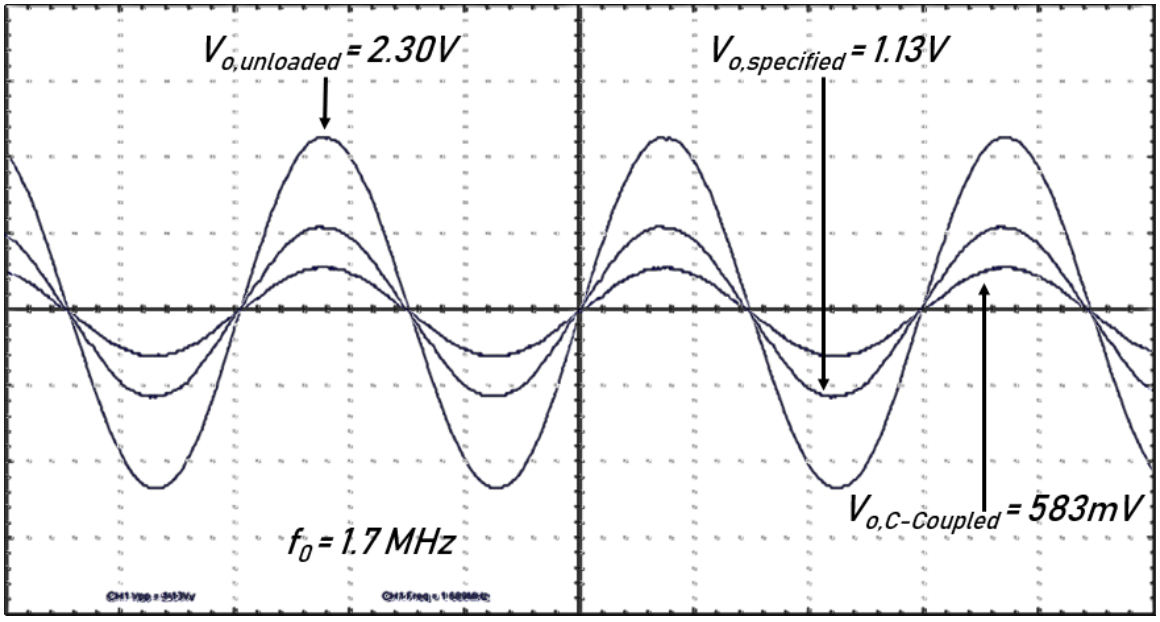

Figure 2.51: Loaded and Unloaded Output Voltages

The output voltage amplitude with this resistor in the specified position is larger than when capacitively coupled, though when simulated the two configurations provide an identical output waveform. All waveform graphs in this thesis are AC voltages as the DC offset is the value of V_{CC}, or very close to it considering the voltage drop across the resistance r. It is interesting that a larger voltage is retained by omitting the capacitive coupling, though the applications of it may be few considering the biasing requirements of follow-on subcircuits. Load placement throughout this work corresponds to the typical load placement for the common-base amplifier. According to Underhill [20] however, phase noise can be improved by placing the load in different positions.

2.2.3 Phase Noise and Distortion

Oscillators are often used in conjunction with mixers. Mixers convert RF signals to a lower frequency for easier amplification and up-convert signals to a higher frequency for transmission. An ideal oscillator output waveform appears on the spectrum analyzer screen as a spike, or delta function. All real oscillators however have a power distribution

centered at the resonant frequency, not to mention at harmonic frequencies (integer multiples of the resonant frequency). Figure 2.52 is the spectrum analyzer image of a 163 kHz oscillator. In addition to the large peak at the center frequency are several harmonics in decreasing amplitude until they eventually reach the noise floor.

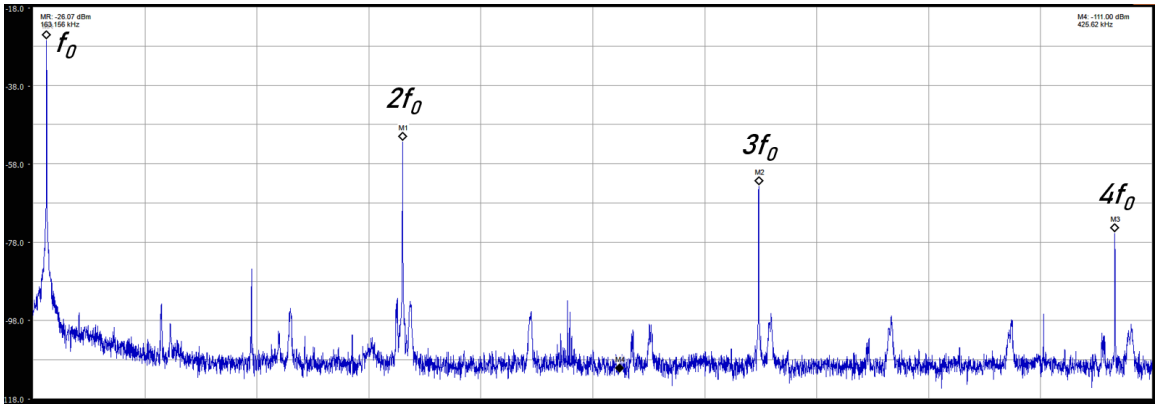

Figure 2.52: 163 kHz Oscillator on Spectrum Analyzer

This power spread around the resonant frequency is termed phase noise. Besides degrading the signal-to-noise ratio of the data to be sent or received, greater phase noise requires a larger bandwidth and decreases the number of communication channels available in a given frequency space.

As described in the Pozar [16] textbook, a simple model consisting of a carrier and modulating signal leads easily to a mathematical representation of phase noise. If the combined signal is represented by $v_o(t) = V\cos(\omega_0 t + \theta(t))$ where V is the voltage amplitude neglecting amplitude noise, then $\theta(t)$ is the phase variation as a function of time. In this model, let $\theta(t) = \Theta\sin(\omega_m t)$, where Θ is the amplitude of the modulating wave and ω_m is its frequency. Substituting this function into the modulated carrier wave yields

$$v_o(t) = V\cos(\omega_0 t + \Theta\sin(\omega_m t)).$$

Carrying through the trigonometry yields

$$v_o(t) = V\cos\omega_0 t\cos(\Theta\sin\omega_m t) - V\sin\omega_0 t\sin(\Theta\sin\omega_m t). \tag{2.24}$$

Trigonometric functions whose arguments are also trigonometric functions have expansions as Bessel functions, seen in equations 2.25 and 2.26.

$$\cos(z\sin\theta) = J_0(z) + 2\sum_{k=1}^{\infty} J_{2k}(z)\cos(2k\theta) \qquad [1, 9.1.42] \tag{2.25}$$

$$\sin(z\sin\theta) = 2\sum_{k=0}^{\infty} J_{2k+1}(z)\sin[(2k+1)\theta] \qquad [1, 9.1.43]. \tag{2.26}$$

Substituting equations 2.25 and 2.26 into equation 2.24 yields equation 2.27.

$$\begin{aligned} v_o(t) = V\Big\{ &\cos\omega_0 t\Big[J_o(\Theta) + 2\sum_{k=1}^{\infty} J_{2k}(\Theta)\cos(2k\omega_m t)\Big] \\ &- \sin\omega_0 t\Big[2\sum_{k=0}^{\infty} J_{2k+1}(\Theta)\sin[(2k+1)\omega_m t]\Big]\Big\} \end{aligned} \tag{2.27}$$

Applying the small-angle approximations of Appendix E results in equation 2.28.

$$v_o(t) = V[\cos\omega_0 t - \Theta\sin\omega_0 t\sin\omega_m t] \tag{2.28}$$

Applying a trigonometric identity to the second term of equation 2.28 results in equation 2.29.

$$v_o(t) = V\big(\cos\omega_0 t - \frac{\Theta}{2}[\cos(\omega_0 - \omega_m)t - \cos(\omega_0 + \omega_m)t]\big) \tag{2.29}$$

Equation 2.29 indicates that for a given modulating frequency, the resulting output voltage will have components at the carrier frequency as well as at the sum and difference of the carrier and modulating frequencies. For a spectrum of modulating frequencies, the output waveform will have the appearance of the first peak of figure 2.52 – a central peak with a distribution decreasing to the noise floor.

A phase noise model encompassing the various sources of noise does exist (Leeson's model). The model however is more instructive than predictive [11, p. 576] and the experiments in the following chapter will investigate phase noise and harmonics comparatively and not mathematically.

CHAPTER 3

EXPERIMENTAL DATA AND RESULTS

The previous chapter provided the concepts and terminology of the Colpitts oscillator but did not provide analysis methods whose predictions corresponded to experimental results – at least given the experimental conditions. This chapter investigates many aspects of the oscillator and provides some basis for controlling the output characteristics of voltage amplitude, resistance and waveform distortion given a set of components.

The oscillators in the following experiments were all constructed on breadboards and measurements were conducted with an oscilloscope (x10 probe), multimeter, and spectrum analyzer. The experimental resonant frequency range was maintained below 10 MHz to minimize the effect of parasitic reactance.

Throughout the course of this work, at least 1,000 oscillators were constructed and measured though not all measurements were included in the data. The transistors used were the S9018, selected for its high transition frequency. All resistors and capacitors were measured with a digital multimeter. The same meter was not able to measure inductances smaller than approximately 4 μH, so instead an RL circuit was constructed and driven with a sine wave. The input and output voltages were compared and the inductance was measured. The method is displayed in figure 3.1.

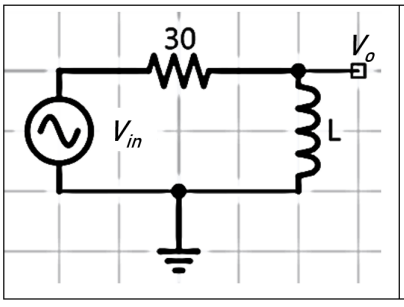

$$\frac{V_o}{V_{in}} = \frac{\omega L}{\sqrt{R^2 + \omega^2 L^2}}$$

$$L = \frac{R}{\omega} \frac{V_o}{\sqrt{V_{in}^2 - V_o^2}}$$

Figure 3.1: Small Inductance Measurement Method

3.1 Output Voltage Amplitude Experiments

The predictions of section 2.2.1 did not accurately correspond to the experimental results obtained from the authors' example circuits. The simulations of their circuits often required modifying initial conditions to attain oscillation, though the correct setting varied depending on the circuit. The simulated voltage amplitudes were consistently much larger than their experiemental counterparts.

This section investigates each component of the common-base Colpitts oscillator and its effect on the output voltage. The goal is to develop a method or set of guidelines for component selection such that an oscillating, unsaturated output voltage is reliably attained. Figure 3.2 is the topology for the experiments in this section unless otherwise specified.

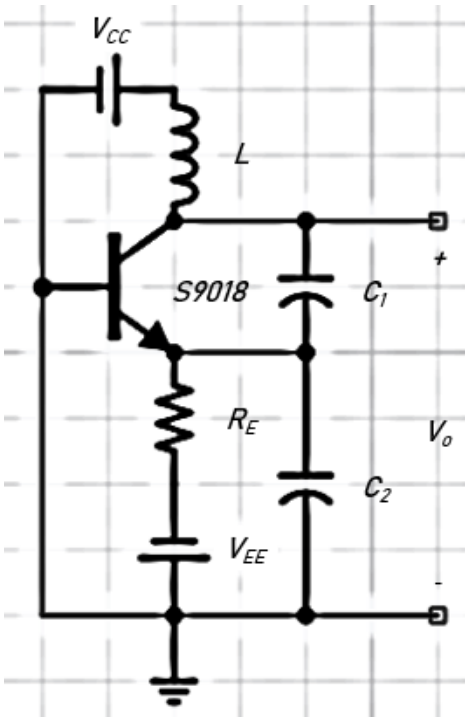

Figure 3.2: Colpitts Oscillator for Extracting Output Voltage Data

The oscillator in figure 3.2 is the simplest possible circuit for studying V_o. The circuit is unloaded except for the oscilloscope probe and free from the complication of extra voltage-divider biasing resistors. Quiescent currents are easily changed with a variable V_{EE}.

3.1.1 V_o Experiment 1: Dependence on Inductance (Constant C_1)

This experiment is intended to demonstrate the effect of inductance on the output voltage. In this experiment, several sets of data were obtained. Throughout the experiment, the C_1 capacitor was kept constant (428 pF) and for each data set, the C_2 capacitor was varied to yield a different capacitance ratio n. For each data set, eleven inductors with values ranging from 100 nH to 15 μH were cycled through and the output voltage obtained. The value of the emitter resistor was 10.3 $k\Omega$ and the DC voltage supplies were set to 10 V.

Figure 3.3 is a plot of the constant C_1 data as well as a weighted linear regression of the data set for $n = 0.31$. That ratio was selected because each inductor in the set produced a non-zero and non-saturated output voltage.

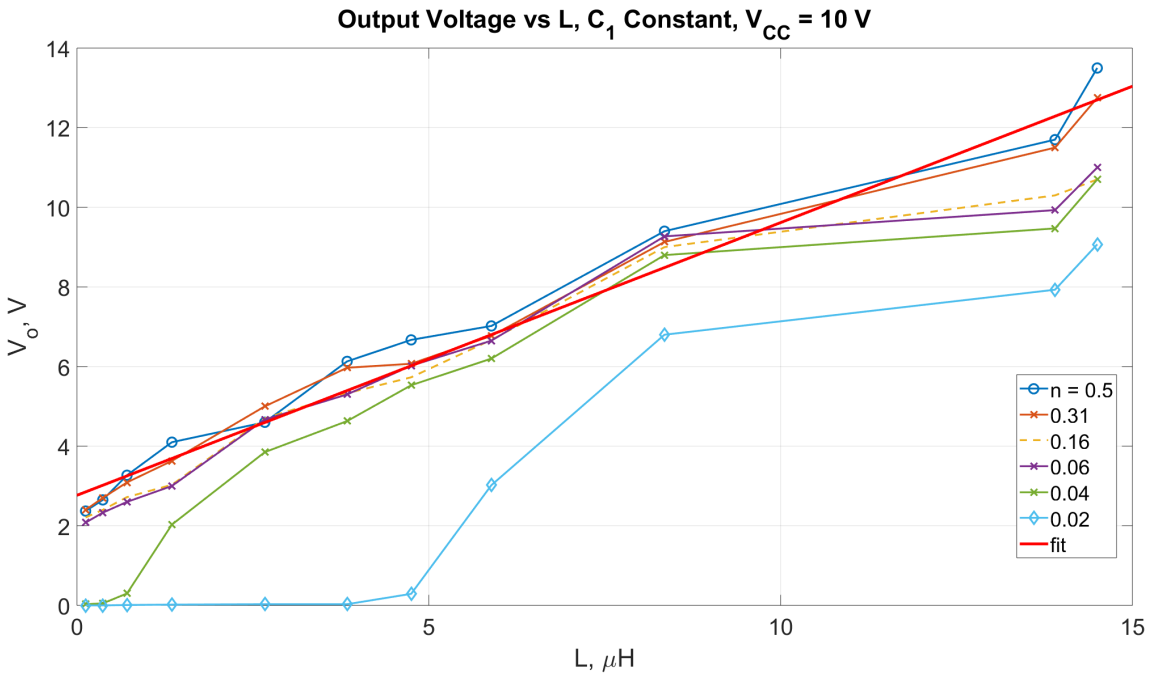

Figure 3.3: First Data Set - V_o vs L, Constant C_1, Slope ($n = 0.31$): 0.68 $V/\mu H$

Because only one component changed with each point, the data lines are quite regular. Figure 3.3 indicates that, at least with these combinations of reactive element values, the output voltage amplitude has a proportional relationship with inductance value. It also shows that a very small capacitance ratio combined with a very small inductor fails to produce oscillation, while that same inductor with a larger capacitance ratio will. Finally, the graph depicts that the output voltage is not strongly correlated with the capacitance ratio, assuming that oscillation is produced. The plots for $n = 0.5$ and $n = 0.04$ differ in most cases inside the extremes of inductance values by less than 2 V, and often are much nearer.

3.1.2 V_o Experiment 2: Dependence on Inductance (Constant f_0)

Each oscillator tested in the previous experiment produced a different resonant frequency. It is possible that the frequency response of the transistor could affect the output voltage amplitude. To remove that possibility, this experiment maintains f_0

instead of C_1. Virtually the same n-ratio data sets are obtained and the same eleven inductors are used. For each oscillator constructed, both capacitors are replaced in order to obtain both the correct capacitive ratio and a tolerably similar resonant frequency.

Figure 3.4 is a plot of the resonant frequencies produced for each oscillator in each data set and it demonstrates that the resonant frequencies were maintained to a range of 3.3 to 3.4 MHz in almost all cases. The sharp drops in the figure indicate that no useable output voltage was obtained for that combination of components. Having removed the frequency variable from the experiment, figure 3.5 is a plot of V_o versus L for the constant resonant frequency data.

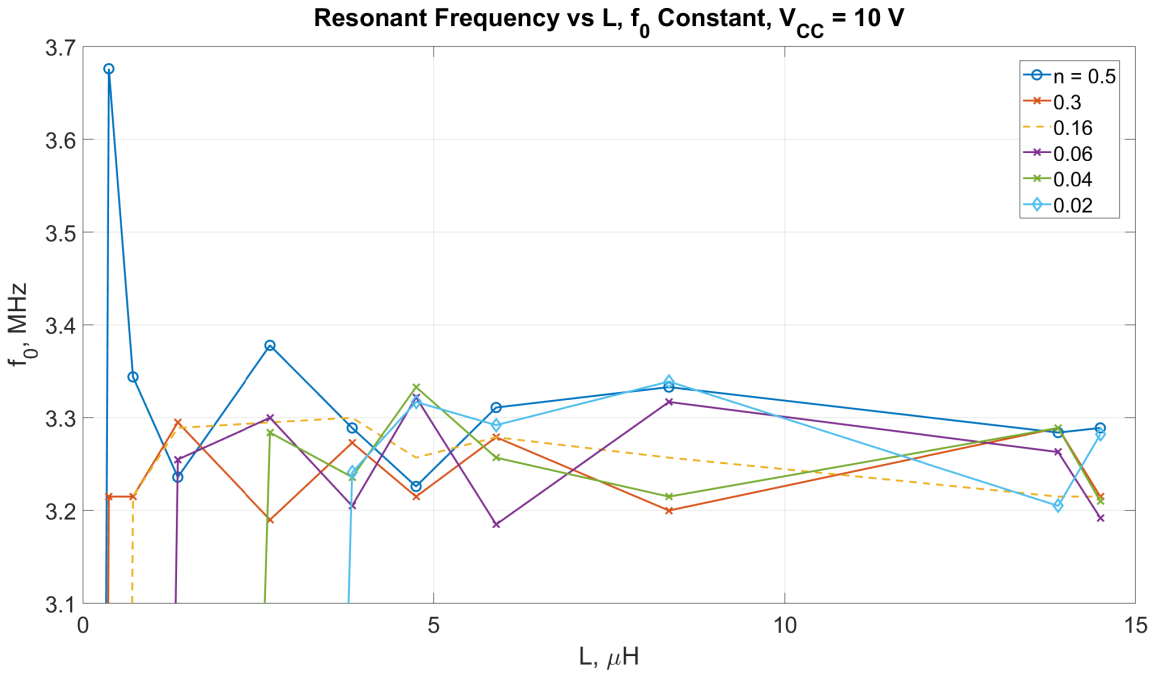

Figure 3.4: Second Data Set - f_0 vs L, Constant f_0

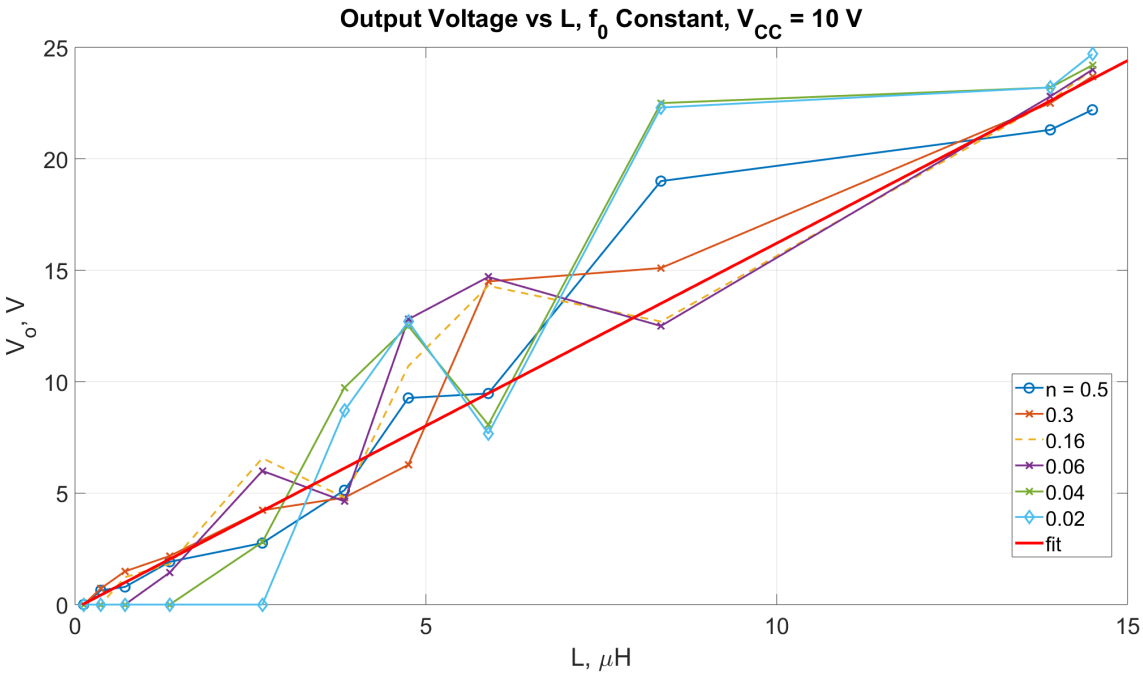

Figure 3.5: Second Data Set - V_o vs L, Constant f_0, Slope ($n = 0.3$): 1.64 $V/\mu H$

There is a range of resonant frequencies for the oscillators constructed in this experiment despite the attempt to maintain resonant frequency constant. Because of this variation, the output voltage plot reflects not only the change in inductance but also an irregular relative change in capacitance. Correspondingly, the data lines in figure 3.5 are less regular than those of figure 3.3.

For this range of inductors at least, whether the C_2 capacitor is kept constant or the resonant frequency is, there is a proportional relationship between the inductor and the output voltage amplitude and it is plausible that this relationship is linear. This relationship accords with the predictive equations from Imani [8] and Huang [7]. A best-fit line for the $n = 0.3$ data set is included in figure 3.5 and its slope is stated in the caption.

3.1.3 V_o Experiment 3: Saturation Dependence on Inductance (Constant C)

The first two experiments sought to demonstrate the dependence of V_o on the inductance, but the range of inductors was limited. A linear relationship was implied but for a given bias scheme, the trend cannot extend indefinitely. The intention of the third experiment is to determine the saturation voltage for an oscillator as a function of inductance. Having demonstrated in the previous experiments that the relationship between output voltage and inductance is proportional whether or not the resonant frequency is maintained, this experiment opts for the simpler method.

For each of the four data sets in this experiment the two capacitors C_1 and C_2 are kept constant and only the inductors vary. The number and range of inductors is much greater in this experiment, from hundreds of nanohenries to nearly one millihenry. The oscillator in this experiment uses voltage-divider biasing, though all quiescent values are kept constant throughout the experiment. The positive DC supply voltage was set to 13.9 V. The resistors used were $R_1 = 359.6\ k\Omega$, $R_2 = 54.9\ k\Omega$, and $R_E = 3.2\ k\Omega$. The coupling and bypass capacitors are each 25 μF. Figure 3.6 is the experimental circuit diagram and 3.7 is a plot of the first data set.

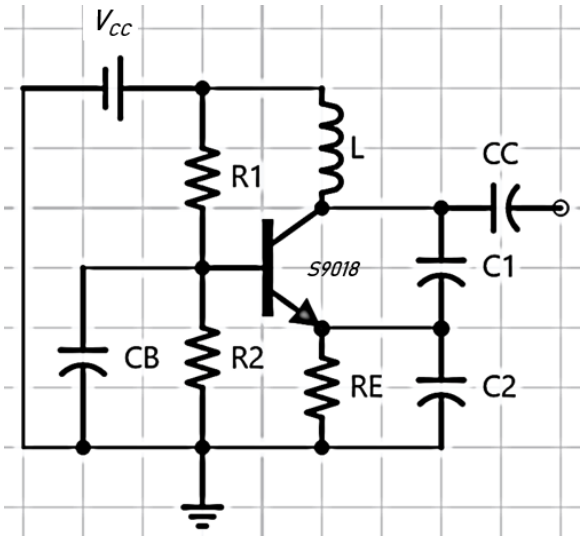

Figure 3.6: Experiment 3 Circuit

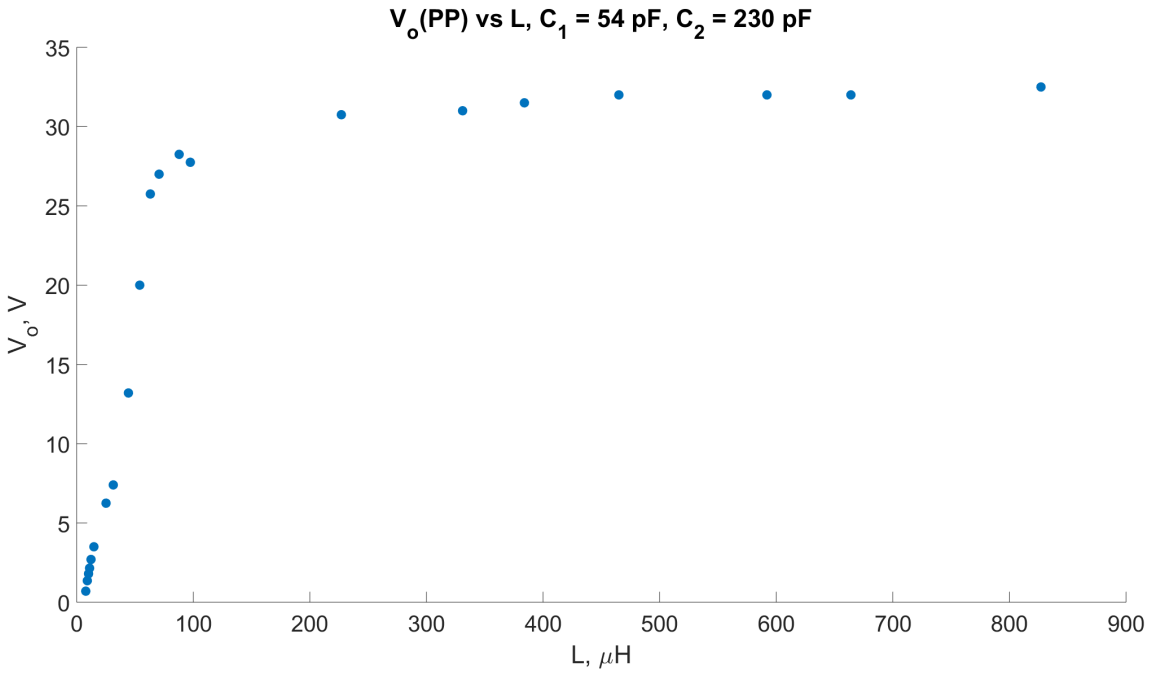

Figure 3.7: Experiment 3, Data Set 1

Figure 3.7 shows a period of output voltage rising with increasing inductance followed by voltage values that cease to rise. Well outside the scope of figure 3.7 is a datapoint at 9.7 mH. The voltage corresponding to that inductance is 31 V - very close to the general saturation values at the upper end of figure 3.7, though this larger inductor has a slightly larger equivalent series resistance.

To better view the rising portion of the data, figure 3.8 is a plot of the unsaturated region of the same data set along with the slope of a linear regression of the data in this region. The significance of the slope is unknown but is included for reference and comparison.

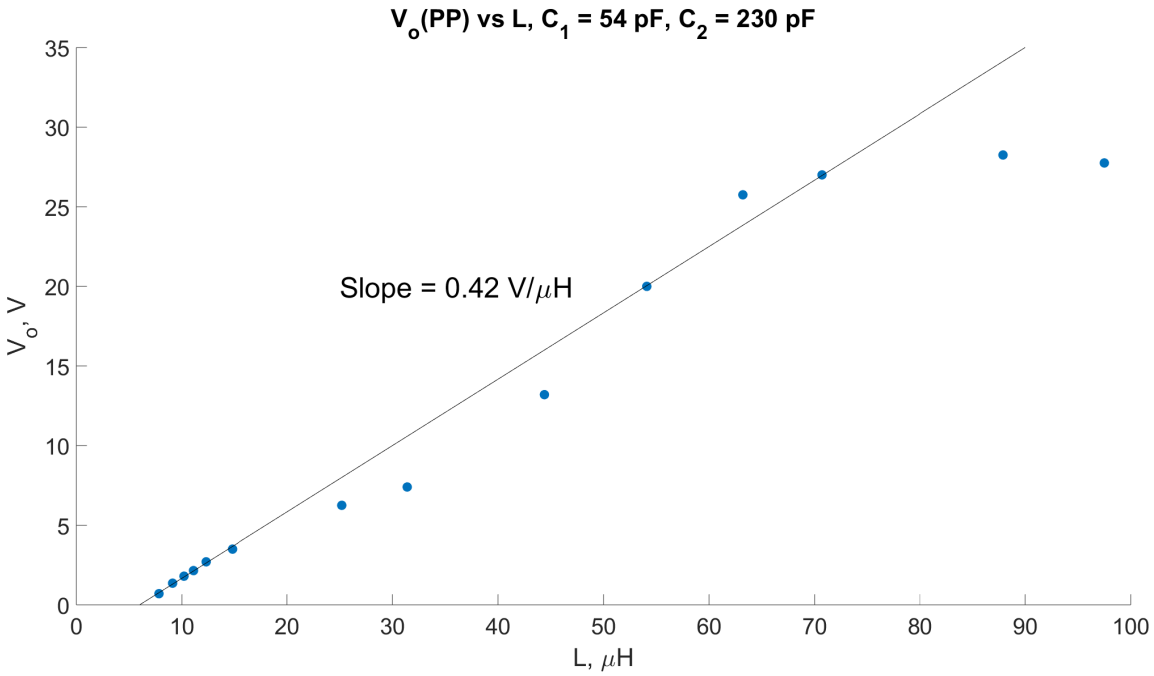

Figure 3.8: Unsaturated Region of Experiment 3, Data Set 1

Without more data points to fill in the plot, a linear relationship between V_o and inductance within a limited range is not certain but is plausible and agrees with the results of the first two experiments.

To be certain that this data is not anomalous, the experiment was conducted three additional times with different capacitor values. Figures 3.9, 3.10, and 3.11 are the V_o versus inductance. The capacitor values are identified in each figure along with best-fit lines for the unsaturated regions.

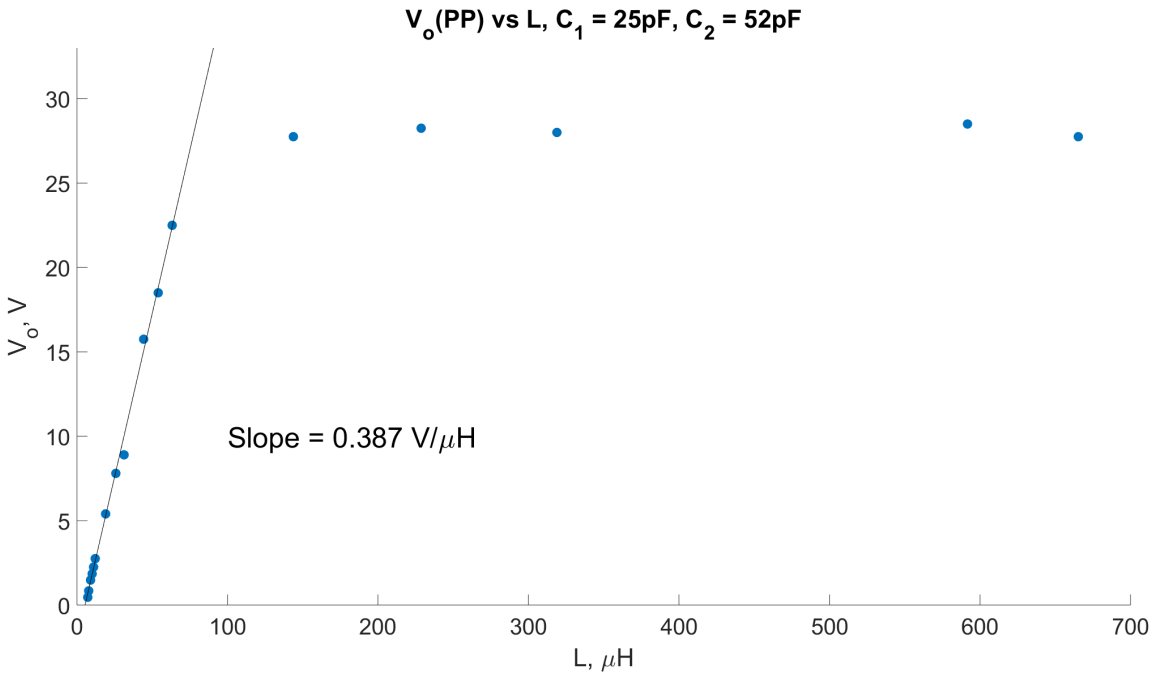

Figure 3.9: Experiment 3, Data Set 2

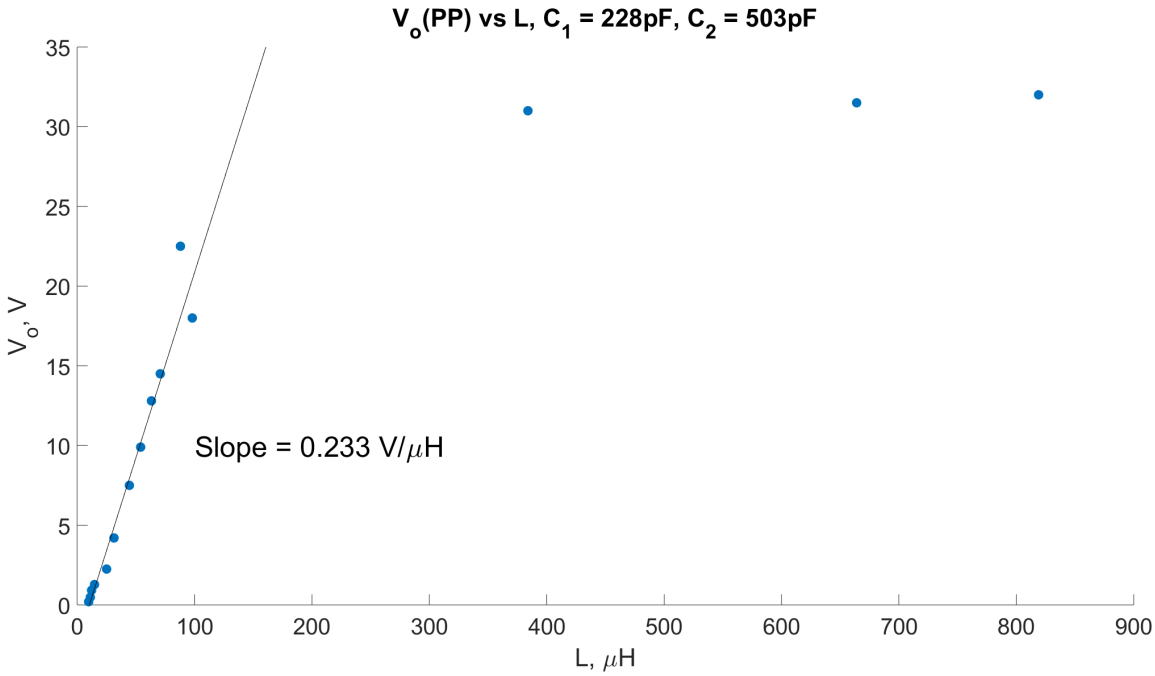

Figure 3.10: Experiment 3, Data Set 3

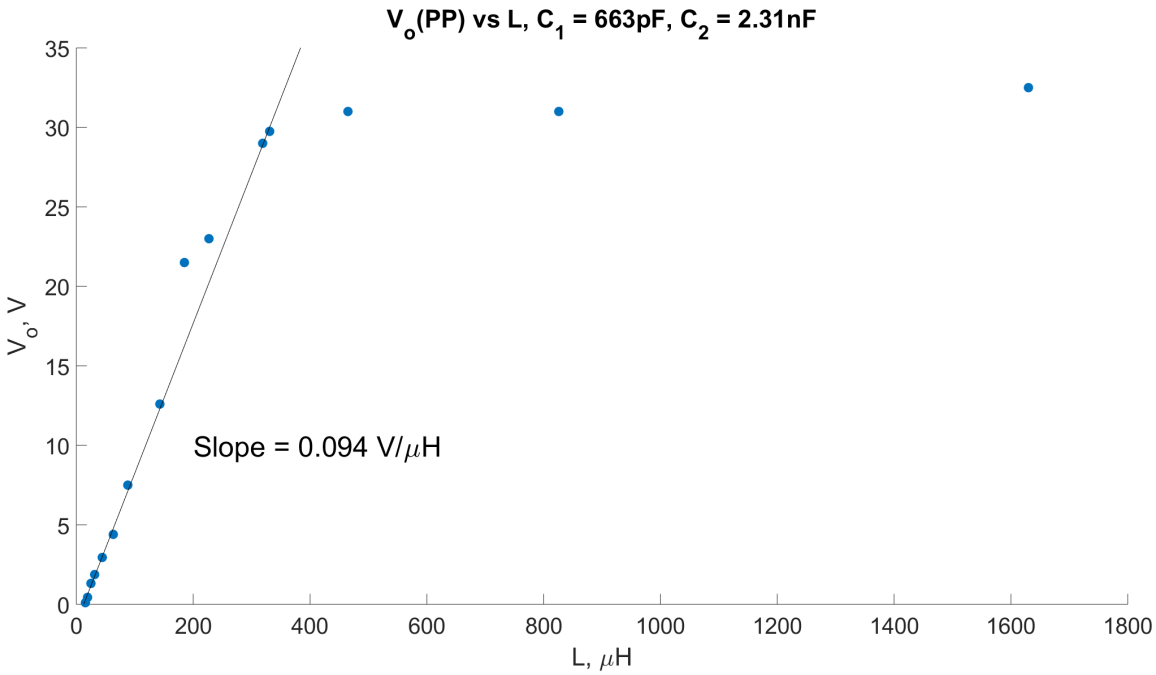

Figure 3.11: Experiment 3, Data Set 4

In each of the four data sets of experiment 3 the voltage is near-linear with inductance and then saturates. As will be shown in section 3.3, saturated oscillators contain powerful harmonics and are undesireable for use as carriers. Automatic gain control circuits can amplify voltages to a desired level but they cannot correct a saturated waveform.

A valuable prediction method would provide a maximum inductance value for a given oscillator such that the output voltage remains unsaturated. The prediction method should involve only component values and theoretical computations to be of ready use and the method must include the inductance. As an attempt to correlate output voltage to a theoretical characteristic involving inductance, the following method offers some insight.

Figures 3.14, 3.12, 3.15, and 3.13 are the same four plots of output voltage versus inductance for different capacitance values as figures 3.7, 3.9, 3.10, and 3.11, with the addition of the plots of theoretical and experimental resonant frequency superposed and

on a different scale.

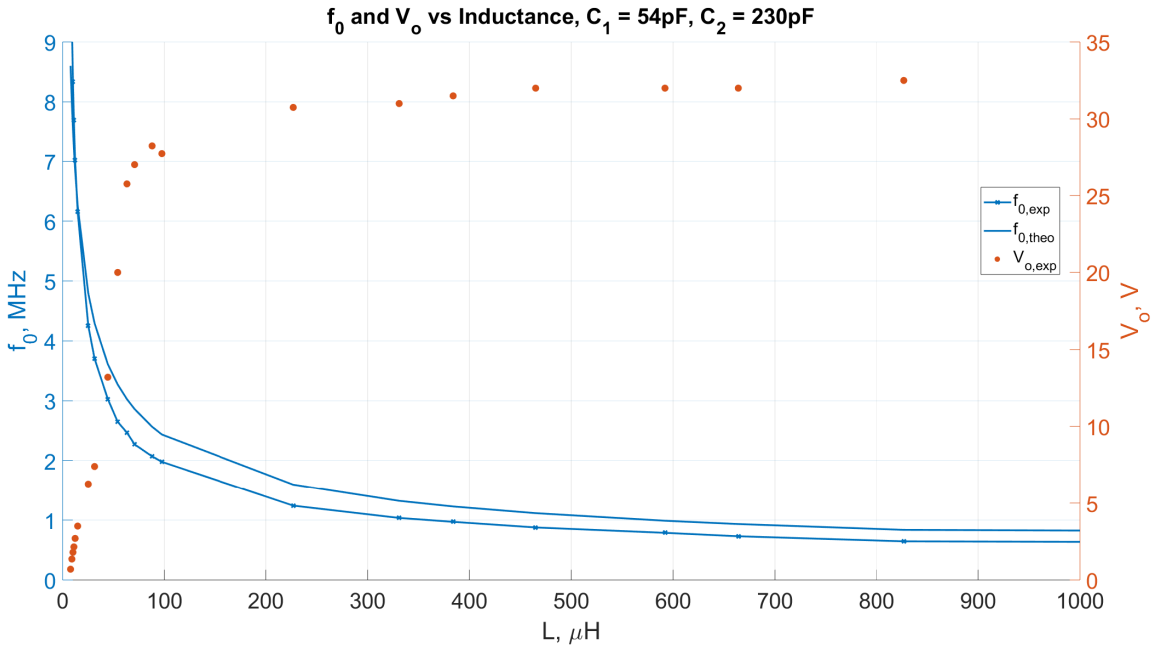

Figure 3.12: Experiment 3, Data Set 1

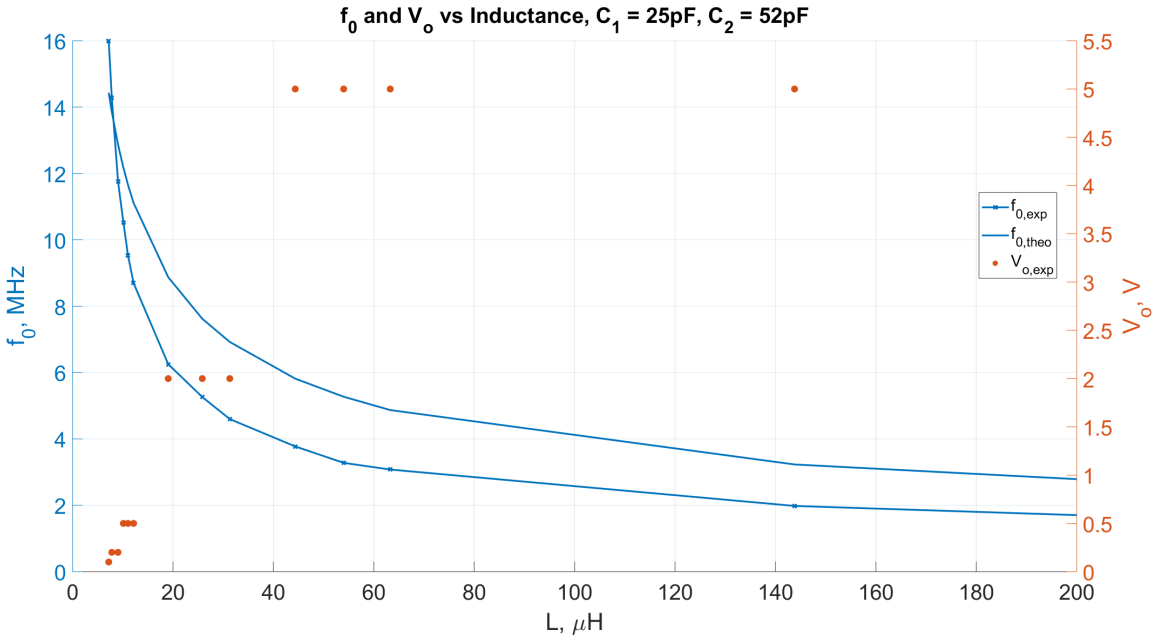

Figure 3.13: Experiment 3, Data Set 2

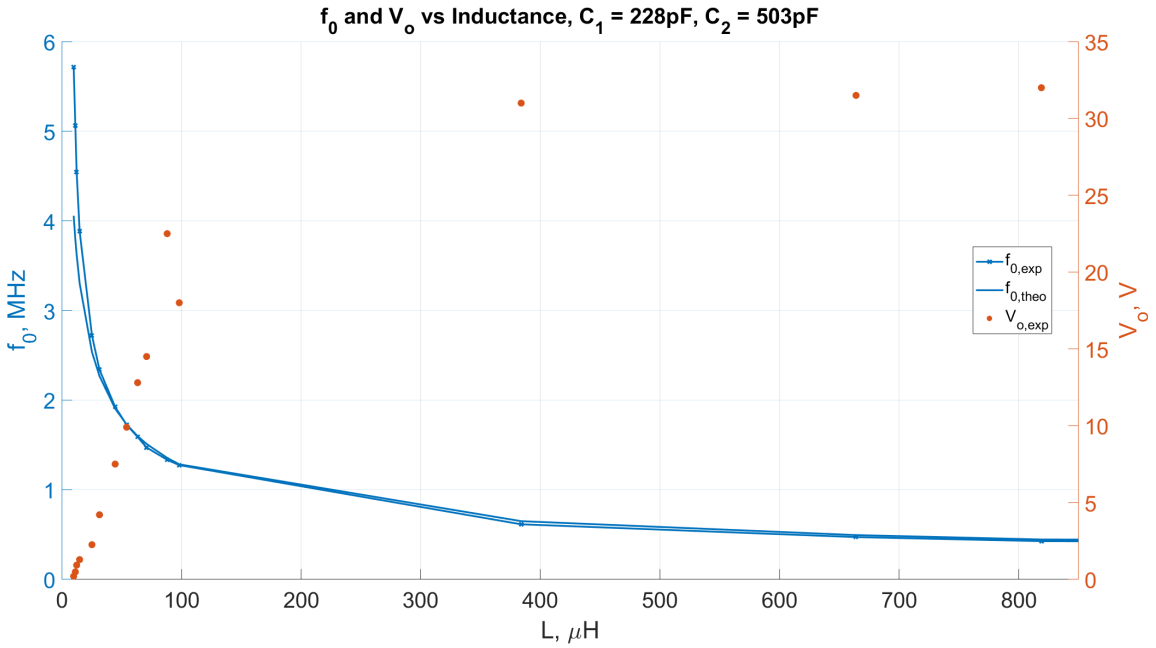

Figure 3.14: Experiment 3, Data Set 3

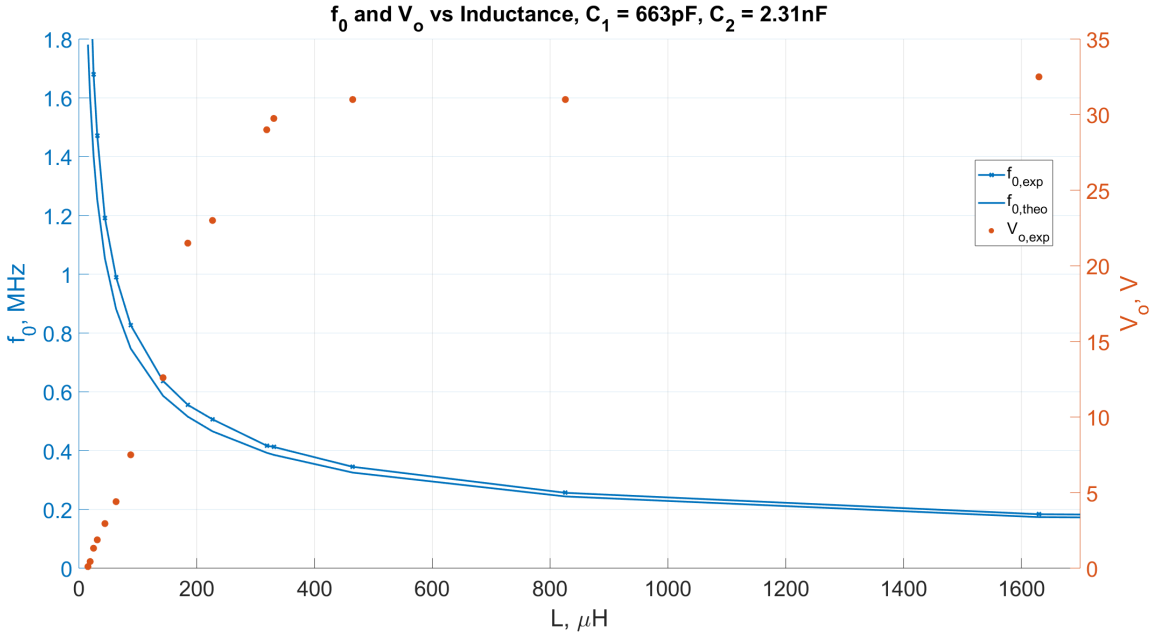

Figure 3.15: Experiment 3, Data Set 4

While equations 2.13 and B.6 provide more sophisticated methods for computing the resonant frequency, the experimental frequencies in figures 3.12, 3.13, 3.14, and 3.15 are of the simplest kind, whereby $f_0 = \frac{1}{2\pi\sqrt{LC}}$ and C is the series combination of the oscillator capacitors. Only in the case of figure 3.13 is there a large discrepancy between the magnitudes of the theoretical and experimental frequencies. Despite the difference in the values of the frequency plots, their behavior is similar.

In all four cases, there is a relationship between the linear (or at least rising) portion of the voltage data and the rapidly falling portion of the frequency. Because the real phenomenon predicting saturation is the derivative of the frequency with respect to inductance, this function could be plotted instead. That curve however is less instructive than the graphics already presented. Figure 3.16 is the same data as figure 3.12 but with the derivative of frequency with respect to inductance plotted alongside output voltage.

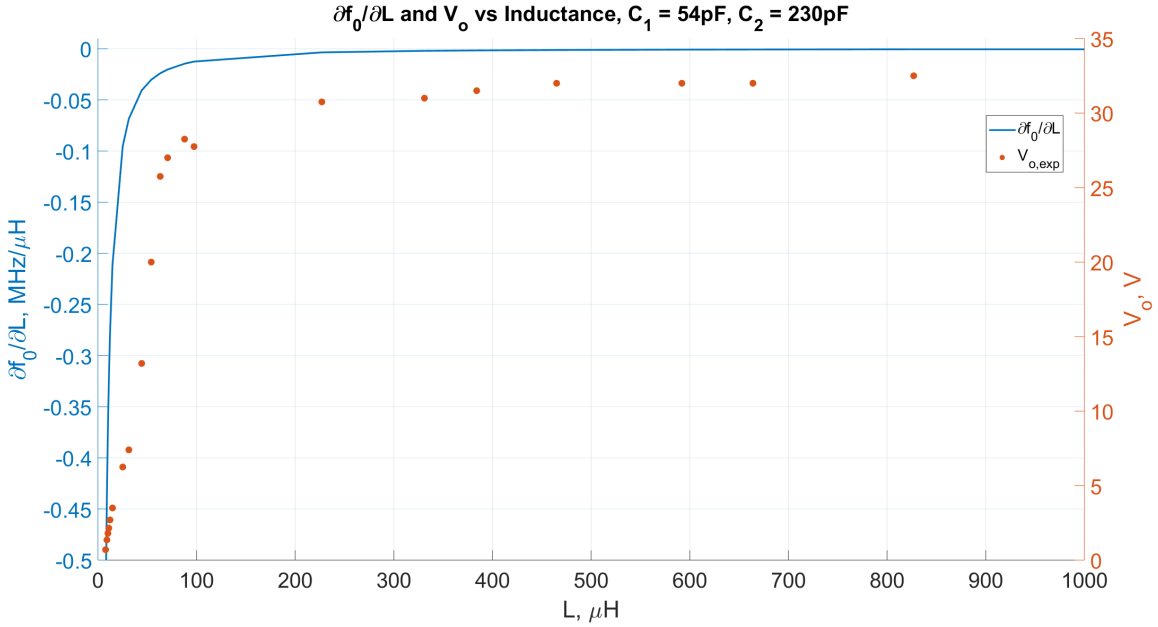

Figure 3.16: Experiment 3, Data Set 1

In the portion of figure 3.16 where the voltage is still rising with inductance, the derivative of the frequency is very near to zero but is not yet asymptotically close. At a

glance, this figure indicates that only a very narrow set of inductors will produce a non-saturated output voltage, while experimentally, the largest tolerable inductance is close to 100 μH. This range is better viewed in figure 3.12, where the graph depicts that a non-saturated output voltage may be obtained while the frequency is not asymptotically flat with increasing inductance.

Experiments 1, 2 and 3 imply a partial method for selecting components when constructing an oscillator. While they do not predict the amplitude of the output voltage, they do provide an indication of a maximum value for the inductor given a desired resonant frequency, bias current, and series capacitance value.

3.1.4 V_o Experiment 4: Dependence on C

The voltage saturation method of the previous experiment is a plot of resonant frequency versus inductance. Resonant frequency is a function of capacitance and inductance. A plot of resonant frequency versus capacitance may then reasonably be expected to be significant.

This experiment is similar to the last three except that in this case, all circuit elements are maintained and only the capacitors are varied. As was seen in experiments 1 and 2, the output voltage is not strongly correlated to the capacitance ratio so any sufficiently large n is acceptable. The simplest choice is $n = 0.5$ where $C_1 = C_2$.

The circuit used in this experiment is that of figure 3.2 with $L = 4.75\ \mu H$ and $V_{CC} = V_{EE} = 10\ V$. The capacitors were measured and selected to be very close to identical, both in value and in type. Figure 3.17 is a plot of the output voltage amplitude and theoretical resonant frequency against the series value of the capacitors.

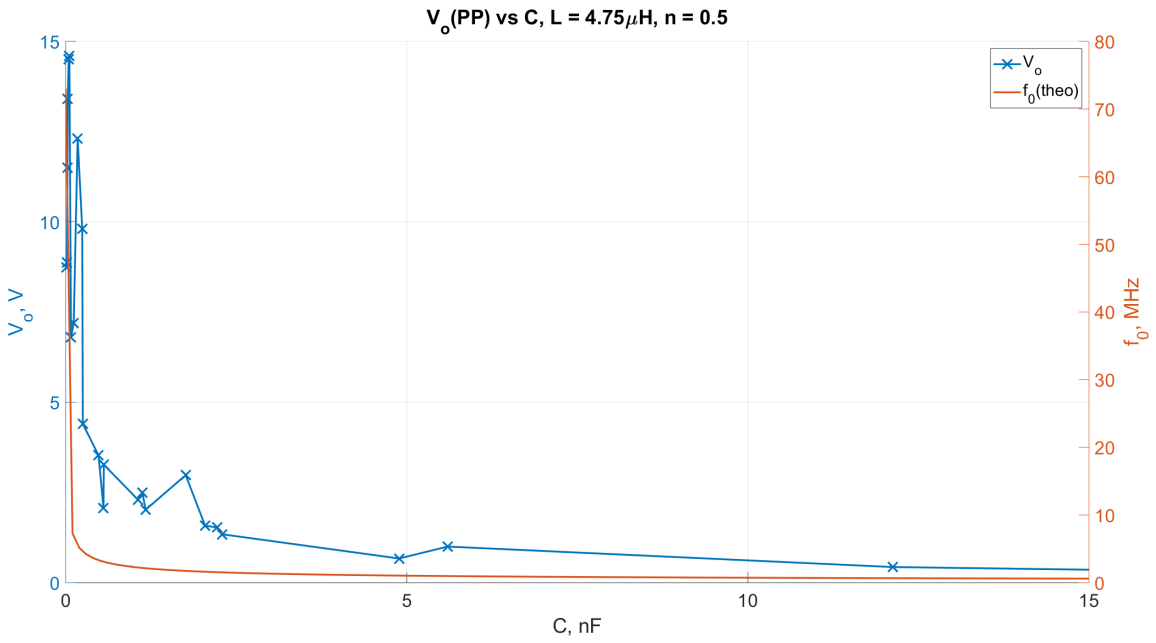

Figure 3.17: Experiment 4 - V_o vs C

Figure 3.17 shows a strong correlation between output voltage amplitude and resonant frequency as functions of capacitance and the data are in agreement with the Huang [7] and Imani [8] predictive equations. Using a plot of resonant frequency versus capacitance, it looks possible to predict a capacitance value that will yield a large output voltage or the point beyond which any increase in capacitance will yield an output voltage amplitude tending very slowly to zero. The oscillation was not measurable past $C_1 = C_2 = 50\ \ nF$.

3.1.5 V_o Experiment 5: Dependence on n

The first two experiments demonstrated that in most cases the capacitive ratio n did not affect the output voltage amplitude much for a given inductor. To investigate the effect of n on the output voltage more comprehensively, only the C_2 capacitor is varied in this experiment. Figure 3.18 is a plot of the data for the C_2 range of 0 (absent) to 700 nF.

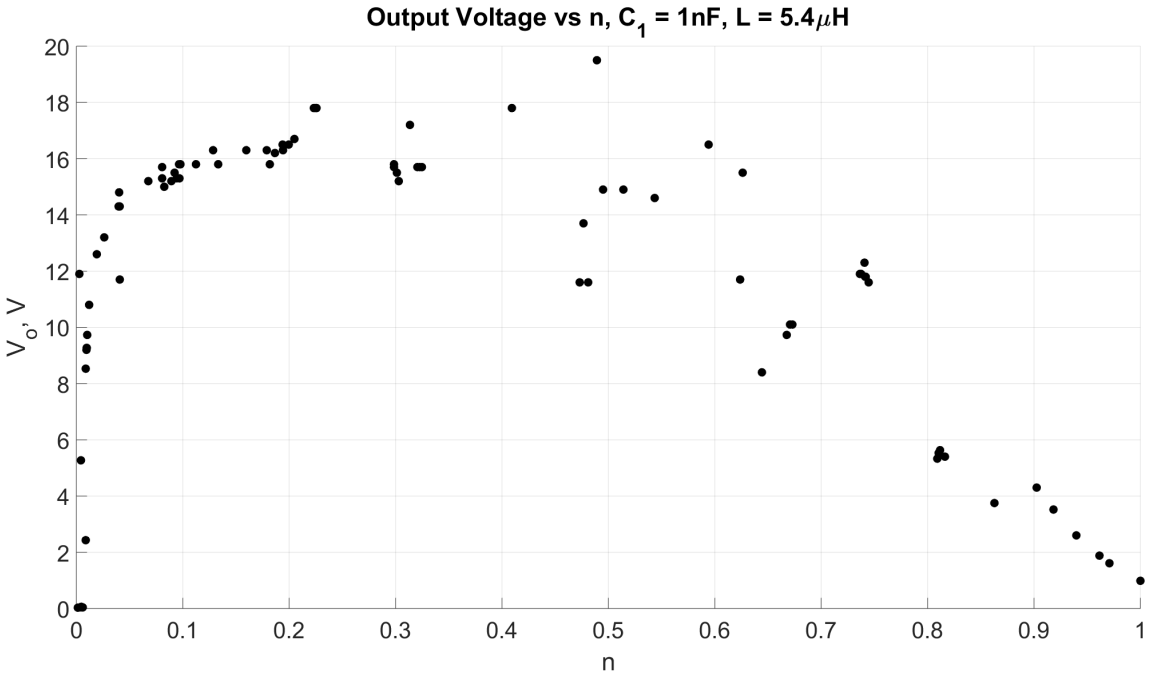

Figure 3.18: Experiment 5 - V_o vs n

Many of the data points appear erratic in figure 3.18. For extremely small n, no oscillation was measurable. As n increased to approximately 0.02, the output voltage was linear with n. Between $n = 0.05$ to $n = 0.35$, the output voltage generally remained constant. When $C_1 \approx C_2$, the plot is erratic but the average corresponds to the stable region for lower n. Beyond $n = 0.5$, the output voltage drops linearly with increasing n. In this experiment there is a measurable output voltage for $C_2 = 0$. This result may be due to the base-emitter junction having enough capacitance to allow for oscillation.

3.1.6 V_o Experiment 6: Dependence on Biasing

This experiment investigates the dependence of output voltage on V_{CC} and V_{EE}. The oscillator used is the baseline oscillator of the first experiment in the frequency domain section (section 3.3.1). The capacitive ratio is 0.46 and the inductor is 2.7 μH. In this experiment, both DC supply voltages were varied at 500 mV increments and peak-to-peak output voltage measurements were taken at each sample. Figure 3.19 is a

plot of the data.

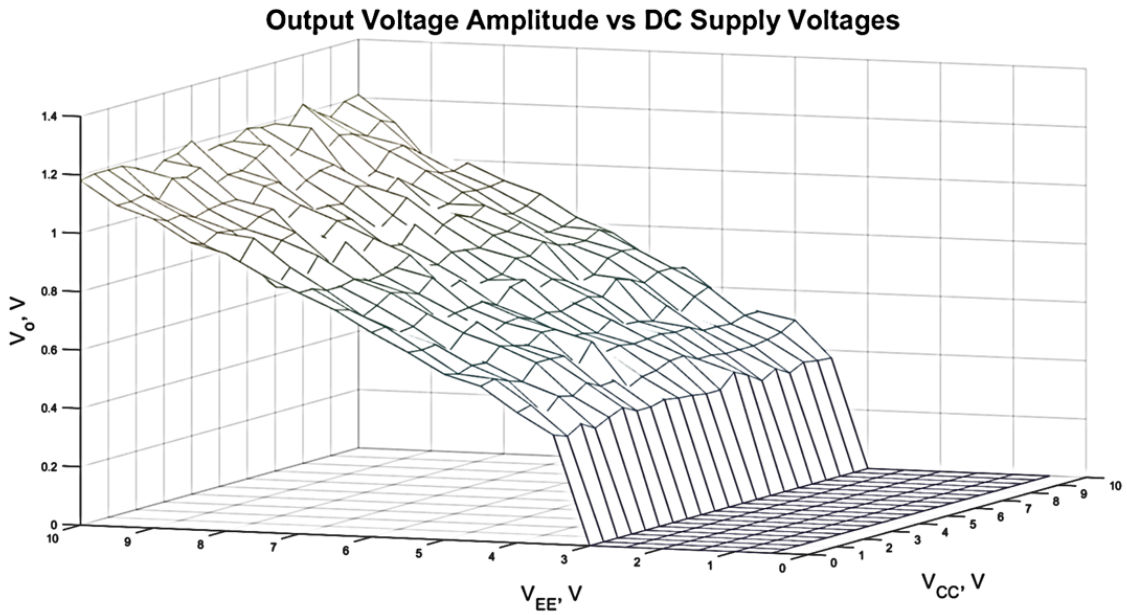

Figure 3.19: V_o Experiment 6 - $V_o(pp) = f(V_{CC}, V_{EE})$

Figure 3.19 shows that in this experiment V_{CC} has no effect on the output voltage and the output voltage amplitude is linear with the emitter current. The relationship between output voltage amplitude and circuit current agrees with the predictions of Huang [7] and Imani [8]. The explanation for the lack of effect of the positive supply voltage on the output voltage amplitude is that the output voltage is small throughout the scope of this experiment.

Though most of the output voltage graphics in this thesis display only the AC waveform, oscillation occurs on top of the positive DC supply, or V_{CC}.[1] For the dual-supply biasing scheme used in this circuit, the emitter voltage is equal to the voltage drop across the base-emitter junction, or $-V_{BEQ}$. The maximum peak output voltage obtained in this experiment is 0.6 V – just smaller than V_{EQ}. The positive voltage swing is not limited in this type of oscillator, but the negative swing cannot drop below V_E. V_{CC}

[1] less the voltage drop across the inductor which is usually negligible.

then is used to lift the offset of the oscillation so that the waveform does not saturate. Thus all of the saturated output voltages obtained in experiment 3 could have been corrected by increasing the positive DC voltage supply, though the voltage-divider biasing would also have to be adjusted to maintain the same emitter current and quiescent emitter voltage level.

To demonstrate that V_{CC} is only necessary if the peak amplitude of oscillation is greater than $-V_{BEQ}$, the circuit of figure 3.20 was constructed.

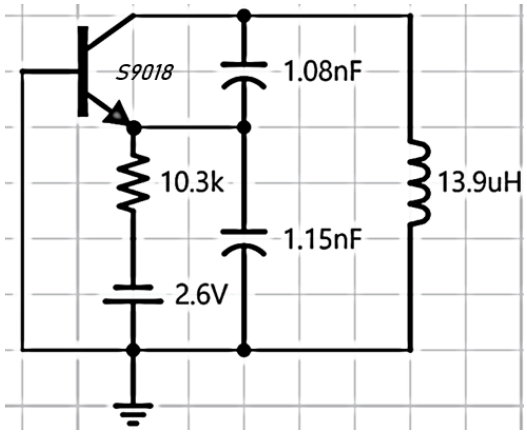

Figure 3.20: Oscillator without Positive DC Voltage Supply

As constructed, the output voltage does not saturate. Increasing the negative DC voltage supply to –5.2 V does cause saturation however. Both waveforms are displayed superposed in figure 3.21.

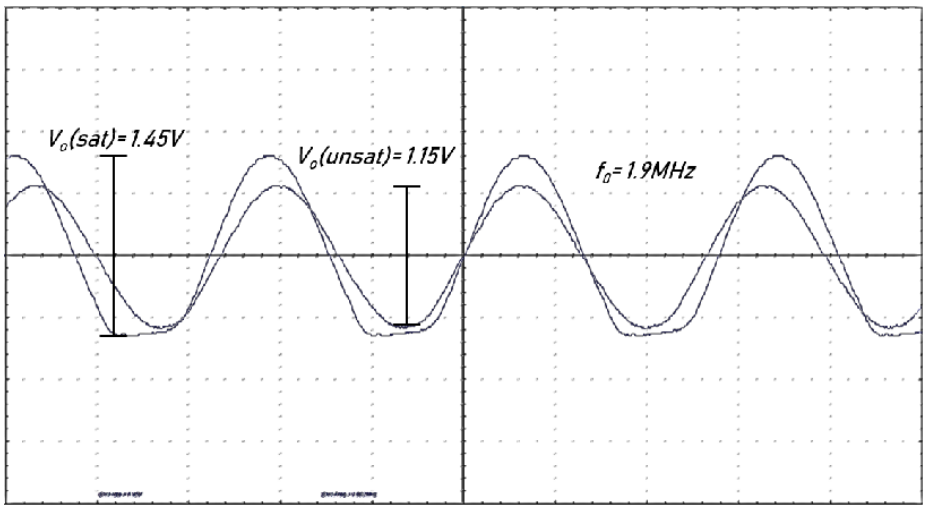

Figure 3.21: Single-Supply Oscillator: Saturated and Unsaturated Output Voltages

To correct the saturated output voltage without changing the emitter current, the circuit is reconfigured to include V_{CC}, which is set to 0.29 V. The corrected output waveform (DC-coupled) is shown in figure 3.22.

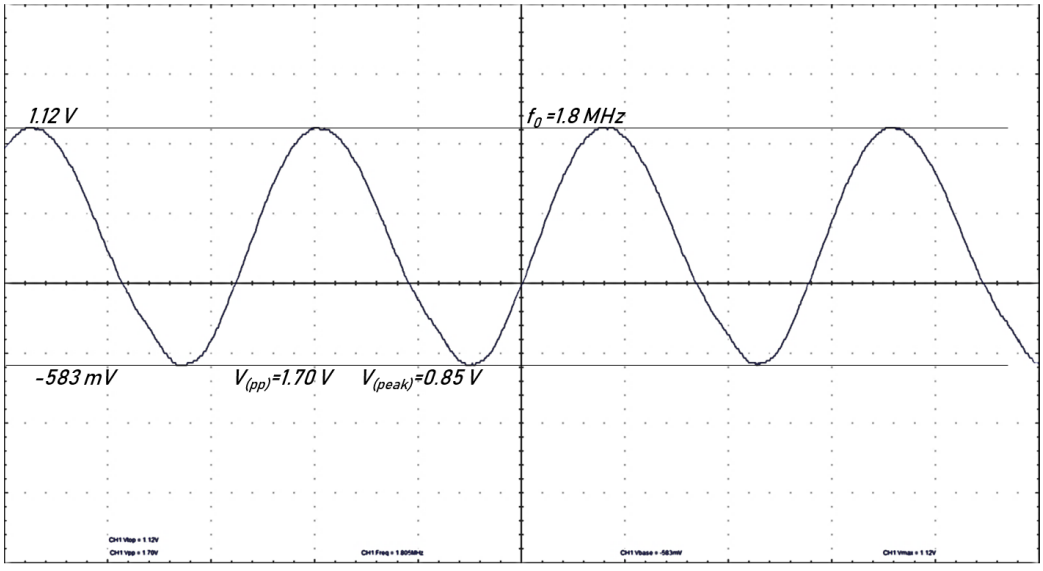

Figure 3.22: Corrected Output Voltage

3.1.7 V_o Experiment 7: Large Inductance Oscillator

To demonstrate that the saturation results of experiment 3 are unnecessary through manipulation of V_{CC}, this experiment investigates an oscillator with a very large inductor and very small capacitors. In all data sets of experiment 3, an inductor greater than 1 mH would have yielded a saturated output voltage. In this experiment, the inductor is approximately 10 mH and saturation is avoided. Figure 3.23 is the circuit schematic with values labeled.

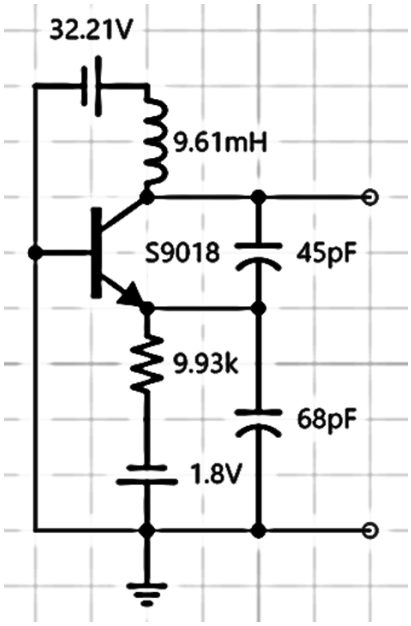

Figure 3.23: Oscillator with Large Inductor, Small Capacitors

The emitter current in this circuit (controlled by the negative DC supply voltage V_{EE}) is very low. It need not be, but accommodating a larger output voltage would have required a large positive DC supply than was available (32 V).

As demonstrated in the first three experiments, the output voltage amplitude is proportional to the inductance and the relationship at least appeared linear. A very large inductor should then cause a very large voltage relative to that of a much smaller inductor. Figure 3.24 is the superposition of the waveform of the circuit as specified in

figure 3.23 and the waveform of the same circuit but with the inductor replaced by one of value $L = 13.9\ \mu H$.

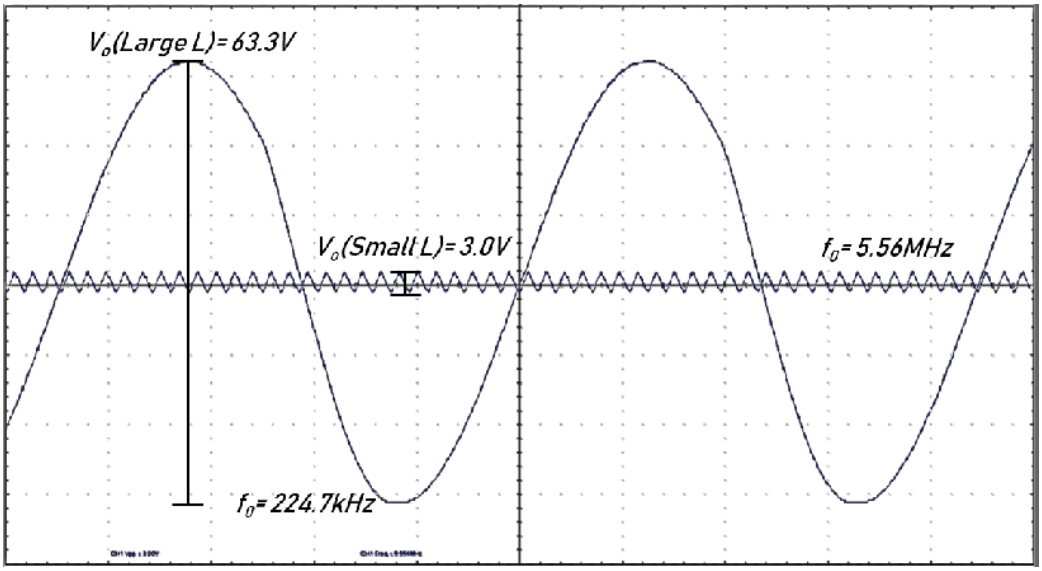

Figure 3.24: Output Waveform for Large Inductance Oscillator

By setting V_{CC} to lift the DC offset voltage and allow for the full swing of the output voltage, saturation is avoided.

3.1.8 V_o Experiment 8: Added Resistance in Series with Inductor

According to equations 2.14 and B.10, there exists a maximum possible equivalent series resistance in an inductor that will still allow oscillation. To test this, the circuit of figure 3.25 was constructed.

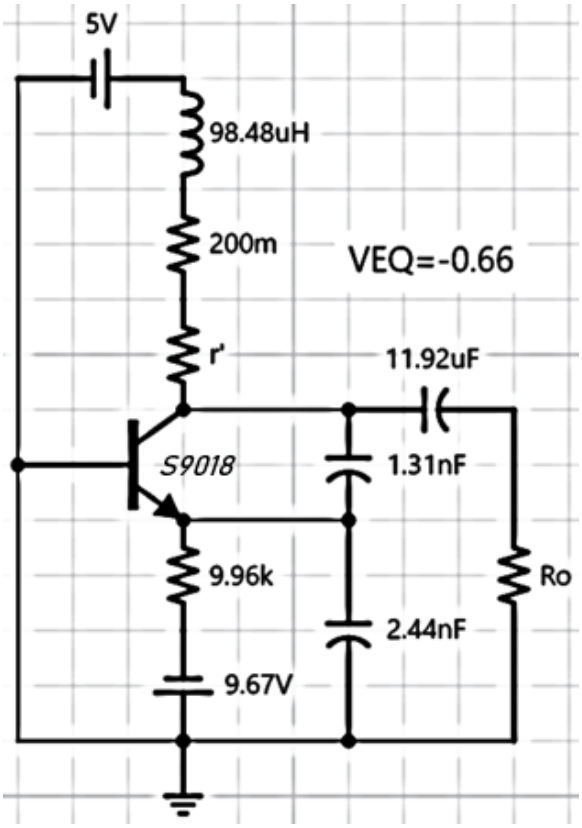

Figure 3.25: Oscillator with Added Resistance r'

Without added resistance, the circuit oscillated at 609.8 kHz with an amplitude of 11.0 V. With a measured current ratio of $\beta = 197.3$, the maximum allowable resistance is $r = 731.9\ \Omega$. As the measured resistance of the inductor is 200 $m\Omega$, this circuit can theoretically support much more resistance. Pushing the maximum value resulted in a very unstable waveform, but adding a discrete resistor $r' = 100.3\ \Omega$ yielded a usable signal. The superposition of the original and augmented output voltages are shown in figure 3.26.

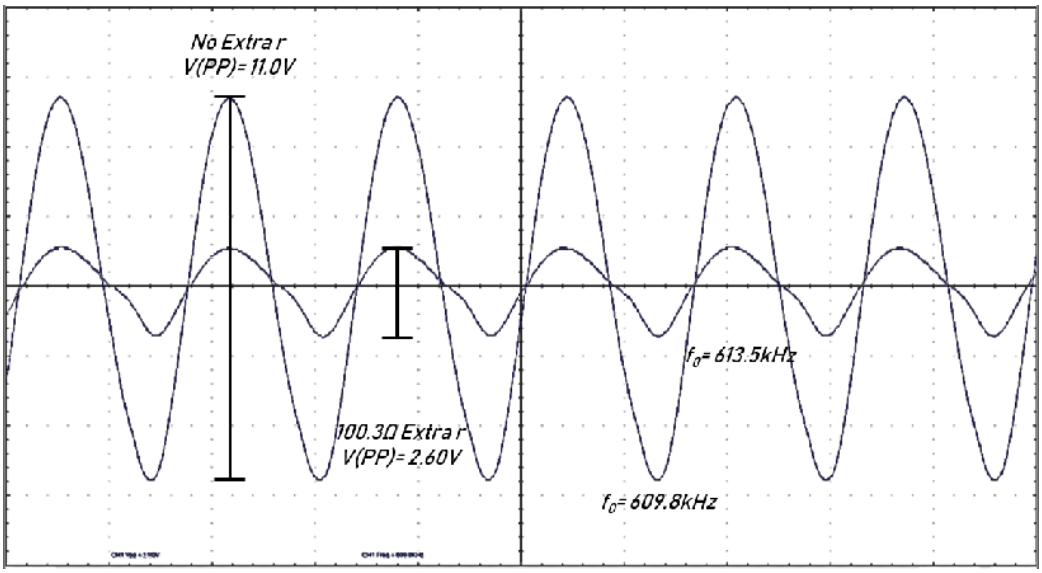

Figure 3.26: Output Voltages of Original and Augmented Circuits

The original signal is nearly sinusoidal except for a small bend in the descending portion. The augmented signal is more distorted. Additionally, the amplitude decreased by 76%. The frequency increased with the additional resistance, though this is predicted by equation B.6. Detectable oscillation was achieved for resistances up to $r' = 552\ \Omega$ though the signal quality was degraded and attenuated to approximately 600 mV with significant amplitude jitter. The analysis of appendix B is confirmed – this circuit was able to support a considerable amount of added resistance though at the cost of distorting the output signal. The effects on output resistance and frequency-domain representation are investigated in sections 3.2 and 3.3.

3.2 Output Resistance Experiments

The first two output resistance experiments were conducted concurrently with the first two output voltage experiments. After each voltage measurement, a potentiometer was coupled through a capacitor to the oscillator and varied until the loaded output voltage dropped to half the unloaded amplitude. The potentiometer was then disconnected and its measured value was taken as the output resistance of the oscillator.

While only the relationship between inductance and output resistance was investigated, the output voltage experiments indicate that all components of the oscillator have an effect on R_o. For the purpose of connecting the oscillator circuit with a follow-on stage, only the order and not the exact value of the output resistance is usually necessary. Measuring resistance through the use of potentiometers is not the ideal method as potentiometers are imprecise and contain parasitics, but the method is sufficient to demonstrate trends.

3.2.1 R_o Experiment 1: Constant C_1

This experiment was conducted concurrently with the first output voltage experiment. The C_1 capacitor was kept constant and the C_2 capacitor varied for each of eleven inductors. Figure 3.27 is a plot of the output resistance versus inductance for each constant-n data set.

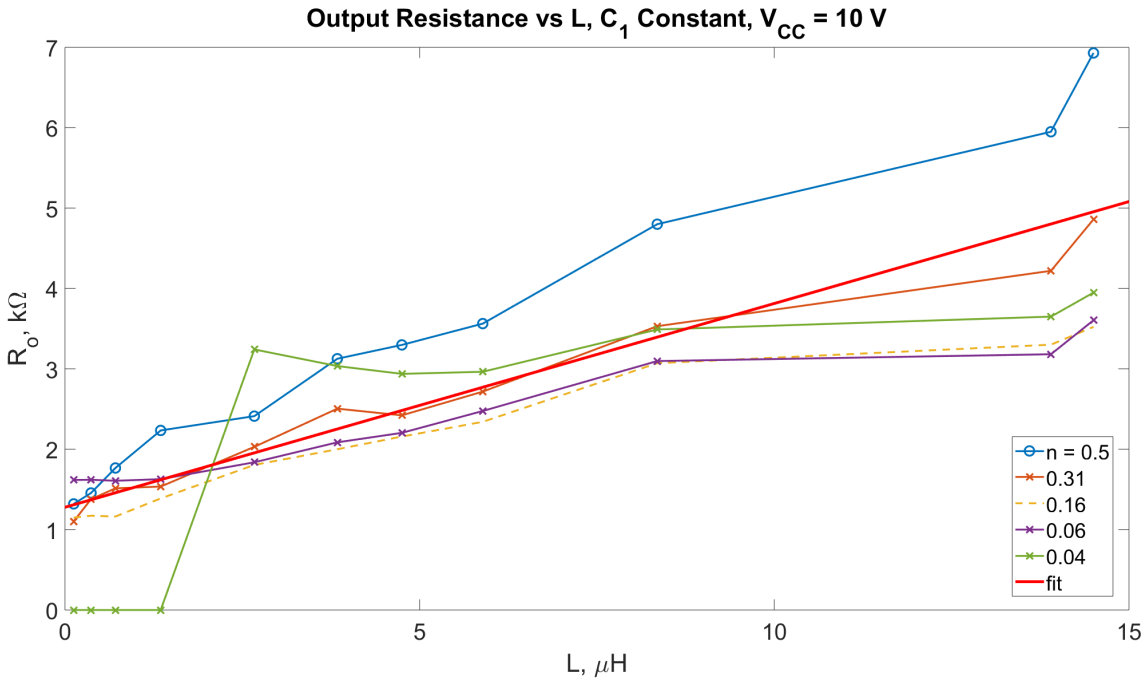

Figure 3.27: R_o vs L, Constant C_1, Slope ($n = 0.31$): 0.25 $k\Omega/\mu H$

With the exception of the portion of the data line corresponding to $n = 0.04$ for very small inductance, the output resistance is nearly linear with inductance. Some of the component combinations did not yield measurable oscillation and they are represented as $R_o = 0$ in figure 3.27. For capacitance ratios smaller than $n = 0.4$, the data became too eratic to include. In addition to the correlation between output resistance and inductance, the data shows that the capacitance ratio has some effect on the output resistance as evidenced by the consistency of the constant-n lines relative to one another. The experiment did not show that this relationship is proportional or linear however.

3.2.2 R_o Experiment 2: Constant f_0

This experiment was conducted concurrently with the second output voltage experiment. In this experiment the resonant frequency is kept constant to determine the validity of the proposed linear relationship between output resistance and inductance. Figure 3.28 is a plot of R_o for constant f_0.

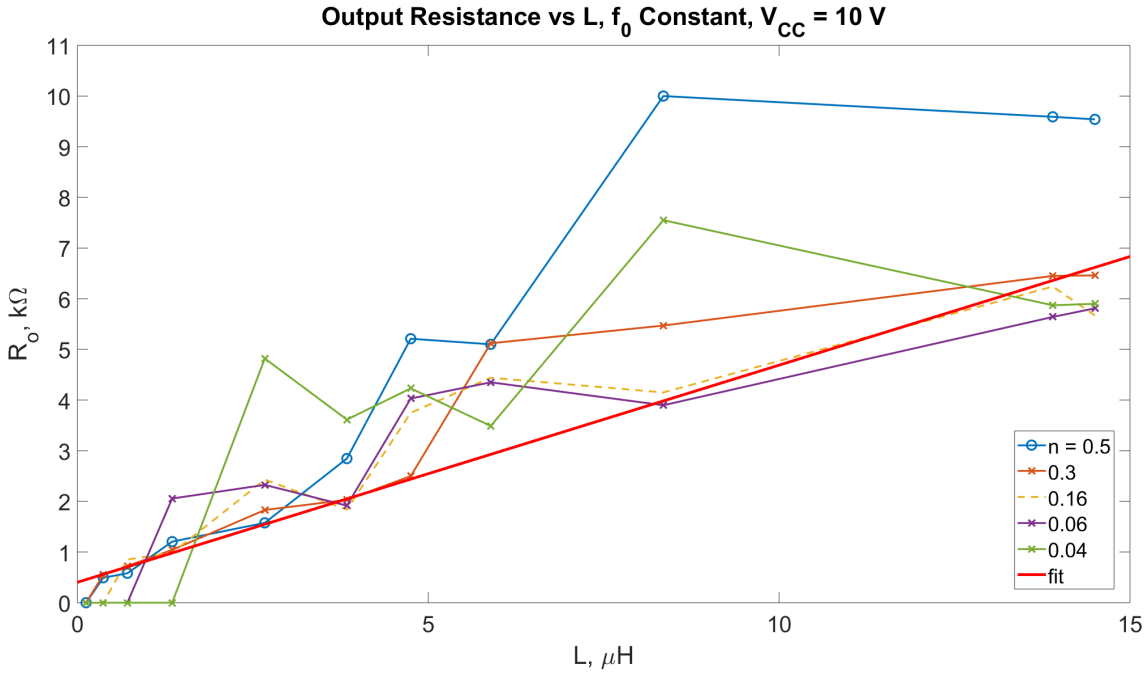

Figure 3.28: R_o vs L, Constant f_0, Slope ($n = 0.3$): 0.43 $k\Omega/\mu H$

Because all three reactive components are replaced for each data point, figure 3.28 is less smooth than figure 3.27. Just as with the output voltage, the data shows a proportional relationship between inductance and output resistance and this experiment further shows that the relationship is a function only of inductance and not resonant frequency.

3.2.3 R_o Experiment 3: Large L, Small C

The first two output resistance experiments indicate that R_o increases with inductance. This experiment tests the output resistance of the circuit of figure 3.23 - an oscillator with a very large inductor and small capacitors.[2] For the R_o vs L trend to be validated, the output resistance measured in this experiment should be extremely large. While that conclusion is indicated by the result of the experiment, no definitive value could be obtained for the output resistance.

The unloaded output voltage for this experiment was 2.4 V peak-to-peak. At $R_L = R_o$, the output voltage should be half its unloaded value, or 1.2 V. Table 3.1 lists the resulting output voltage amplitude for a selection of discrete load resistors.

$V_o(PP)$, mV	R_L, MΩ
0	0.161
60	0.990
265	5.640
700 (avg)	10.200

Table 3.1: R_L and V_o for Large L Oscillator

At $R_L = 10$ MΩ, the output voltage amplitude varied quickly between approximately 500 mV and 2 V. Adding additional 10 MΩ resistors did not improve the result. The 5 MΩ load resistor provided a reasonably stable waveform but its magnitude is much lower than $V_{o,unloaded}/2$. It is likely that the very high resistance above 5 MΩ is

[2]The DC biases for this experiment were very slightly different from those of the V_o discussion in section 3.1.7.

affecting the probe. The results indicate that the output impedance of this circuit is greater than 5 MΩ but additional methods, possibly a transformer or an emitter-follower, are required to determine its value.

3.2.4 R_o Experiment 4: Added Resistance in Series with Inductor

According to equation B.10, there is a maximum allowable resistance in series with the inductor such that oscillation is still possible. According to the analysis of appendix C, the output resistance of a Colpitts oscillator is a function of the equivalent series resistance, such that r reduces R_o. In theory, it is possible to reduce the output resistance of an oscillator by introducing extra resistance r' in series with the inductor. This experiment tests that theory.

The circuit of figure 3.29 was constructed and output resistances were measured for $r' = 0$ and $r' = 100.3\ \Omega$. The resonant frequency of the original circuit is 609.1 kHz.

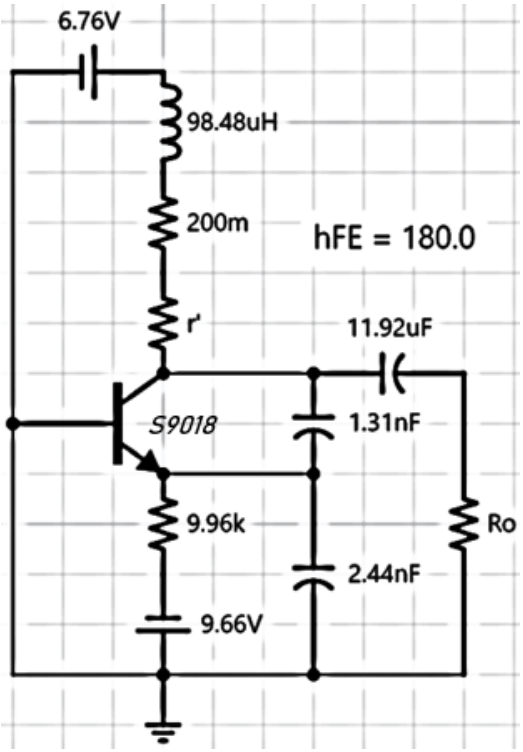

Figure 3.29: Oscillator with Added Resistance r'

The experimental output resistance of the original circuit is 4.79 $k\Omega$ and for the augmented circuit, $R_o = 1.15\ \ k\Omega$. These values are compared with their theoretical counterparts using the Smith [18] method of section 2.2.2. This method identifies different output resistance values depending on the inclusion of the effects of frequency on the admittance transformation (section 2.1.3) and the effect of the inductor's resistance r. These values are listed in table 3.2.

Resistance Type	Value (Ω)
R_o	235.1
$R_{o,\omega}$	1,619
$R_{o,r}$	235.0
$R_{o,\omega,r}$	**1,615**
$R_{o,r'}$	203.5
$R_{o,\omega,r'}$	**782.8**

Table 3.2: Theoretical Output Resistances of Oscillator with Added Resistance r

In table 3.2, R_o is the output resistance assuming no frequency effects and no resistance r. $R_{o,\omega}$ includes the frequency effects of transforming the input resistance across the output. $R_{o,r}$ includes the effect of the inductor's resistance but ignores the transformation effects, and $R_{o,\omega,r}$ includes both effects. The label r' indicates the inclusion of the extra resistance in series with the inductor.

While the predicted and measured values are very different, adding the extra resistance resulted in a drastic drop in both theoretical and experimental output resistances.

3.3 Frequency Domain Experiments

The experiments in this section exhibit the frequency-domain representations of oscillators of various characteristics. The first experiment is an exhibition of a well-behaved oscillator with nearly sinusoidal output voltage and balanced dual-supply biasing. The second experiment compares the frequency plots of a saturated and

unsaturated oscillator. The third compares the frequency plots of an oscillator with and without extra resistance in series with the inductor.

In the case of the oscillator with the large inductor, the output resistance was too large to couple the circuit physically with the spectrum analyzer without resort to extra components or transistor stages. By fashioning a sort of antenna to the spectrum analyzer probe, the data was obtained and values are relative. However, the difference between the fundamental level and the harmonic levels are accurate.

In the other two cases, a large and small load resistor were capacitively coupled to the oscillator. The probe was then connected in parallel with the small resistor in order to keep prevent the spectrum analyzer from loading the circuit and completely killing the oscillation.

3.3.1 Frequency Domain Experiment 1: Baseline Oscillator

This experiment was designed to provide baseline results to compare the data from the remainder of the oscillators in this section. Table 3.3 identifies the component values for the dual-source biasing oscillator of the type in figure 3.2 and throughout this thesis. The transistor used was the S9018. Figure 3.30 is the output voltage waveform.

V_{CC}	10 V
V_{EE}	10 V
L	2.67 μH
r	200 $m\Omega$
C_1	9.57 nF
C_2	11.3 nF
R_E	9.92 $k\Omega$
n	0.46

Table 3.3: Baseline Oscillator Component and Bias Values

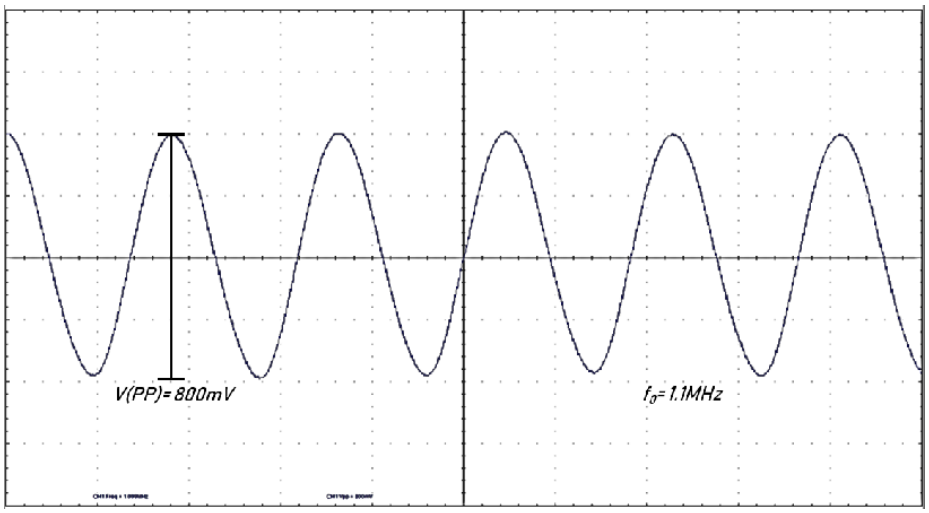

Figure 3.30: Baseline Oscillator Waveform

The component values comply with the frequency-vs-inductance method introduced in section 3.1 and the waveform is generally free from distortion, though there is some jitter present not visible in the plot. The voltage amplitude is much smaller than either of the DC voltage sources and should not be a problem for a follow-on stage using the same DC sources.

The resolution bandwidth was set to 1 kHz for measuring harmonics. Figure 3.31 is a plot of the output voltage in the frequency spectrum and table 3.4 lists the relative power at each harmonic of significant power. The noise below the fundamental frequency in figure 3.31 was present before turning on the oscillator, as was the small peak between the third and fourth harmonics.

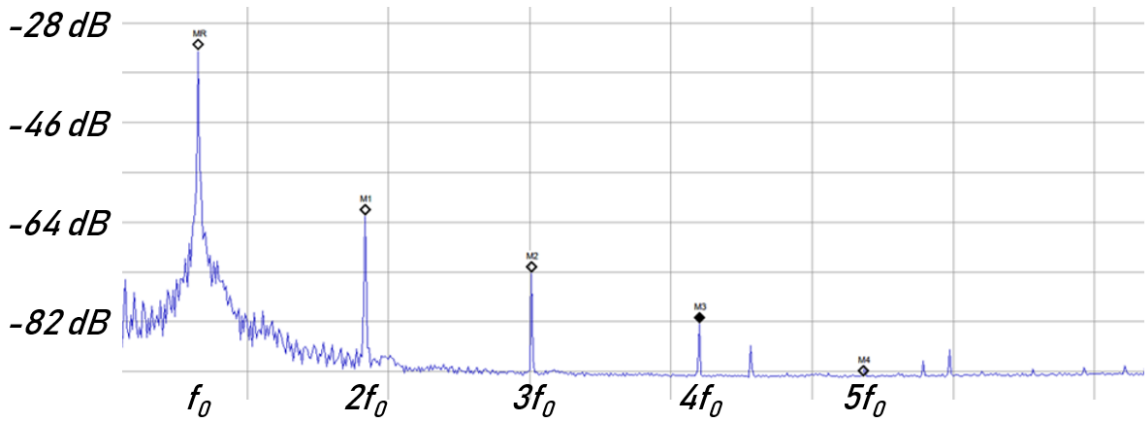

Figure 3.31: Baseline Oscillator Harmonics

f_0 = 1.1175 MHz		
Harmonic	Frequency (MHz)	ΔP (dB)
$2f_0$	2.246	-29.83
$3f_0$	3.362	-40.23
$4f_0$	4.490	-49.42
$5f_0$	5.594	-59.04

Table 3.4: Baseline Oscillator - Relative Power at Harmonics

While harmonics are present, their power contribution is quite small compared to the carrier. This oscillator does not have perfect characteristics but it also has no large defects. All remaining experiments exhibit deviations from this example.

3.3.2 Frequency Domain Experiment 2: Large L, Small C

In this experiment, the circuit of figure 3.23 is supplied by two sets of DC voltages. Because the oscillator features a very large inductor and two very small capacitors, the emitter current must be very small to avoid saturation. In the first scenario, with $V_{CC} = 1.20\ \ V$ and $V_{EE} = -2.51\ \ V$, the waveform is nearly sinusoidal. In the second, $V_{CC} = 21.0\ \ V$ and $V_{EE} = -4.01\ \ V$ and the oscillator is driven into saturation. Because of the extremely high output resistance of this circuit, the frequency spectrum data was

obtained via radiation to the spectrum analyzer and not directly through physical connection with the probe.

Unsaturated Large-Inductor Oscillator Figure 3.32 is the waveform in the unsaturated case and figure 3.33 is its frequency-domain representation out to 5 MHz.

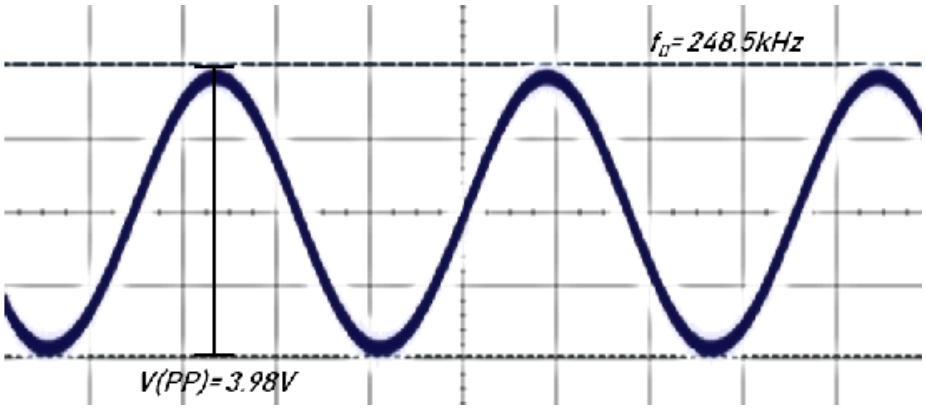

Figure 3.32: Large-Inductor Oscillator - Unsaturated Waveform

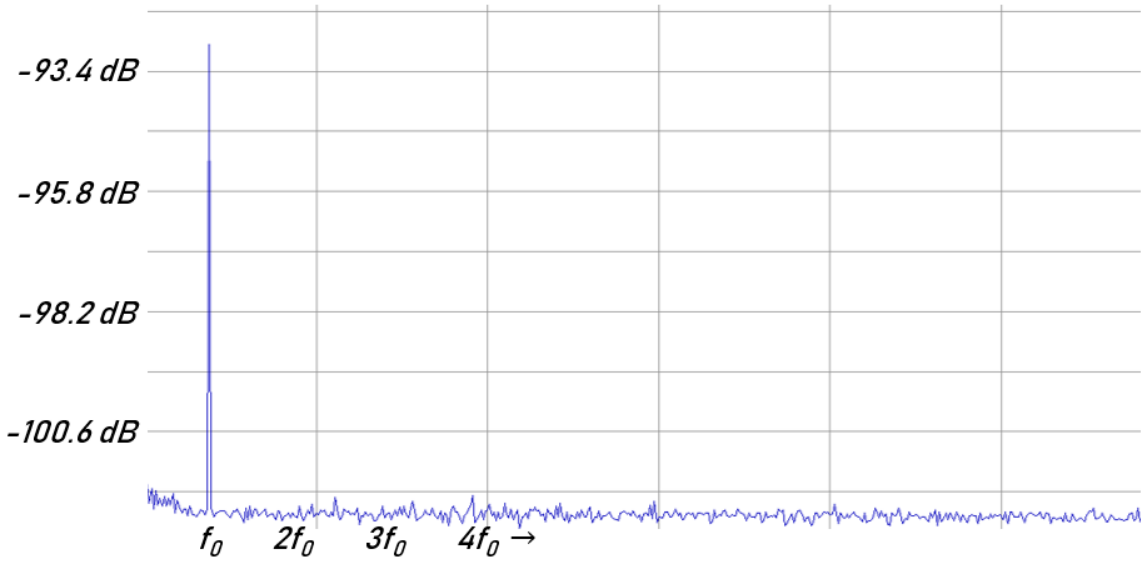

Figure 3.33: Large-Inductor Oscillator Harmonics - Unsaturated

The waveform in figure 3.32 is very sinusoidal and only the fundamental frequency appears on the spectrum analyzer as seen in figure 3.33. However, the oscillator's DC supply voltages are very low. The resonant frequency is only 8.3 dBm above the noise floor and presumably harmonics would appear with higher radiated power. In the case of the baseline oscillator, the first harmonic was almost 30 dB lower than the fundamental frequency.

Saturated Large-Inductor Oscillator Figure 3.34 is the output voltage for the oscillator supplied by larger DC voltages. The waveform is distorted both by clipping at the bottom portion and also by the linear descending leg of the waveform.

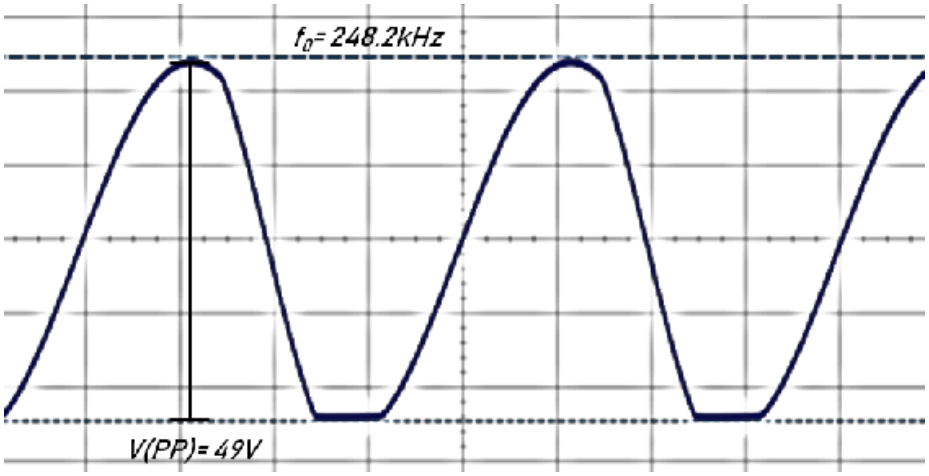

Figure 3.34: Large-Inductor Oscillator - Saturated Waveform

Figure 3.35 is its frequency-domain representation again out to 5 MHz. There are significant components at the first five harmonics and non-negligible components through the span of the measurement. Table 3.5 lists the differences in power from the fundamental frequency at each harmonic.

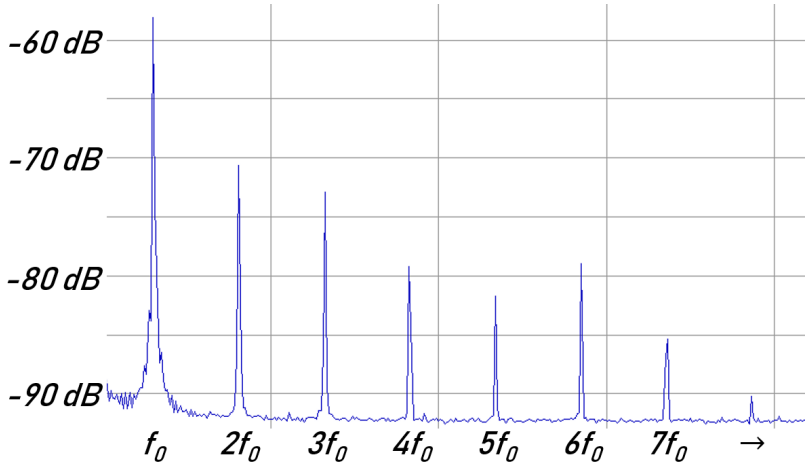

Figure 3.35: Large-Inductor Oscillator Harmonics - Saturated

f_0 = 247 kHz		
Harmonic	Frequency (kHz)	ΔP (dB)
$2f_0$	498.1	-12.59
$3f_0$	749.2	-14.69
$4f_0$	994.2	-20.81
$5f_0$	1,245	-23.67
$6f_0$	1,496	-20.91
$7f_0$	1,742	-25.77

Table 3.5: Large-Inductor Oscillator (Saturated) - Relative Power at Harmonics

The power at each harmonic for this oscillator is much larger than those of the baseline oscillator, although the relative waveforms' appearances predict this. The same result should be obtained from a comparison with the unsaturated large-inductor oscillator, although the impedance limitation makes this measurement impractical.

The harmonics of the saturated oscillator are formidable. If a carrier is desired at the frequency achieved by this oscillator, a different set of reactive components should be selected - specifically, a smaller inductor and larger capacitors.

3.3.3 Frequency Domain Experiment 3: Added Resistance in Series with Inductor

It is possible to add resistance in series with the inductor and still achieve oscillation. The primary benefit is a decrease in output resistance but at the cost of output voltage amplitude. This experiment compares the original oscillator with its added-resistance counterpart in the frequency domain to determine the effects of added resistance on the relative size of harmonics.

Oscillator with No Added Resistance Figure 3.36 is the output waveform of the circuit in figure 3.25 with no additional resistor r' added.

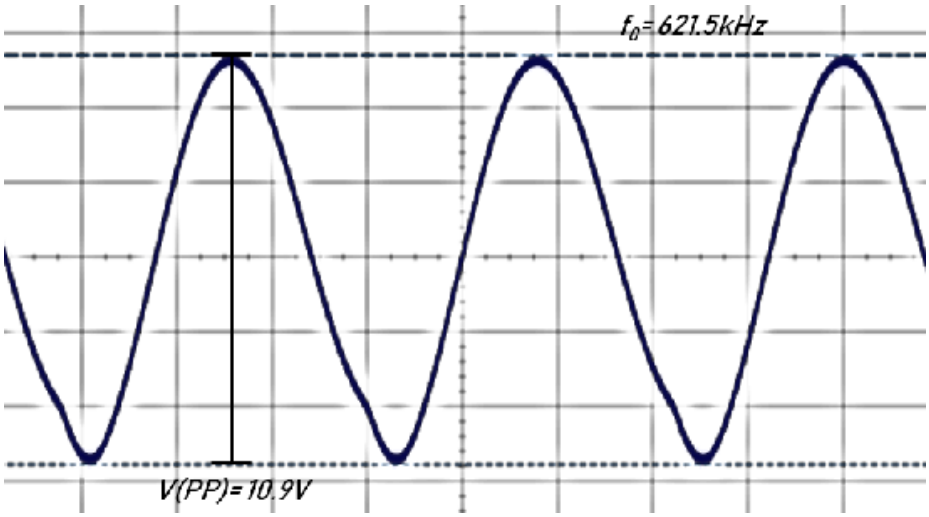

Figure 3.36: Oscillator with No Added Resistance - Waveform

The waveform exhibits some small distortion because of its large inductor relative to the small capacitors, however it is this combination that allows for so much added resistance.

Figure 3.37 is a plot of the harmonics and table 3.6 lists the relative power at those harmonics.

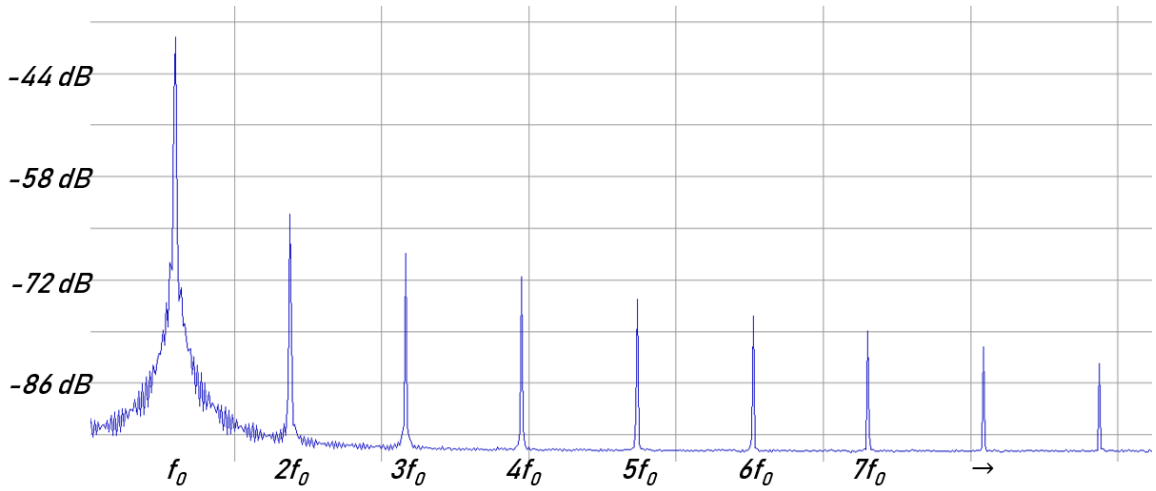

Figure 3.37: Oscillator with No Added Resistance - Harmonics

f_0 = 621 kHz		
Harmonic	Frequency (MHz)	ΔP (dB)
$2f_0$	1.229	-24.05
$3f_0$	1.848	-29.34
$4f_0$	2.466	-32.55
$5f_0$	3.084	-35.56
$6f_0$	3.702	-37.83
$7f_0$	4.310	-39.82

Table 3.6: Oscillator with No Added Resistance - Relative Power at Harmonics

This oscillator compares poorly with the baseline oscillator and favorably with the saturated large-inductor oscillator in terms of harmonics though the distortion in the output voltage waveform in the time domain predicts this.

Oscillator with Added Resistance Figure 3.38 is the output waveform of circuit 3.25 with an additional resistance $r' = 98.2\ \Omega$.

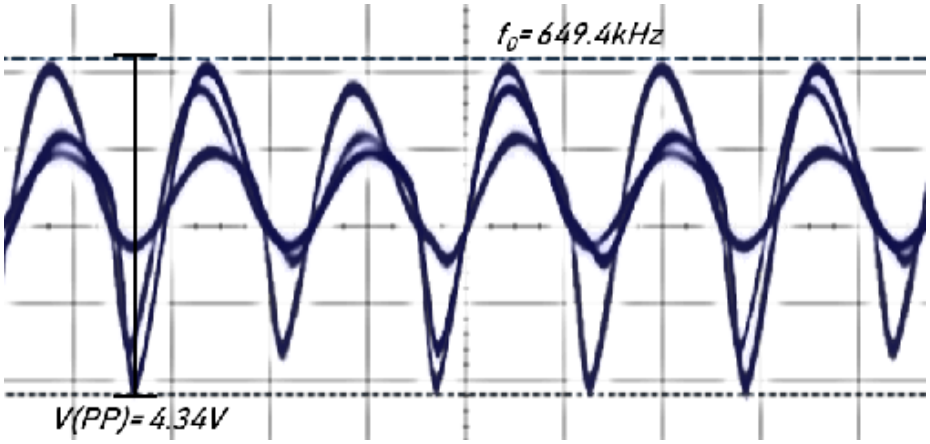

Figure 3.38: Oscillator with Added Resistance - Waveform

The waveform of figure 3.38 is periodic and to some extent sinusoidal but also highly distorted.

Figure 3.39 is the frequency plot of this oscillator and table 3.7 lists the relative power values at the significant peaks, though clearly there are more frequencies present than solely integer-multiples of the fundamental frequency.

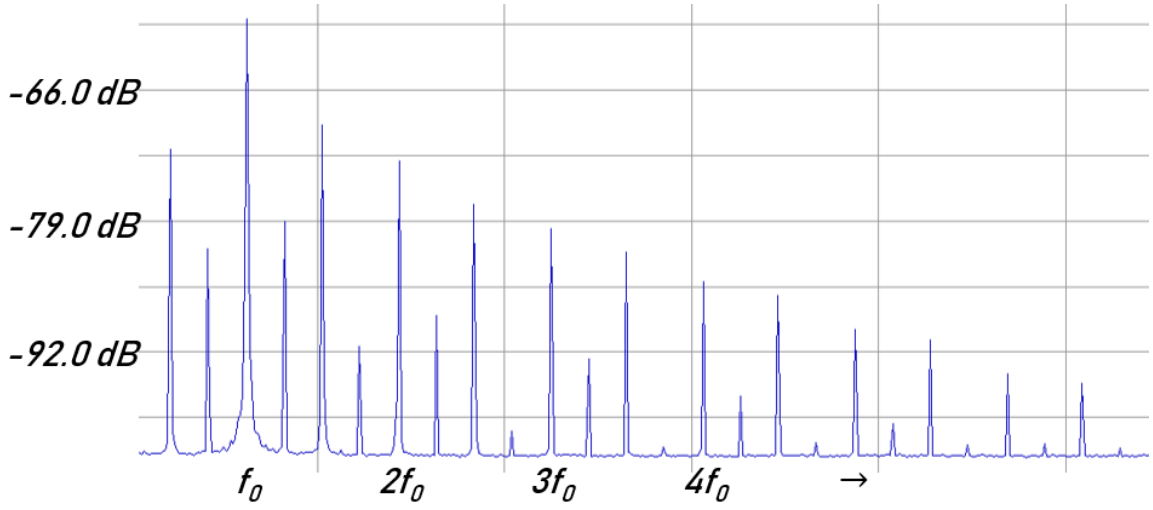

Figure 3.39: Oscillator with Added Resistance - Harmonics

f_0 = 640.9 kHz		
Harmonic	Frequency (MHz)	ΔP (dB)
$1.25 \times f_0$	0.801	-20.14
$1.5 \times f_0$	0.961	-10.64
$1.75 \times f_0$	1.121	-32.52
$2f_0$	1.271	-14.24
$3f_0$	1.911	-20.84
$4f_0$	2.551	-26.18
$5f_0$	3.191	-30.79

Table 3.7: Oscillator with Added Resistance - Relative Power at Harmonics

Figure 3.39 shows significant power components at all quarter-integer multiples of the fundamental frequency as well as nearly identical power values reflected on the opposite side of the fundamental frequency at the same relative distances. The drop in power from the fundamental frequency to the first harmonic is poor with respect to that of the baseline oscillator (-14 dB vs -30 dB). This oscillator would need a high-Q bandpass filter to be of any use. It appears that adding resistance to the inductor is not worth the distortion to the oscillating signal, whatever the benefit to the decreased output resistance.

CHAPTER 4

DISCUSSION

The previous chapter investigated many facets of the common-base Colpitts oscillator and identified several trends. This chapter seeks to combine those trends into a set of guidelines for selecting components for the purpose of constructing an oscillator and especially for controlling the characterists of output voltage amplitude, output resistance, and waveform purity. Areas where further analysis is required will also be discussed as well as other interesting points.

4.1 Output Voltage Amplitude

The primary trends observed in section 3.1 are that output voltage is linear with (or at least proportional to) emitter current and inductance, and inversely proportional to the series-combined capacitance. These relationships were all predicted by Huang [7] and Imani [8] for their circuits. Additionally, as long as C_2 is at least as large but not exceedingly larger than C_1, the output voltage amplitude is generally unaffected by the capacitance ratio. The simplest ratio is 1:1. These observations can be exploited to the extreme to configure an oscillator with a very large output voltage swing or balanced through controlled trial and error to provide an output voltage of any desired amplitude.

The next significant trend seen in the previous chapter is that the positive supply voltage only shifts the DC offset but does not contribute to the output voltage amplitude. This is because the positive supply does not contribute to the emitter or collector currents. If the output voltage amplitude is very large, correctly setting V_{CC} will enable the full swing by keeping the waveform above ground. If a very small output voltage amplitude is desired (peak amplitude less than the size of the voltage drop across the base-emitter junction), then only a single voltage supply acting as a current source may be used.

The final significant trend seen is the frequency-vs-inductance method which helps to identify appropriate inductance values. In the previous chapter, this method was used to predict the maximum inductance value that would not cause saturation of the

output voltage. With the subsequent analysis of the purpose of V_{CC}, voltage saturation need never occur. The frequency rule remains a useful predictor of large output voltage amplitude for a given combined capacitance.

4.1.1 Feedback Gain vs Output Voltage Amplitude

The capacitive ratio n appears throughout the analysis of the Colpitts oscillator. It contributes one third of the expression of the loop gain satisfying Barkhausen's criteria: $ng_mR_o \geq 1$. At first glance, the larger the feedback gain n, the larger the loop gain. The third factor in the loop gain expression is R_o and it is inversely proportional to n^2.[1] Thus the loop gain is reduced to an inverse relationship with n, and a smaller capacitive ratio should result in a larger output voltage.

The analysis of the previous chapter showed a more complicated relationship between the capacitive ratio and the output voltage. As n increases from infinitessimally small to 0.04, the output voltage rises linearly with n. Between $n = 0.04$ and $n = 0.50$, the output voltage remains fairly constant. For n greater than 0.5, the output voltage drops linearly with increasing n. These relationships correspond with the data from experiment 5 of the output voltage amplitude section. According to Smith [18, p. 247], a large loop gain enables the oscillator to self-start and no claim is made about a relationship between loop gain and output voltage amplitude.

4.1.2 Output Voltage as a Function of Inductance

The data from the first three experiments confirm that output voltage is a function of inductance. This is indicated in the Huang [7] and Imani [8] articles. Inductance and emitter current have similar effects on the output voltage so it is possible to compensate for one with the other.

[1] If the approximation for R_o is not applied, output resistance is roughly inversely proportional to n^2.

4.1.3 V_o-Inductance Slope

Confirming the analysis of Huang [7] and Imani [8], the experimental data confirm that the inductance and emitter current have at least an approximately linear relationship to output voltage amplitude and the combined capacitance has an approximately inverse relationship to it. The data in V_o experiments 1-3 identify a slope corresponding to increasing inductance for a set C and I_E. This slope is unique to the components and biasing of each oscillator, but deriving a general formula for $V_o = f(L, I_E, C)$ through experimentation may be possible for this type of circuit.

4.2 Output Impedance

The experiments of section 3.2 sought to discover the relationship of output resistance to inductance and the only attempt to reconcile the theoretical values with experimental occurred in section 2.2.2. Even with the limited scope, the experiments demonstrated the general trend that output resistance is proportional to inductance, a concept absent from the analysis methods of section 2.2.2. The relationship was confirmed with the large-inductance oscillator whose output resistance was too large to make an accurate measurement through use of a laboratory oscilloscope probe as well as the unsuccessful attempt to couple the circuit physically to the spectrum analyzer. The other components of the oscillator certainly affect output resistance and their relationships are likely to mirror those identified for output voltage amplitude.

4.3 Waveform Distortion

The experiments of section 3.3 were selected to demonstrate the differences between the frequency representation of a well-behaved oscillator and those of undesirable oscillators. While experiment 7 of the output voltage amplitude section showed that virtually any inductor can be paired with any capacitor pair [2], larger inductors cause slight distortions in the form of straight, non-sinusoidal, descending legs

[2] assuming a reasonable capacitance ratio.

of the output waveform. These may be due to nonlinear inductor effects. These and other distortions appear as strong harmonics which must be filtered if the oscillator is to be used as a carrier. The analysis did not show a degradation in the peak of the fundamental frequency (i.e. phase noise) regardless of the distortion of the waveform and in fact the baseline oscillator displayed only average performance in that respect compared to the other oscillators investigated. The technique of adding resistance, or by implication using an inductor with very high resistance, was shown to distort the waveform and add strong harmonics and subharmonics to the frequency representation.

4.4 Guidelines for Oscillator Construction

Regrettably, no formula predicting output voltage and output resistance for a given set of components was produced in this work. In place of a definitive prediction method is an informed process of trial and error. To demonstrate the reliability of the relationships between output voltage and L, C, and I_E, two example oscillators will be constructed for two arbitrary sets of design requirements. Some intermediate incorrect choices will be omitted but the process for component selection will remain.

Guidelines for Oscillator Construction The general guidelines in no particular order are presented here. In the absence of specific requirements, setting the emitter current to 1 mA and the capacitive ratio to 0.5 are reasonable starting points. While the choice of transistor will affect the output characteristics, the relationships described below are independent of any specific NPN BJT transistor model.

(a) Increase inductance to increase output voltage amplitude.

(b) Increase emitter current to increase output voltage amplitude.

(c) Decrease capacitance to increase output voltage amplitude.

(d) Decrease inductance to decrease output resistance.

(e) Apply the resonant frequency-vs-inductance curve to determine suitability of inductor.

(f) Vary C_1 and C_2 to tune frequency and output voltage amplitude.

(g) Construct oscillator with separate positive and negative DC voltage supplies and then convert to single-supply circuit for difficult design requirements.

(h) Use single negative supply if desired peak output voltage amplitude is smaller than V_{BEQ}.

(i) Vary I_E with a potentiometer as the emitter resistor to tune the output voltage amplitude.

4.4.1 Oscillator 1

Requirements

1. f_0 = 2 MHz
2. V_o = 2 V peak to peak
3. Single DC Supply: 9 V
4. Maximum Output Resistance - 4 $k\Omega$

Process The amplitude of the desired output voltage is larger than a typical V_{BEQ}, so a single negative DC supply voltage will not suffice and guideline (h) is not applicable. The desired output voltage amplitude is small compared to the positive supply, so guideline (g) is not required and the circuit may be easily designed with only one positive DC supply. The biasing may be set first and the output voltage amplitude managed by the selection of the components of tank circuit.

The choice of reactive elements will place the initial output voltage near the desired value but V_o will likely require tuning. The output voltage is easily changed by varying I_E through a potentiometer as the emitter resistor so single base resistor with the emitter potentiometer was chosen as the biasing scheme. Selecting $I_E = 1\ \ mA$ for fast calculation and using a 5 $k\Omega$ potentiometer as R_E (guideline (i)), the base resistor is calculated to be 415.8 $k\Omega$ and selected as $R_B = 448\ \ k\Omega$. The calculated quiescent emitter voltage with these biasing components is 4.9 V, low enough to pass the full 1-V-peak waveform. Because this circuit is a common-base oscillator, a 1 μF bypass capacitor is added to the base to tie it to AC-ground.

In an effort to keep the output resistance low, a small inductor is desirable (guideline (d)). Selecting a value $L = 1.35\ \mu H$, the corresponding combined capacitance for the specified resonant frequency is 4.7 nF. Using this combined capacitance, the $f_0\ vs\ L$ curve is plotted in figure 4.1.

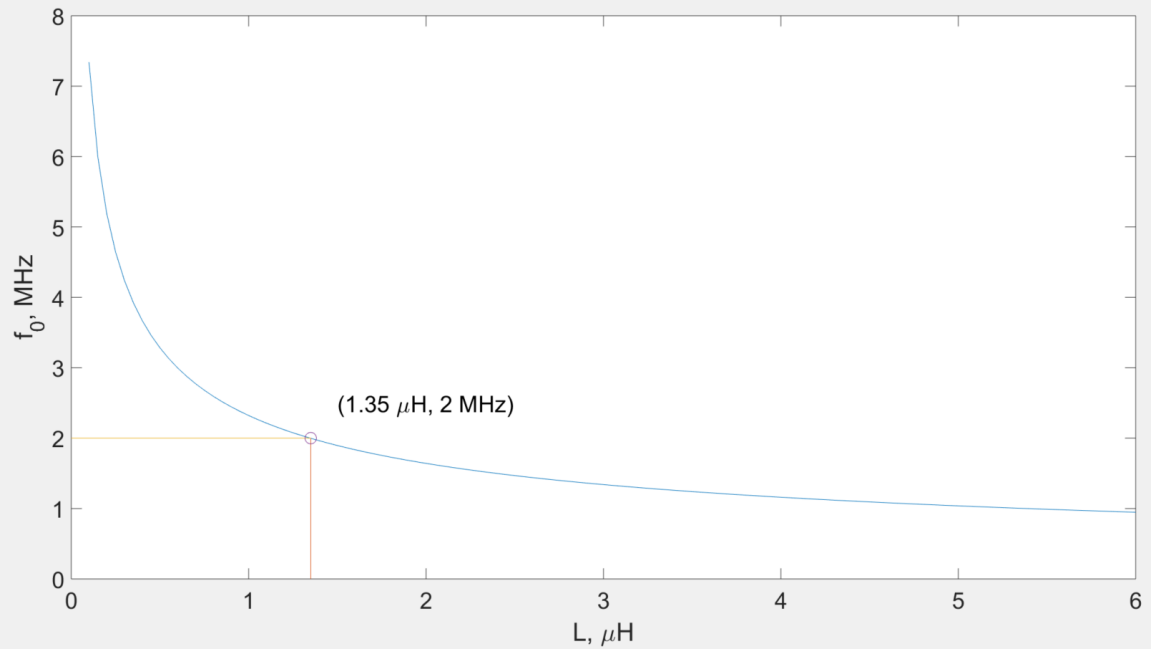

Figure 4.1: Resonant Frequency vs Inductance Curve, $C = 4.7\ nF$

In chapter 3, the output voltage amplitude was shown to be small when the resonant frequency-vs-inductance curve had a steep slope and large when the resonant frequency had a shallow slope. In this case, the point of intersection in figure 4.1 is between the extremes. The output voltage amplitude should correspondingly be moderate and susceptable to tuning. Roughly matching the capacitors to achieve the desired combined value of 4.7 nF, the values C_1 = 9.1 nF and C_2 = 9.5 nF are selected.

Turning on the power supply and varying the potentiometer until a maximum output voltage was reached yielded a peak-to-peak voltage amplitude of 747 mV and a frequency of 1.4 MHz. Because both the frequency and amplitude were too low, guideline (c) suggests that a possible solution for both problems is to decrease capacitance. After

tuning the capacitors to achieve the correct frequency, the amplitude was still too low. The potentiometer was varied in accordance with guideline (i) and a satisfactory output voltage was reached. The potentiometer was replaced by a discrete resistor and the output voltage amplitude and resonant frequency were verified not to have changed.

To test the output resistance, a 3.9 $k\Omega$ resistor was capacitively coupled to verify that the output voltage amplitude did not drop by more than half. Figure 4.2 is the final circuit with component values listed, and figure 4.3 is the superposed loaded and unloaded output voltage waveforms.

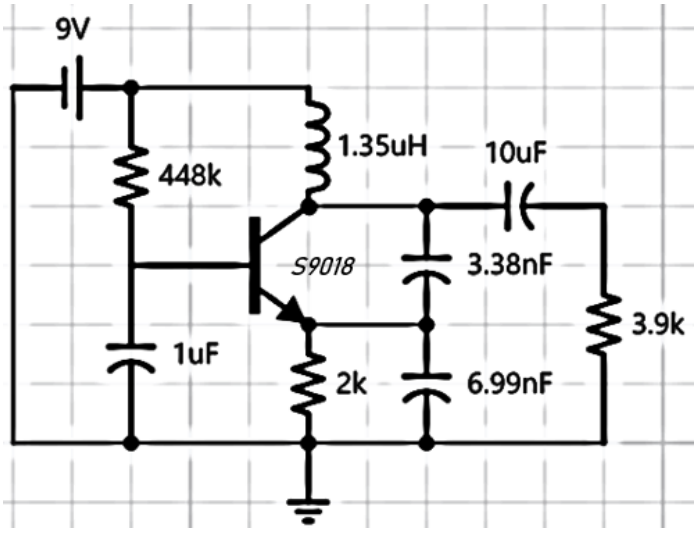

Figure 4.2: First Example Oscillator Circuit

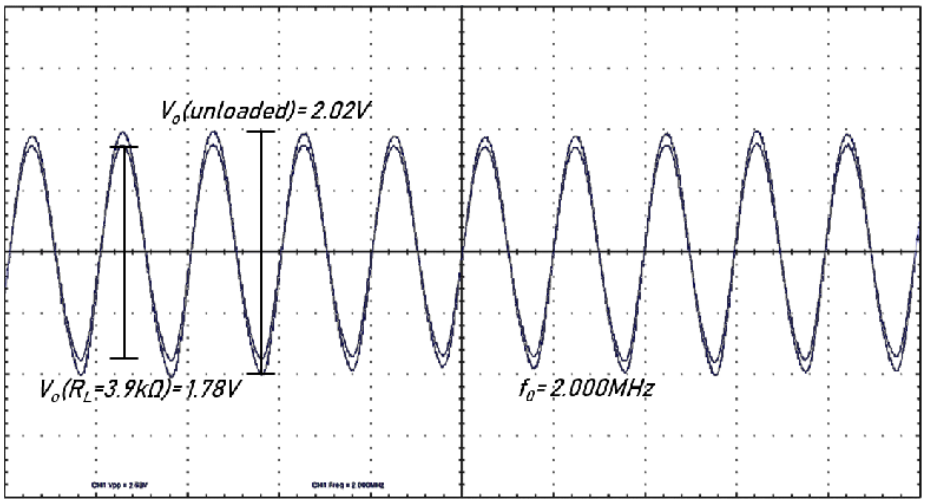

Figure 4.3: First Example Oscillator Waveforms

The circuit of figure 4.2 was simulated for comparison using the PN2222 transistor. Applying the *startup* modifier resulted in no oscillation. Applying *uic* resulted in oscillation for less than 1 ms followed by DC voltage at the level of the supply. With no modifiers applied, the simulated output waveform of figure 4.4 was generated.

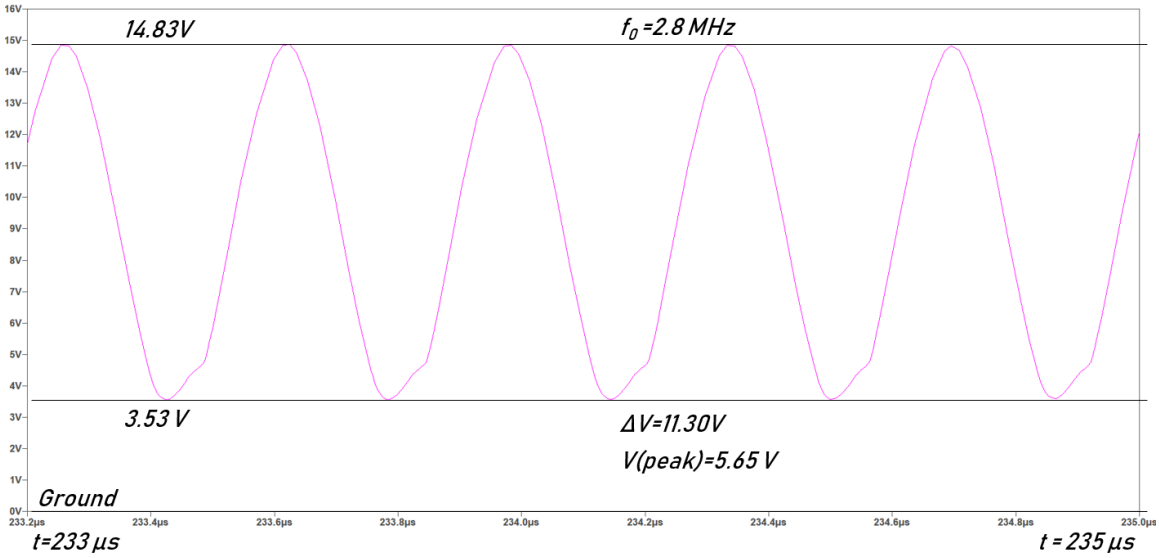

Figure 4.4: First Example Oscillator Simulation: No Initial Conditions

The simulation for this circuit predicts a saturated waveform of greater amplitude and frequency than the experimental circuit generates. This does not prove that the simulation is incorrect, but it does indicate that constructed circuits may be expected to deviate from both theoretical and simulated values. Applying the guidelines of this chapter allows the designer to control the output when this occurs.

4.4.2 Oscillator 2

Requirements

1. f_0 = 8 MHz
2. V_o = 8 V peak to peak
3. Single DC Supply: 5 V
4. Maximum Inductance - 500 nH

Process The requirements of the first oscillator were not difficult to satisfy. The DC voltage supply was large compared to the desired output amplitude so it was not necessary to set the bias values very carefully. In this example, there is little additional room between the bottom of the voltage swing and ground.

The process for the first oscillator was to set up reasonable bias conditions and then tune the circuit with the potentiometer and the capacitance ratio. In this example, it was necessary to build a dual-supply oscillator first in accordance with guideline (g) to ensure that meeting the requirements was possible. Using two supplies replaces the minimum voltage of V_E with $-V_{BE}$ and allows a maximum possible sinusoidal peak-to-peak output voltage amplitude of $2V_{CC} + V_{BE}$. The DC waveform for the dual-supply oscillator is shown in figure 4.5.

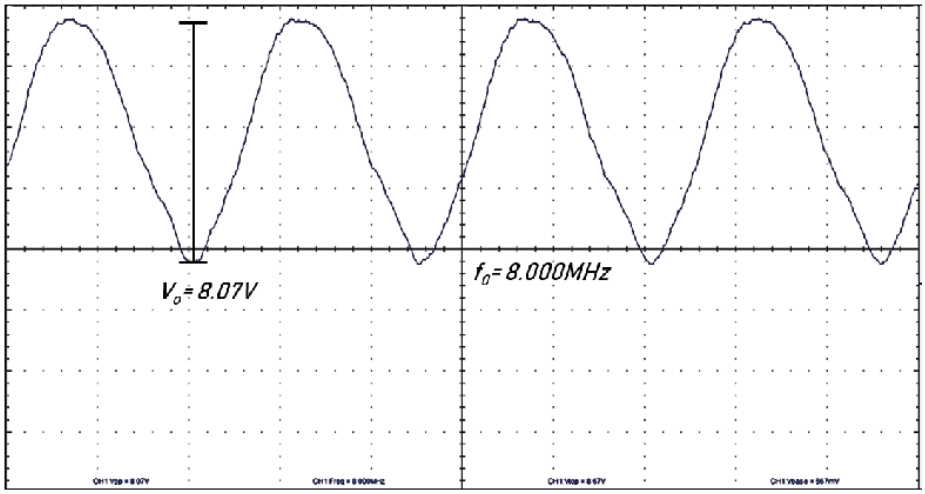

Figure 4.5: Second Example Oscillator Waveform - Dual Supply

Both supplies were set to 5 V and a 1 $k\Omega$ potentiometer was used as the emitter resistor. After finding the correct capacitors and achieving the correct output amplitude, the potentiometer was measured and the oscillator's single-supply fixed-bias counterpart was configured. After converting the biasing scheme, the circuit required tuning and the only available variable was the capacitance (guideline (f)). While both capacitors affect both output characteristic, the C_2 capacitor has more of an effect on output voltage amplitude and the C_1 capacitor has a larger effect on frequency. The final circuit is displayed in figure 4.6 and its waveform is shown in figure 4.7.

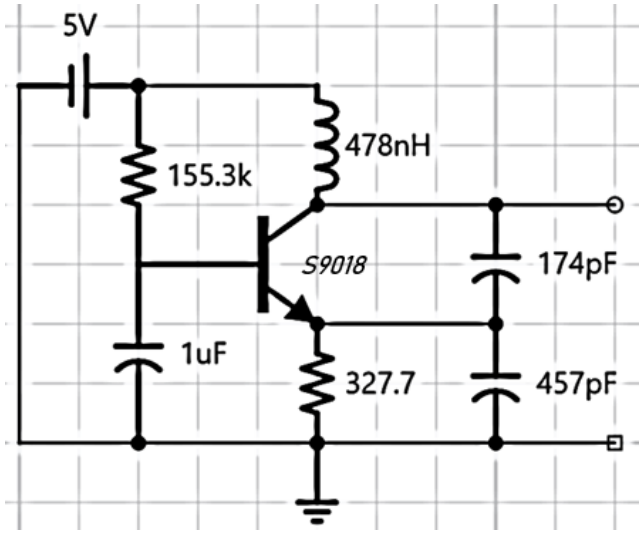

Figure 4.6: Second Example Oscillator Circuit

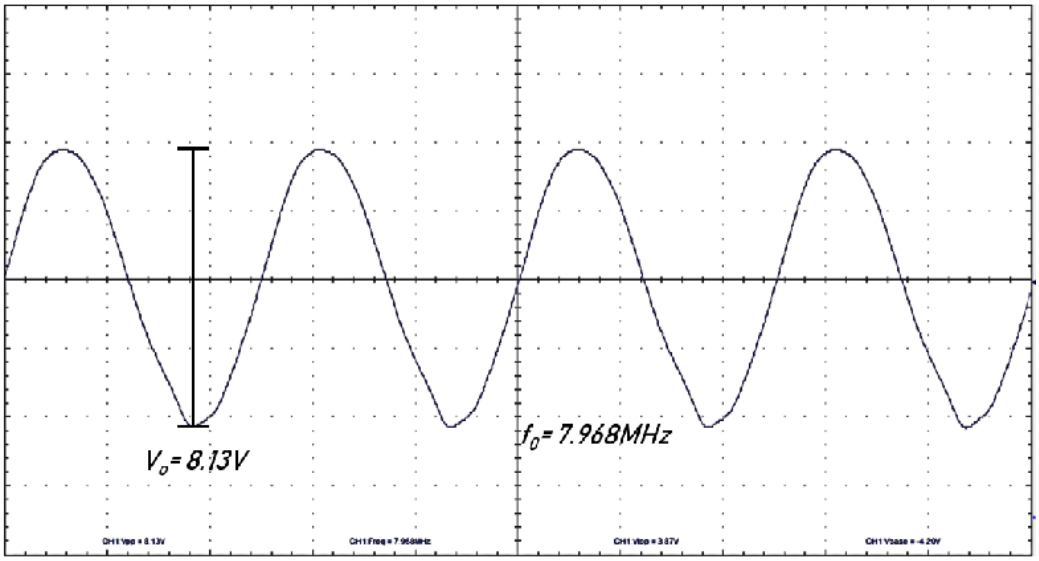

Figure 4.7: Second Example Oscillator Waveform - Single Supply

The circuit of figure 4.6 was simulted for comparison. Applying the *startup* modifier resulted in a 20 μs ramp up of voltage followed by a stead DC voltage at the level of the supply. Applying *uic* yielded the waveform of figure 4.8 and applying no special conditions produced the waveform of figure 4.9.

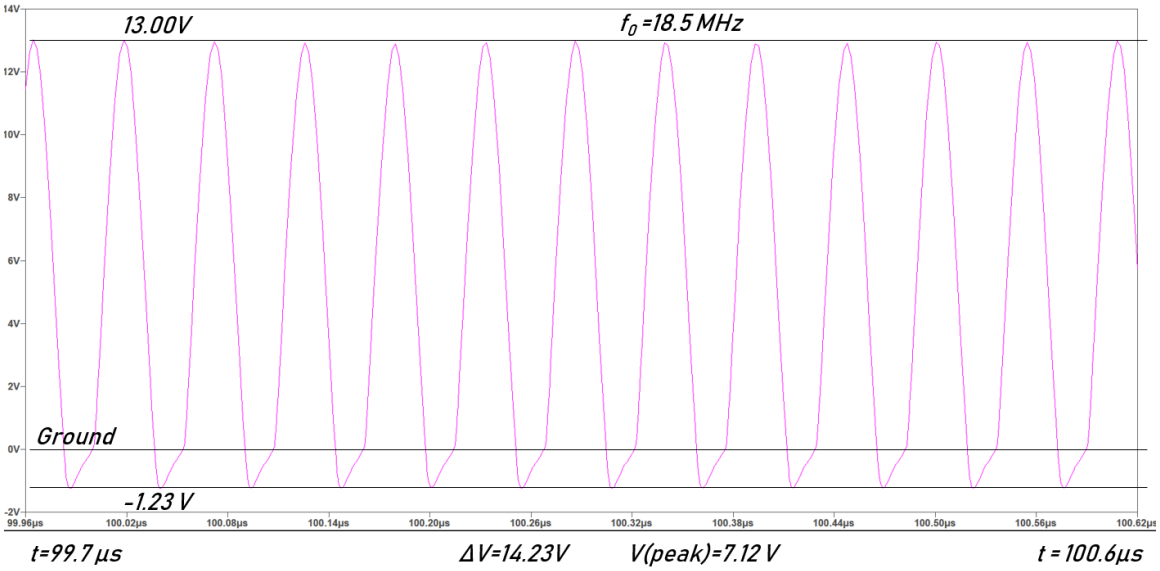

Figure 4.8: Second Example Oscillator Simulation: *uic* Applied

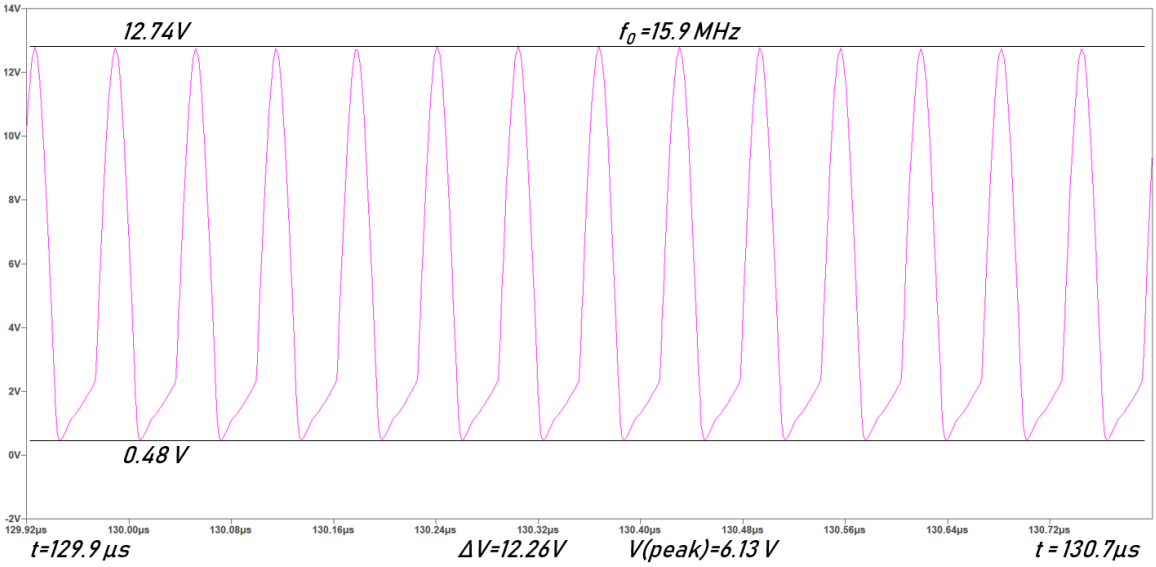

Figure 4.9: Second Example Oscillator Simulation: No Initial Conditions

The simulations both predict that this circuit will oscillate though at significantly different amplitudes and frequencies. Neither simulation predicted results close to the experimental values.

Conclusion Neither oscillator in this example exactly met the specifications precisely but they could have with more tuning. The purpose of this section was to show how the circuit parameters of the Colpitts oscillator may be manipulated.

CHAPTER 5

CONCLUSIONS AND SUGGESTIONS FOR FURTHER RESEARCH

The objective of this thesis was to determine a method to control the output voltage amplitude, output resistance, and waveform purity of the Colpitts oscillator. To accomplish this, theory, simulation, and experimentation were all used. In many cases, the theoretical and simulated results were similar. In no case did the experimental results accord with either theory or simulation. This is to be expected because of the parasitic reactance and unaccounted-for resistance in actual circuits as well as the variance in β and other parameters of the transistors.

5.1 Contributions

The relationships of current, inductance and capacitance to output voltage stated in the articles by Huang [7] and Imani [8] were confirmed experimentally and became the basis for the first three guidelines for experimental oscillator construction described in chapter 4. Additional analysis of the Colpitts oscillator circuit demonstrated the effects of V_{CC} and the capacitive ratio n on the output voltage. By controlling these variables, the amplitude of oscillation may be set to any desired level with no limit indicated experimentally.

Component selection was also shown to affect the magnitude of output resistance and the quality of the waveform. Because of the diversity of output voltage control mechanisms, the circuit may be manipulated to balance these three requirements.

While the process is iterative, the guidelines identified in chapter 4 provide a method for Colpitts oscillator construction to satisfy design criteria. The effects of the guidelines were all demonstrated in the output voltage amplitude and output resistance sections of chapter 3. The guidelines do not specify any particular NPN transistor model. The effect of changing the transistor model had little effect on the simulated output voltage and the guideline relationships are independent of the model selected.

5.1.1 Output Voltage Amplitude Guidelines

The first guideline (increase inductance to increase output voltage amplitude) was implied in the first three output voltage amplitude experiments (output voltage as a function of increasing inductance) and tested in the seventh (Large Inductance Oscillator). The second guideline (increase emitter current to increase output voltage amplitude) was demonstrated in the sixth output voltage experiment. In this experiment the output voltage was measured and only the positive and negative voltage supplies were varied.

The third guideline (decrease capacitance to increase output voltage amplitude) was demonstrated in the fourth output voltage experiment by measuring the output voltage amplitude and varying only the capacitance. The fifth guideline (apply the resonant-frequency curve to select inductance) was presented in the third output voltage experiment as a method to prevent saturation for a given biasing scheme. If biasing may be varied, saturation need not occur. The frequency curve is still useful as an indicator of relative output voltage amplitude.

The sixth guideline (vary C_1 and C_2 to tune resonant frequency and output voltage amplitude) was demonstrated in output voltage experiment 5. In this experiment the C_1 capacitor was maintained constant and the C_2 capacitor was varied to produce a capacitive ratio n between values 0 and 1. Except at n values very close to the extremes, a measurable output voltage was obtained. For n between approximately 0.04 and 0.50, there was only minor change in the output voltage amplitude. Slight changes in n result in slight changes in the resonant frequency and output voltage amplitude and thus these parameters may be tuned.

Guidelines 7-9 (design with positive and negative DC supplies and then convert to single supply; use only a negative supply if the desired output voltage is less than V_{BEQ}(peak); and determine appropriate I_E through use of a potentiometer) and the recommendations to begin with $I_E = 1\ mA$ and $n = 0.5$ are practical considerations. An oscillator designer may have only a specific resonant frequency in mind before construction and must begin somewhere. These design considerations allow the designer

to begin with a simple but flexible circuit that may be easily manipulated to meet requirements before conversion to a single supply.

5.1.2 Output Resistance Guideline

While several experiments investigating output resistance were conducted, only one guideline emerged (decrease inductance to decrease output resistance). The effect of output resistance increasing with inductance was demonstrated in the first two output resistance experiments and tested in the third.

5.2 Suggestions for Further Research

Through the discoveries of this thesis, a circuit with undesirable characteristics may in some respects be corrected. This was displayed in experiments 6 and 7 in chapter 3 and the example circuits of chapter 4. With more data, an equation in the style of equations 1.1 and 1.2 based on experimental results could be attempted.

While much of this thesis focused on the effect of circuit parameters on the output voltage, the same process should be conducted for the output resistance. The output resistance was shown to be proportional to the inductance but its dependence on the other parameters is unknown.

The output voltage waveforms throughout this thesis exhibited varying levels of distortion other than saturation. Possible reasons for the distortion were mentioned but a comprehensive investigation could be completed in terms of qualitative appearance (sawtooth, e.g.) and total harmonic distortion.

A final recommended future undertaking would be the reconciliation of experimental results with the large-signal analysis methods used by Clark, Hess [3], Rohde and Apte [17]. Their prediction methods largely corresponded to simulation but further analysis is required to account for the discrepancy with experimental results. The experimentation should be focused on a lower frequency range (hundreds of kilohertz) to minimize the effect of parasitics.

BIBLIOGRAPHY

[1] Milton Abramowitz and Irene A. Stegun, editors. *Handbook of Mathematical Functions - Formulas, Graphs, and Mathematical Tables*. National Bureau of Standards - Applied Mathematics Series 55, Washington, DC, June 1964.

[2] Robert L. Boylestad and Louis Nashelsky. *Electronic Devices and Circuit Theory*. Prentice-Hall, Inc., Upper Saddle River, New Jersey, 7th edition, 1999.

[3] Kenneth K. Clarke and Donald T. Hess. *Communication Circuits: Analysis and Design*. Addison-Wesley Publishing Company, Reading, Massachusetts, 1971.

[4] Analog Devices. Ltspice. 2019.

[5] Jon B. Hagen. *Radio-Frequency Electronics: Circuits and Applications*. Cambridge University Press, New York, 2nd edition, 2009.

[6] Ian Hickman. *Newnes Practical RF Handbook*. Butterworth-Heinemann Ltd, Oxford, 1993.

[7] Qiuting Huang. Exact calculation of oscillation amplitude and predicting power consumption for CMOS Colpitts oscillators. *IEEE International Symposium on Circuits and Systems*, pages 1401–1404, June 9-12 1997.

[8] Alireza Imani and Hossein Hashemi. Frequency and power scaling in mm-wave Colpitts oscillators. *IEEE Journal of Solid-State Circuits*, 53 Issue 5, May 2018.

[9] N. N. Lebedev. *Special Functions & Their Applications*. Dover Publications, Inc., New York, 1972.

[10] Jae-Young Lee and Kyu-Bok Lee. Design of K-band Gunn oscillator. *2005 Asia-Pacific Microwave Conference Proceedings*, December 2016.

[11] Reinhold Ludwig and Gene Bogdanov. *RF Circuit Design - Theory and Applications*. Pearson Education, Inc., New Jersey, 2nd edition, 2009.

[12] Kartikeya Mayaram. Output voltage analysis for the mos colpitts oscillator. *IEEE Transactions on Circuits and Systems I: Fundamental Theory and Applications*, 42 Issue 6, 2000.

[13] Donald A. Neamen. *Microelectronics: Circuit Analysis and Design*. McGraw-Hill, Inc., New York, 4th edition, 2009.

[14] Norio Nomura and Yuji Aoyagi. A colpitts-type crystal oscillator for gigahertz frequency. *2006 IEEE International Frequency Control Symposium and Exposition*.

[15] G. Palumbo M. Pennisi and S. Pennisi. Approach to analyse and design nearly sinusoidal oscillators. *IET Circuits, Devices & Systems*, 3 Issue 4, 2009.

[16] David M. Pozar. *Microwave Engineering*. John Wiley & Sons, Inc, Hoboken, New Jersey, 4th edition, 2012.

[17] Ulrich L. Rohde and Anisha M. Apte. Everything you always wanted to know about Colpitts oscillators. *IEEE Microwave Magazine*, pages 59–76, August 2016.

[18] Jack Smith. *Modern Communication Circuits*. McGraw-Hill, Inc., New York, 1986.

[19] Leonard Strauss. *Wave Generation and Shaping*. McGraw-Hill Book Company, Inc., New York, 1960.

[20] M J Underhill. Reduction of phase noise in single transistor oscillators. *Tenth European Frequency and Time Forum EFTF 96*, 1996.

APPENDIX A

OUTPUT IMPEDANCE OF COMMON-BASE AMPLIFIER

To determine the output impedance of the common-base amplifier, a slightly more robust model is required[1].:

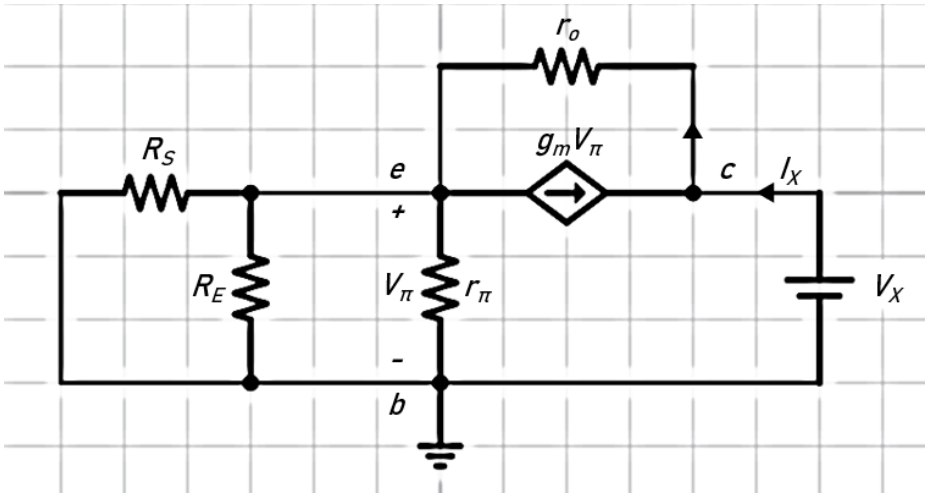

Figure A.1: Common-Base Amplifier Small-Signal Equivalent Circuit Including r_o and R_S

Figure A.1 is the same common-base amplifier small-signal equivalent circuit as figure 2.4, with the addition of the intrinsic transistor output resistance r_o and including the signal source output resistance R_S, which will be removed later. The collector and load resistors are also removed, as they are both considered as the load.

To determine the output resistance, the DC source is treated as a short circuit and a voltage V_X is applied back into the circuit, resulting in a current I_X. The ratio $\frac{V_X}{I_X}$ is the output resistance, Z_o.

To simplify figure A.1, the input-side resistors are combined in parallel to become R_{eq}, so that $R_{eq} = R_S||R_E||r_\pi$, as seen in figure A.2:

[1]The concept and final results of this problem are stated in [13, p. 434].

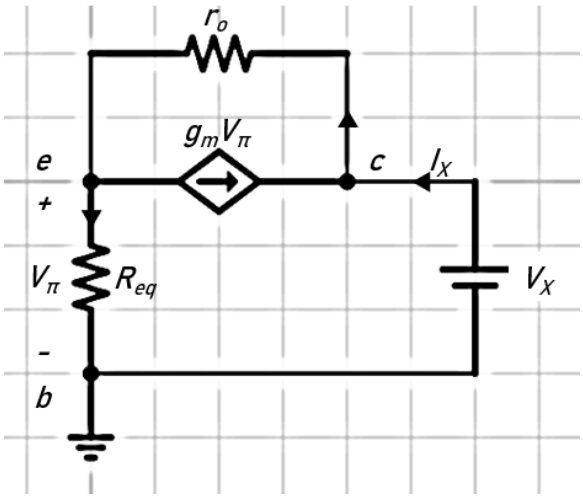

Figure A.2: CB Amplifier Equivalent Circuit for Calculating Z_o

Kirchhoff's current law is applied at both the emitter and collector nodes. At the collector:

$$I_X + g_m V_\pi - \frac{V_X - V_\pi}{r_o} = 0.$$

Solving for $\frac{V_\pi}{r_o}$ yields:

$$\frac{V_\pi}{r_o} = \left(\frac{V_X}{r_o} - I_X\right) \cdot \frac{1}{(g_m r_o + 1)}. \tag{A.1}$$

At the emitter:

$$\frac{V_X - V_\pi}{r_o} - g_m V_\pi - \frac{V_\pi}{R_{eq}} = 0.$$

Again solving for $\frac{V_\pi}{r_o}$ yields:

$$\frac{V_\pi}{r_o} = \frac{V_X}{r_o} \cdot \frac{1}{\left(1 + g_m r_o + \frac{r_o}{R_{eq}}\right)}. \tag{A.2}$$

Equating A.1 and A.2 and moving the multiterm factors in the denominators yields: $\cancel{\frac{V_X}{r_o}(1 + g_m r_o)} + \frac{V_X}{R_{eq}} - I_X\left(1 + g_m r_o + \frac{r_o}{R_{eq}}\right) = \cancel{\frac{V_X}{r_o}(1 + g_m r_o)}$ Finally, solving for $\frac{V_X}{I_X}$ yields:

$$Z_o = r_o(1 + g_m R_{eq}) + R_{eq} \tag{A.3}$$

If the source resistance R_S is zero, then $R_{eq} = 0$ and:

$$Z_o = r_o \tag{A.4}$$

In this case the total output impedance of the common-base amplifier including the collector and load resistors is the parallel combination:

$$Z_{o,loaded} = r_o||R_C||R_L.$$

APPENDIX B

RESONANT FREQUENCY, MAXIMUM EQUIVALENT SERIES RESISTANCE, AND NEGATIVE RESISTANCE

A method for determining the frequency of oscillation and the maximum value for the equivalent series resistor in the inductor makes use of a generalized oscillator. The oscillator, seen in figure B.1, consists of a small-signal transistor model (G_i, g_m, G_o), and a feedback network (Y_1, Y_2, Y_3).

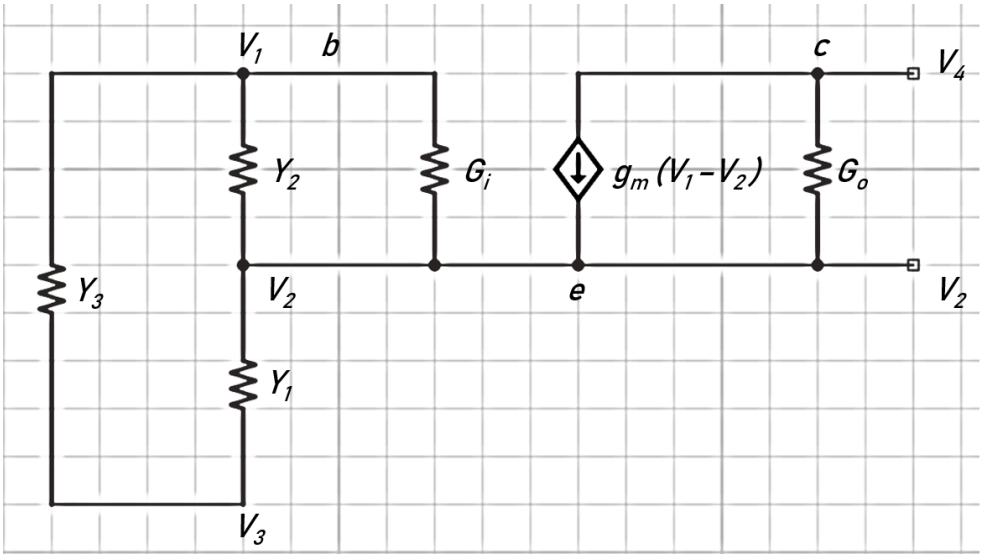

Figure B.1: Generalized Positive Feedback Transistor Oscillator

Identification of a common node indicates the oscillator configuration. Selection of component types for the feedback network indicates the type of oscillator (Hartley, Colpitts) and the phase relationship (inverted, non-inverted). Finally, a feedback path must be identified by connecting two voltage nodes. Not all combinations result in functional oscillators, but all functional oscillators may be configured using this model.

Figure B.1 may be converted to an admittance-voltage matrix that satisfies Kirchhoff's current law, [Y][V] = 0, as in figure B.2.

$$\begin{bmatrix} Y_2+Y_3+G_i & -(Y_2+G_i) & -Y_3 & 0 \\ -(Y_2+g_m+G_i) & Y_1+Y_2+G_i+G_o+g_m & -Y_1 & -G_o \\ -Y_3 & -Y_1 & Y_1+Y_3 & 0 \\ g_m & -(G_o+g_m) & 0 & G_o \end{bmatrix} \begin{bmatrix} V_1 \\ V_2 \\ V_3 \\ V_4 \end{bmatrix} = \begin{bmatrix} 0 \\ 0 \\ 0 \\ 0 \end{bmatrix}$$

Figure B.2: Complete Generalized KCL Matrix

As can readily be determined from figure B.1, terminal V_1 is the base. As the base is grounded in a common-base amplifier or oscillator, the associated rows of the matrix equation convert to 0. Further, as the feedback path in a common-base oscillator connects the collector terminal (V_4) to the first of two series-connected elements ($Y_1 \Rightarrow C_1$), V_4 and V_3 must be connected and the corresponding rows (3 and 4) must be added in all three terms. Finally, the intrinsic output admittance shunting the controlled current source in the small-signal BJT model may be ignored for simplicity. All of these operations yield the matrix in figure B.3.

$$\begin{bmatrix} Y_1+Y_2+G_i+g_m & -Y_1 \\ -(Y_1+g_m) & Y_1+Y_3 \end{bmatrix} \begin{bmatrix} V_2 \\ V=V_3+V_4 \end{bmatrix} = \begin{bmatrix} 0 \\ 0 \end{bmatrix}$$

Figure B.3: Reduced KCL Matrix

If V_2 and V are non-zero, the only possible solution to the system in figure B.3 requires that the determinant of the admittance matrix be zero. Figure B.3 could be made to show that the Y_1 and Y_2 must have a different sign from Y_3, but because the circuit has already been established as a common-base Colpitts oscillator, the identities of the admittances are already known. Of course $Y_1 = j\omega C_1$ and $Y_2 = j\omega C_2$. Y_3, the inductor, however, also includes the series resistance r, leading to an admittance $Y_3 = \frac{r-j\omega L}{r^2+\omega^2 L^2}$. The emitter-base conductance $G_i = \frac{1}{r_\pi} = \frac{I_B}{V_T}$, and $g_m = \frac{I_C}{V_T}$. Setting the determinant of the admittance matrix in figure B.3 to zero results in the equation:

$$0 = Y_1Y_3 + Y_1Y_2 + Y_2Y_3 + Y_1G_i + Y_3G_i + Y_3g_m$$

which after substitution yields a real part:

$$0 = \frac{\omega^2 L(C_1 + C_2)}{r^2 + \omega^2 L^2} + \frac{r(G_i + g_m)}{r^2 + \omega^2 L^2} - \omega^2 C_1 C_2 \tag{B.1}$$

and an imaginary part:

$$0 = j\Big(\frac{\omega r(C_1 + C_2)}{r^2 + \omega^2 L^2} - \frac{\omega L(G_i + g_m)}{r^2 + \omega^2 L^2} + \omega C_1 G_i\Big) \tag{B.2}$$

B.1 Resonant Frequency

To determine the resonant frequency, equations B.1 and B.2 are solved in terms of $(G_i + g_m)$:

$$real : G_i + g_m = \omega^2 C_1 C_2 r + \frac{\omega^4 C_1 C_2 L^2}{r} - \frac{\omega^2 L(C_1 + C_2)}{r} \tag{B.3}$$

$$imag : G_i + g_m = \frac{r(C_1 + C_2)}{L} + \frac{C_1 G_i r^2}{L} + \omega^2 C_1 G_i L \tag{B.4}$$

Setting equations B.3 and B.4 equal to each other and carrying through the algebra to solve for ω^2 yields:

$$\omega^2 = \frac{1}{L}\Big(\frac{1}{C_1} + \frac{1}{C_2} + \frac{G_i r}{C_2}\Big)$$

and to simplify by letting $C_2' = \frac{C_2}{1+G_i r} = \frac{C_2}{1+r/r_\pi}$, the resonant frequency including the equivalent series resistance r is:

$$f_0 = \frac{1}{2\pi}\sqrt{\frac{1}{L}\Big(\frac{1}{C_1} + \frac{1}{C_2'}\Big)}. \tag{B.5}$$

Carrying through the same operations while including the emitter resistance R_E yields

$$f_0 = \frac{1}{2\pi}\sqrt{\frac{1}{L}\Big(\frac{1}{C_1} + \frac{1}{C_2} + \Big(\frac{1}{R_E} + \frac{1}{r_\pi}\Big)\frac{r}{C_2}\Big)}. \tag{B.6}$$

B.2 Condition for Oscillation

To determine the maximum allowable value for the equivalent series resistance r in the inductor, equations B.1 and B.2 are solved in terms of $(C_1 + C_2)$:

$$real : C_1 + C_2 = \frac{C_1 C_2 r^2}{L} - \frac{r(G_i + g_m)}{\omega^2 L} + \omega^2 C_1 C_2 L \tag{B.7}$$

$$imag : C_1 + C_2 = \frac{L(G_i + g_m)}{r} - \frac{C_1 G_i \omega^2 L^2}{r} - C_1 G_i r \tag{B.8}$$

Setting equations B.7 and B.8 equal to each other and carrying through the algebra to solve for $r \cdot r_\pi$ yields

$$rr_\pi = \frac{\beta + 1}{\omega^2 C_1 C_2} - \frac{L}{C_2} \tag{B.9}$$

Including R_E into the operation yields

$$rr_\pi = \frac{\beta + 1}{\omega^2 C_1 C_2} - \frac{L}{C_2} - \frac{r_\pi}{R_E}\left(\frac{\omega^2 C_1 L - 1}{\omega^2 C_1 C_2}\right)$$

Finally, dividing both sides by r_π results in the maximum possible equivalent series resistance for the circuit, factoring in the emitter resistor, that will allow oscillation:

$$r_{max} = \frac{\beta + 1}{r_\pi \omega^2 C_1 C_2} - \frac{L}{r_\pi C_2} - \left(\frac{\omega^2 C_1 L - 1}{\omega^2 R_E C_1 C_2}\right). \tag{B.10}$$

B.3 Negative Resistance

Ignoring the emitter resistor, equation B.9 could be solved for r alone by dividing both sides by r_π. The first term on the right side of the equation is then:

$$\frac{(\beta + 1)/r_\pi}{\omega^2 C_1 C_2} \approx \frac{\beta / r_\pi}{\omega^2 C_1 C_2} = \frac{g_m}{\omega^2 C_1 C_2}, \tag{B.11}$$

the result of which is the input impedance of a negative-resistance oscillator such as the common-base Colpitts.

Figure B.4 is the same as figure B.1, configured as a common-base Colpitts oscillator, and including a load.

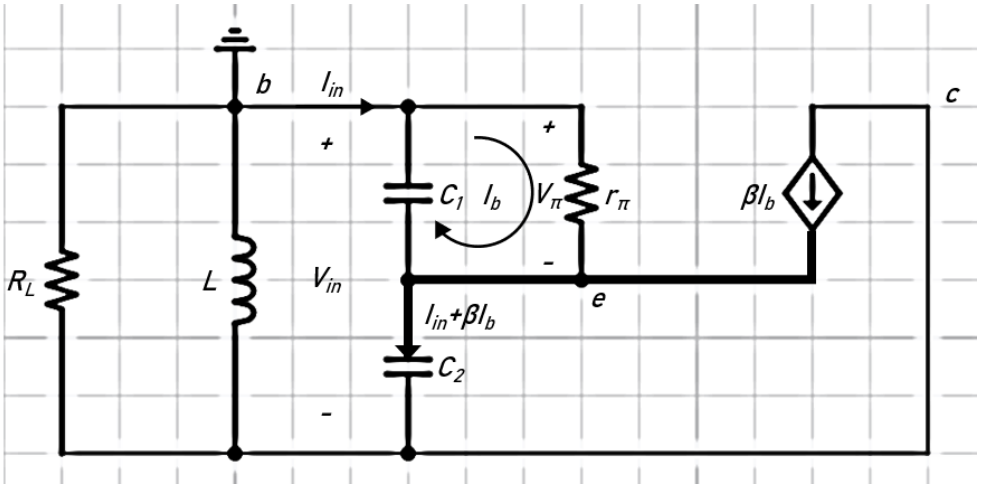

Figure B.4: Common-Base Colpitts Oscillator - Alternative View

The input resistance is the ratio of V_{in} to I_{in}. Using Kirchhoff's voltage law at V_π and V_{in} yields:

$$V_{in} = (I_{in} - I_b)X_{C_1} + (I_{in} + \beta I_b)X_{C_2} \Rightarrow I_b = \frac{V_{in} - I_{in}(X_{C_1} + X_{C_2})}{\beta X_{C_2} - X_{C_1}} \tag{B.12}$$

and

$$(I_{in} - I_b)X_{C_1} = I_b r_\pi \Rightarrow I_b = \frac{I_{in}X_{C_1}}{r_\pi + X_{C_1}} \tag{B.13}$$

Setting equations B.12 and B.13 equal to each other and solving for V_{in}/I_{in} yields:

$$Z_{in} = \frac{V_{in}}{I_{in}} = \frac{(\beta+1)X_{C_1}X_{C_2}}{r_\pi + X_{C_1}} + \frac{r_\pi(X_{C_1} + X_{C_2})}{r_\pi + X_{C_1}}. \tag{B.14}$$

Assuming that r_π is much larger than X_{C_1}, equation B.14 simplifies to

$$Z_{in} \approx \frac{-(\beta+1)/r_\pi}{\omega^2 C_1 C_2} - \frac{j}{\omega}\left(\frac{1}{C_1} + \frac{1}{C_2}\right).$$

Simplifying again by ignoring the "+1" in the numerator of the real term, the input resistance of the common-base Colpitts oscillator is approximately

$$r_{in} \approx \frac{-g_m}{\omega^2 C_1 C_2}. \tag{B.15}$$

Dividing both sides of equation B.9 by r_π now yields a maximum allowable value for the equivalent series resistance r, which is the input resistance of the oscillator less a factor $L/(r_\pi C_2)$.

APPENDIX C

CONTRIBUTION OF EQUIVALENT SERIES RESISTANCE OF INDUCTOR TO OUTPUT IMPEDANCE

Naturally the small resistance of the inductor has some effect on the value of the inductance and the value of the output impedance of the Colpitts oscillator. Because the Colpitts oscillator operates primarily at a single frequency, it is convenient to transform the combined impedance of the inductor with its small resistance and the load resistance to a pure equivalent inductance in parallel with a pure resistance as in figure C.1:

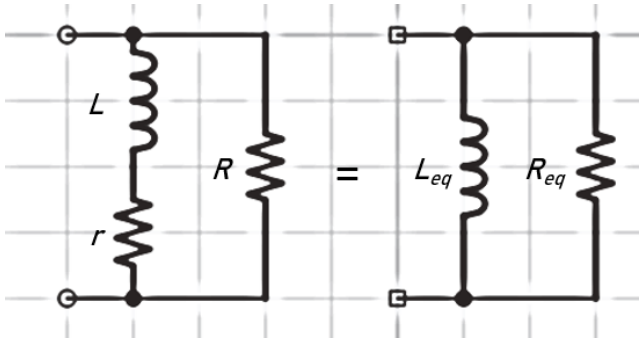

Figure C.1: Inductor Admittance Transformation

The process for the transformation is as follows:

$$Z = \frac{R(r + j\omega L)}{(R + r) + j\omega L}$$

and

$$Y = G - jB_L = \frac{1}{R}\Big(\frac{rR + r^2 + \omega^2 L^2}{r^2 + \omega^2 L^2}\Big) - j\Big(\frac{\omega L}{r^2 + \omega^2 L^2}\Big).$$

Then

$$R_{eq} = \frac{1}{G} = \frac{R(r^2 + \omega^2 L^2)}{rR + (r^2 + \omega^2 L^2)} \tag{C.1}$$

and

$$-jB_L = -\frac{j}{\omega L_{eq}} = -j\Big(\frac{\omega L}{r^2 + \omega^2 L^2}\Big) \Rightarrow L_{eq} = \frac{\omega^2 L^2 + r^2}{\omega^2 L}. \tag{C.2}$$

The equivalent inductance does not depend on any parallel resistance and if r is very small, the inductance is almost unaffected. A 100 mΩ resistance at 1 MHz transforms a 1

μH inductor into a 1.0003 μH inductance. At 5 Ω, the inductor has a value of 1.63 μH, though at 50 Ω, L_{eq} = 64 μH, which is substantial. In practice, inductances in the nano-, micro-, and even milli-Henry ranges have resistance of less than 10 Ω though this factor should always be considered.

The load resistance, however, is very dependent on the inductor resistance. Using the circuit from section 2.2.2, a load resistance of 5 kΩ becomes 2.6 kΩ with a very small *r* of 100 mΩ. At r = 2Ω, R_{eq} becomes 266 Ω.

APPENDIX D

DERIVATION OF LARGE-SIGNAL EMITTER CURRENT AND TRANSCONDUCTANCE FOR SINUSOIDAL INPUT

According to Clarke and Hess [3, p. 4], the small-signal model for a standard transistor amplifier, for example the circuit of figure 2.2, ceases to apply for an input voltage exceeding approximately 260 mV. Beyond this threshold, the input signal causes a significant shift to the bias values and the AC and DC circuits cannot be treated separately. Because the terminal currents are related by the parameters $I_C = \beta I_B = \alpha I_E$, it is sufficient to solve for one current. While this is applicable to all configurations, it is easily displayed in the common-base amplifier of figure D.1. This figure could be achieved with either the two sources displayed or with the base source and base resistor as their Thévenin equivalents.

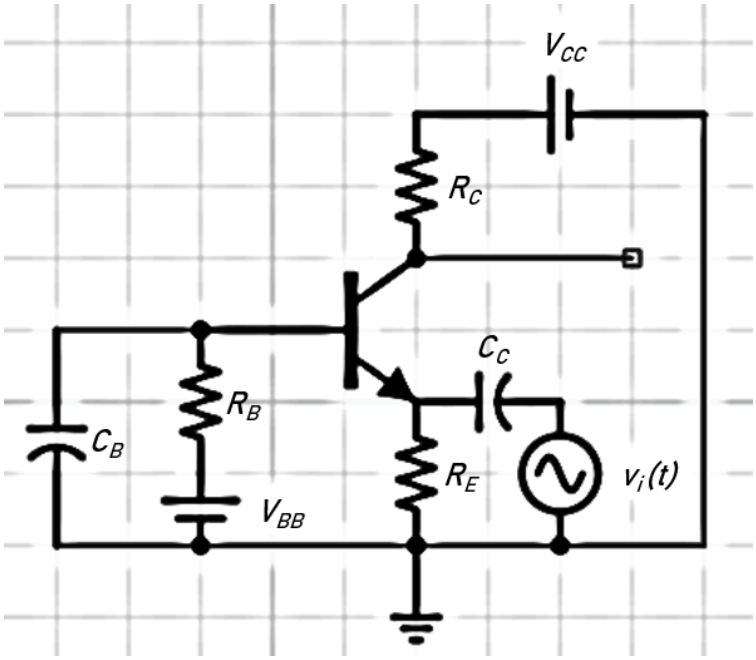

Figure D.1: Common-Base Amplifier with Simplified Biasing

In figure D.1, the voltage across the base-emitter junction is the sum of the DC voltage (V_{dcQ}) from V_{CC} and the AC input voltage $v_i(t)$. Using the Shockley diode

equation (slightly simplified) applied to the base-emitter junction:

$$i_E = I_{ES} e^{v_{BE}/V_T} = I_{ES} e^{V_{dcQ}/V_T} e^{v_i(t)/V_T} \tag{D.1}$$

where I_{ES} is the reverse bias saturation current of the emitter and $V_T = kT/q$ is the thermal voltage, the total emitter current is the product of a constant factor and a time-varying factor f($v_i(t)$). With no applied voltage, equation D.1 reduces to

$$I_{EQ} = I_{ES} e^{V_{dcQ}/V_T} \tag{D.2}$$

and the emitter current as a function of time is

$$i_E(t) = I_{EQ} e^{v_i(t)/V_T}.$$

If the input voltage is sinusoidal (or cosinusoidal), the total emitter current is

$$i_E(t) = I_{EQ} e^{V_1 \cos(\omega t)/V_T} = I_{EQ} e^{x \cos(\omega t)} \tag{D.3}$$

where the input voltage is $v_i(t) = V_1 \cos(\omega t)$ and $x = V_1/V_T$ for brevity. According to [1, eq. 9.6.34, p. 376],

$$e^{x \cos\theta} = I_0(x) + 2 \sum_{n=1}^{\infty} I_n(x) \cos(n\theta) \tag{D.4}$$

where $I_n(x)$ is the modified Bessel function of the first kind of order n. Substituting, the emitter current becomes:

$$i_E(t) = I_{EQ} \left[I_0(x) + 2 \sum_{n=1}^{\infty} I_n(x) \cos(n\omega t) \right] = I_{EQ} I_0(x) \left[1 + 2 \sum_{n=1}^{\infty} \frac{I_n(x)}{I_0(x)} \cos(n\omega t) \right]. \tag{D.5}$$

Observing that the cosine factor averages to zero over any number of cycles, the DC emitter current becomes:

$$I_{dc} = I_{EQ} I_0(x).$$

Having demonstrated that the average, or DC, value of the emitter current in a circuit with an applied signal is different from its quiescent emitter current, it is helpful to define two new placeholder terms. These terms will simplify the derivation of the average large-signal transconductance.

First, as seen in equation D.2, the quiescent voltage drop across the base-emitter junction is V_{dcQ}. Let the average DC voltage drop with an applied signal be V_{dc}. Then the difference between the two is

$$\Delta V = V_{dcQ} - V_{dc},$$

where ΔV is the base-emitter voltage bias suppression.

Second, as shown in equation D.3, the emitter current due to the input signal is $I_{ES}e^{v_i(t)/V_T} = I_{ES}e^{x\cos(\omega t)}$ for an input signal $v_i(t) = V_1\cos(\omega t)$ and $x = V_1/V_T$. Define W as the ratio of the time-varying emitter current to its peak value:

$$W(t) = \frac{i_E(t)}{I_P} = \frac{I_{ES}e^{x\cos(\omega t)}}{I_{ES}e^{x}} = \frac{e^{x\cos(\omega t)}}{e^{x}}; \tag{D.6}$$

now let $\overline{W}$ be the average value of the emitter current due to the input signal:

$$\overline{W} = \frac{\overline{i_e(t)}}{I_P} = \frac{I_{E0}}{I_P} = \frac{\frac{1}{T}\int_0^T \Big(I_0(x) + 2\sum_{n=1}^{\infty} I_n(x)\cos(n\omega t)\Big)dt}{e^{x}} = \frac{I_0(x)}{e^{x}}. \tag{D.7}$$

With the concept of a signal-induced shift in the DC bias voltage and the introduction of the assistant functions ΔV, W, and $\overline{W}$, the derivation of $i_E(t)$ can now be completed.

Substituting the waveform function W into the Shockley diode equation (equation D.1) yields

$$i_E(t) = I_{ES}e^{V_{dcQ}/V_T}e^{V_1/V_T}W(t)$$

and again substituting the quiescent emitter current equation yields:

$$i_E(t) = I_{EQ}e^{-\Delta V/V_T}e^{V_1/V_T}W(t).$$

The average, or DC, emitter current, including the contribution from the input signal is then

$$I_{E0} = I_{EQ}e^{-\Delta V/V_T}e^{V_1/V_T}\overline{W}. \tag{D.8}$$

From the perspective of the circuit of figure D.1, the average emitter current is also

$$I_{E0} = \frac{V_{BB} - V_{dc}}{R_E + R_B/(\beta+1)} = I_{EQ} + \frac{\Delta V}{R_E + R_B/(\beta+1)} = I_{EQ}\Big(1 + \frac{\Delta V}{V_\lambda}\Big) \tag{D.9}$$

where V_λ is the quiescent voltage at the base terminal. Equating D.8 and D.9 and approximating $\Delta V / V_\lambda$ as negligible, ΔV can be solved as

$$\Delta V = V_1 + V_T \ln \overline{W}. \tag{D.10}$$

Substituting the value of $\overline{W}$ from equation D.7 into equation D.10 yields:

$$\Delta V = V_1 + V_T \Big(\ln(I_0(x)) - \ln\left(e^{\frac{V_1}{V_T}}\right)\Big) = V_1 + V_T \ln(I_0(x)) - V_T \frac{V_1}{V_T} = V_T \ln(I_0(x)). \tag{D.11}$$

Finally, using the relationship from equations D.6 and D.7 that $W(t)/\overline{W} = i_E(t)/I_{E0}$, $i_E(t)$ may be calculated as

$$i_E(t) = I_{E0} \frac{W(t)}{\overline{W}} = I_{EQ}\Big(1 + \frac{\Delta V}{V_\lambda}\Big) \frac{e^{x\cos(\omega t)}}{I_0(x)},$$

and expanded using the substitution from equation D.4:

$$i_E(t) = I_{EQ}\left(1 + \frac{\ln(I_0(x))}{V_\lambda / V_T}\right)\left(1 + 2\sum_{n=1}^{\infty} \frac{I_n(x)}{I_0(x)} \cos(n\omega t)\right). \tag{D.12}$$

Now the large-signal average fundamental transconductance, defined in [3, 177] as

$$G_m(x) = \frac{\alpha I_{E1}}{V_1} = \frac{I_{C1}}{V_1} \tag{D.13}$$

may be found. The subscripts on the emitter and collector currents indicate that they are the fundamental components. As in section 2.1.1, the small-signal quiescent transconductance is $g_m = I_{CQ}/V_T$, and again, $x = V_1/V_T$. Substituting these into equation D.12 yields:

$$G_m(x) = g_{mQ}\left(1 + \frac{\ln(I_0(x))}{V_\lambda / V_T}\right) \frac{2I_1(x)}{xI_0(x)} \tag{D.14}$$

and for the analysis of section 2.2.1,

$$\frac{G_m(x)}{g_{mQ}} = \frac{2I_1(x)}{xI_0(x)}\left(1 + \frac{\ln(I_0(x))}{V_\lambda / V_T}\right). \tag{D.15}$$

APPENDIX E

PLOTS OF RELEVANT BESSEL FUNCTIONS

Bessel functions are a family of solutions to certain forms of second order differential equations [9, p. 98]. Two such functions are used in this thesis. They are the Bessel function of the first kind of order n and argument x ($J_n(x)$) and the modified Bessel function of the first kind of order n and argument x ($I_n(x)$). These functions arise as series expansion factors for composite functions, e.g. $\cos(\sin(x))$ and $e^{\cos(x)}$.

These functions are not commonly seen at the electrical engineering undergraduate level. Their plots are presented here for familiarization and to confirm the results of their use and approximations throughout the thesis.

E.1 Bessel Functions of the First Kind

Figure E.1 is a plot of the first four orders (n = 0:3) of the Bessel function of the first kind in the variable x.

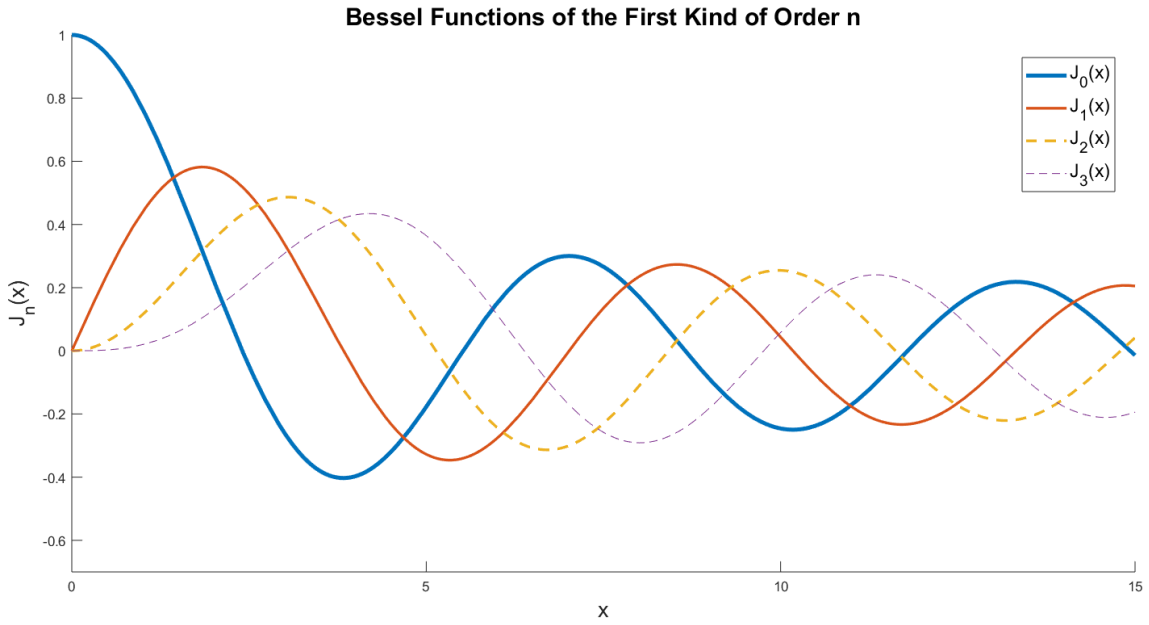

Figure E.1: $J_n(x)$

The functions oscillate but are not periodic. The zeroth-order J function equals 1 at argument 0, whereas all subsequent orders originate at 0.

E.2 Modified Bessel Functions of the First Kind

Figure E.2 is a plot of the first four orders of the modified Bessel function of the first kind.

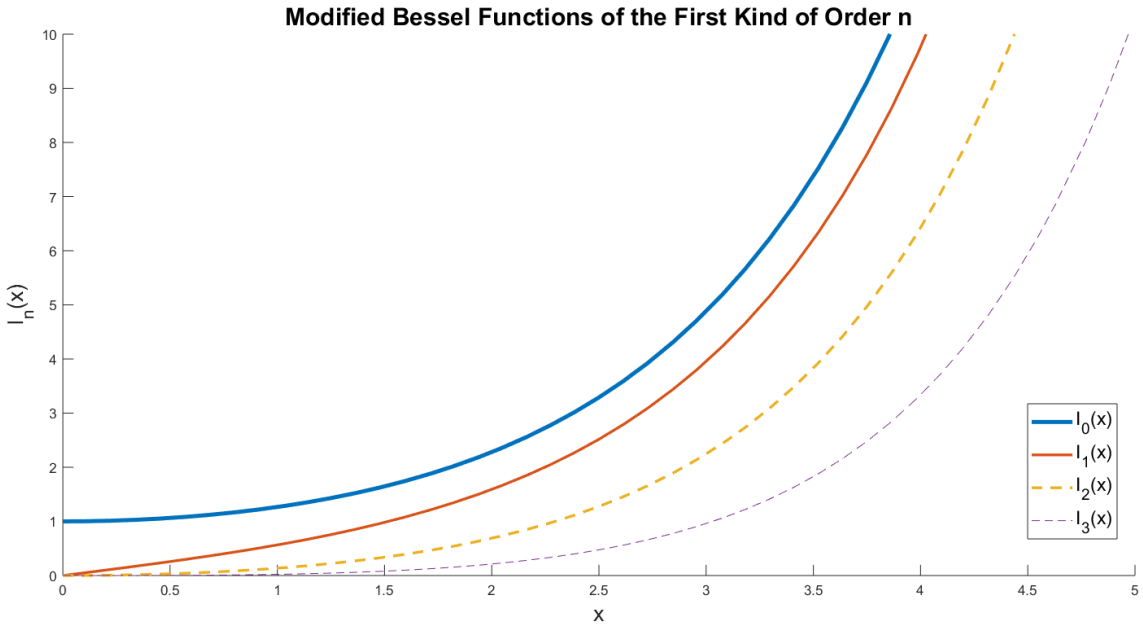

Figure E.2: $I_n(x)$

Again, the 0 order originates at 1 and all subsequent orders originate at 0.

E.3 Small-Angle Approximations

Equation 2.27, the modulated carrier wave for determining phase noise, contains the factors

$$J_0(\Theta) + 2\sum_{k=1}^{\infty} J_{2k}(\Theta)\cos(2k\omega_m t) \tag{E.1}$$

and

$$2\sum_{k=0}^{\infty} J_{2k+1}(\Theta)\sin[(2k+1)\omega_m t]. \tag{E.2}$$

In an effort to approximate these cumbersome terms, a further inspection of Bessel function plots is helpful. The first term of E.1 is $J_0(\Theta)$. Figure E.3 is a plot of $J_0(x)$ near $x = 0$.

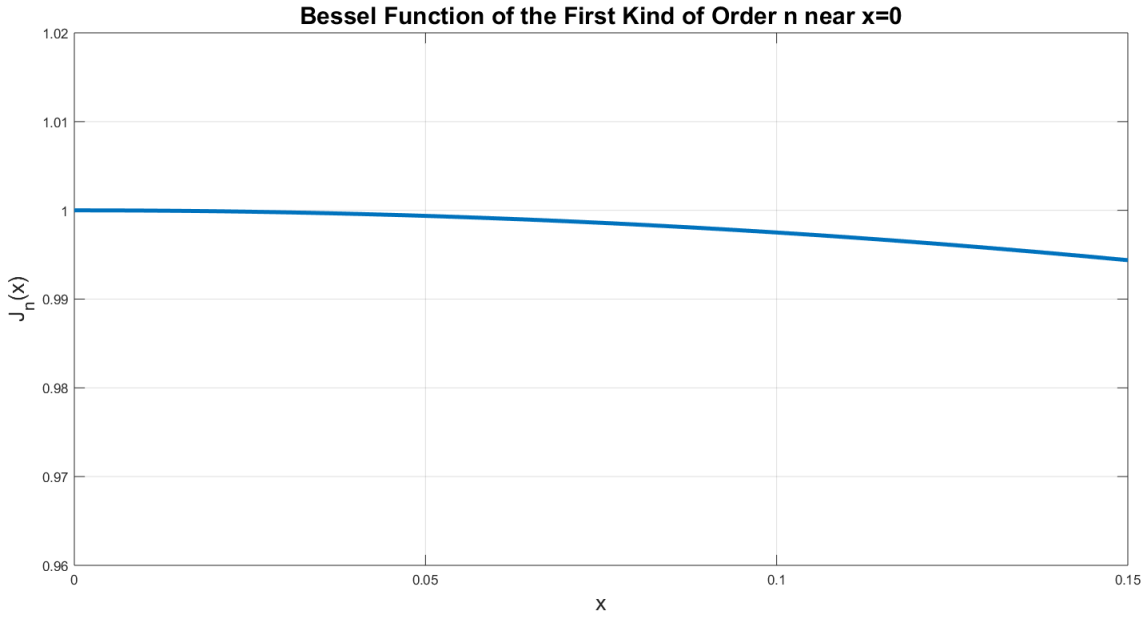

Figure E.3: $J_0(x)$

Near $x = 0$, $J_0(x) \approx 1$. The next term of E.1 is a summation of the even terms of $J_n(x)$ for $n > 0$. Figure E.4 is a plot of the first four such functions assuming the maximum value of unity for the cosine factor.

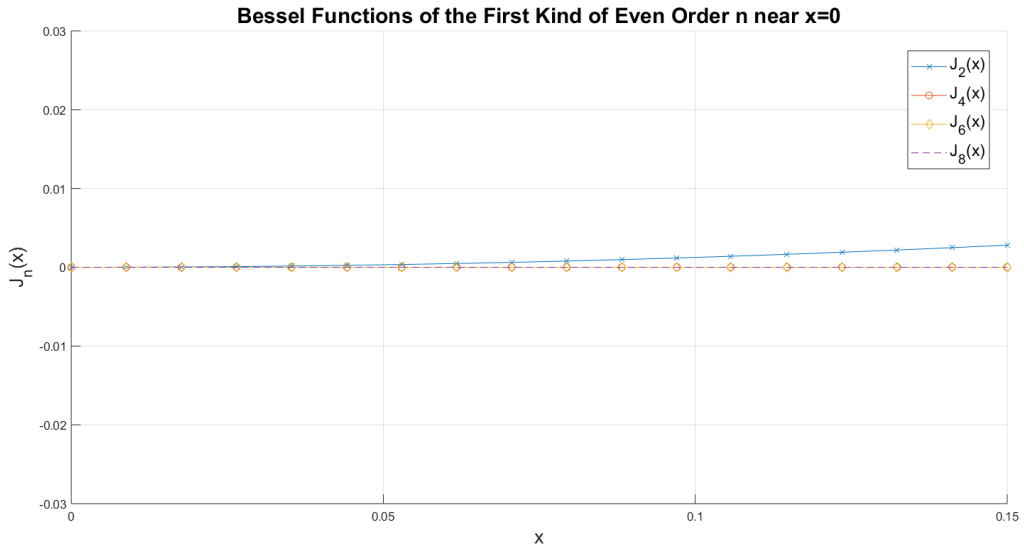

Figure E.4: $J_n(x)$, $n > 0$, even

The second term of E.1 is thus approximately 0 and the entire expression equals approximately 1.

In the case of E.2, the expression is a summation of the odd orders of $J_n(x)$. Figure E.5 is the plot of the first four such terms again assuming unity for the sine factor.

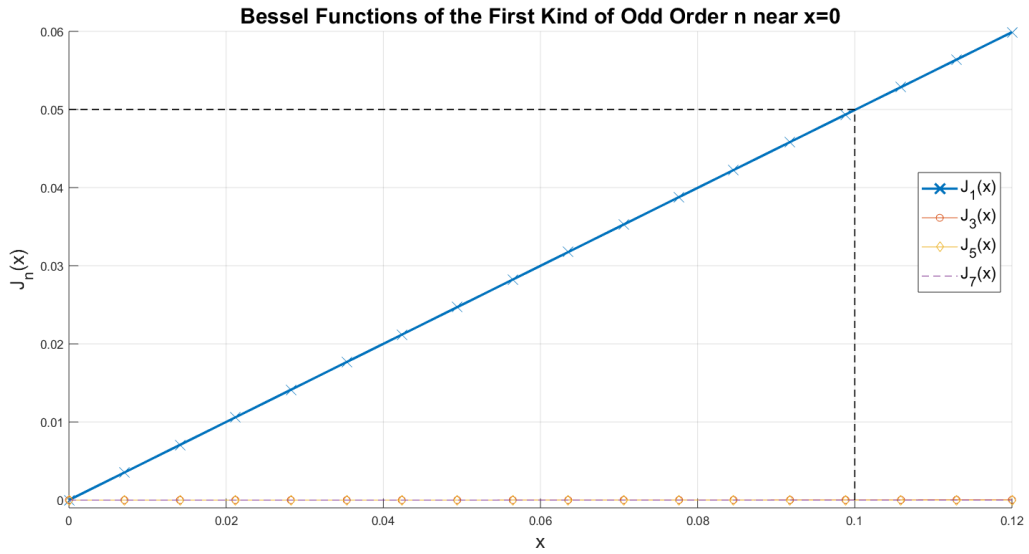

Figure E.5: $J_n(x)$, $n > 1$, odd

The plot contains some assisting constant lines to demonstrate the slope of $J_1(x)$, which is $\frac{1}{2}$. All included subsequent orders are very close to 0, so the value of expression E.2 is $2(\frac{\Theta}{2}\sin\omega_m t + 0 + \cdots) = \Theta \sin\omega_m t$.